

Fall 2009

# Study of additives used in a copper via filling chemistry

Sheik Ansar Usman Ibrahim  
*University of New Hampshire, Durham*

Follow this and additional works at: <https://scholars.unh.edu/thesis>

---

## Recommended Citation

Usman Ibrahim, Sheik Ansar, "Study of additives used in a copper via filling chemistry" (2009). *Master's Theses and Capstones*. 482.  
<https://scholars.unh.edu/thesis/482>

This Thesis is brought to you for free and open access by the Student Scholarship at University of New Hampshire Scholars' Repository. It has been accepted for inclusion in Master's Theses and Capstones by an authorized administrator of University of New Hampshire Scholars' Repository. For more information, please contact [nicole.hentz@unh.edu](mailto:nicole.hentz@unh.edu).

## **NOTE TO USERS**

**This reproduction is the best copy available.**

**UMI<sup>®</sup>**



# **STUDY OF ADDTIVES USED IN A COPPER VIA FILLING**

## **CHEMISTRY**

BY

Sheik Ansar Usman Ibrahim

B.Tech, Central Electrochemical Research Institute, 2006

THESIS

Submitted to the University of New Hampshire  
in Partial Fulfillment of  
the Requirements for the Degree of

Master of Science  
In  
Chemical Engineering

September 2009

UMI Number: 1472067

### INFORMATION TO USERS

The quality of this reproduction is dependent upon the quality of the copy submitted. Broken or indistinct print, colored or poor quality illustrations and photographs, print bleed-through, substandard margins, and improper alignment can adversely affect reproduction.

In the unlikely event that the author did not send a complete manuscript and there are missing pages, these will be noted. Also, if unauthorized copyright material had to be removed, a note will indicate the deletion.

UMI<sup>®</sup>

---

UMI Microform 1472067  
Copyright 2009 by ProQuest LLC  
All rights reserved. This microform edition is protected against  
unauthorized copying under Title 17, United States Code.

---

ProQuest LLC  
789 East Eisenhower Parkway  
P.O. Box 1346  
Ann Arbor, MI 48106-1346

This thesis has been examined and approved.



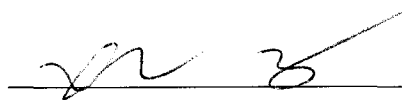
---

Thesis Director, Dr. Dale P. Barkey,  
Professor of Chemical Engineering



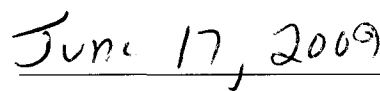
---

Dr. Palligarnai T. Vasudevan,  
Chair and Professor of Chemical Engineering



---

Dr. Xiaowei Teng,  
Assistant Professor of Chemical Engineering



---

Date

## DEDICATION

To all my family;

especially my parents, Razia and Usman Ibrahim, Mehaboob and Vedhasri.

## ACKNOWLEDGMENTS

I would want to extend the deepest gratitude to all the people who helped me accomplish my dissertation work.

The person who was instrumental in me doing research in electrochemical engineering is my thesis advisor, Dr. Dale P. Barkey. He has always been patient in helping me understand key concepts and I have learnt a lot from his expertise in electrochemical science. I am very grateful for all the opportunities he extended for me to conduct research under his guidance.

I would also like to take this opportunity to thank Dr. P. Vasudevan and Dr. Xiaowei Teng for serving on the thesis committee and for their valuable advice and suggestions.

Mr. Jonathan E. Newell, the technician at the Chemical Engineering department, has always been very helpful in providing tools and troubleshooting the entire lab related issues.

I am also grateful to Mrs. Nancy Littlefield for all the help she extended during my graduate study at the university.

I also thank my fellow lab associate and graduate student, Yi-Shi Chen for helping me run several experiments and also for his invaluable inputs from his industrial experience.

I am grateful to Mr. Stephen Christian, manager Rohm and Haas Electronic Materials, NY, for his support and interest shown in me during the course of my internship. He also helped me get a feel of the direct application of my research work in actual production.

I thank my parents, Usman and Razia Begum, my brother Mehaboob, and friends, Vedhasri, Aravind and Amit for all their patience, support and encouragement over the years.



## TABLE OF CONTENTS

DEDICATION.....	iii
ACKNOWLEDGEMENTS.....	iv
LIST OF TABLES.....	ix
LIST OF FIGURES.....	x
ABSTRACT.....	xiv

CHAPTER	PAGE
<b>I</b> INTRODUCTION.....	1
1.1 Overview.....	1
1.2 Electrochemical cell.....	2
1.3 Electrochemistry.....	3
1.4 Mass transport in electrochemical reactions.....	4
1.5 Rotating disk electrode.....	6
1.6 Electrodeposition of copper.....	8
1.7 Types of filling.....	9
1.8 Additive systems.....	12

## **II** LITERATURE REVIEW

2.1	Copper plating bath.....	14
2.2	Effect of Polyethylene glycol.....	14
2.3	Effect of chloride .....	17
2.4	Effect of SPS and MPSA .....	18
2.5	Mechanisms of via filling .....	19

## **III** EXPERIMENTAL

3.1	Introduction.....	21
3.2	Experimental apparatus and instrumentation.....	21
3.2.1	Experimental cell .....	21
3.2.2	Electrodes.....	22
3.2.3	Potentiostat.....	23
3.2.4	Polishing tool .....	24
3.2.5	Chemical reagents.....	25
3.2.6	Computer software and hardware .....	25
3.3	Model .....	27

## IV RESULTS AND DISCUSSION

4.1	Effect of frequency .....	30
4.1.1	Frequency variation with no additives.....	31
4.1.2	Effect of suppressor .....	33
4.1.3	Frequency variation with 400ppm PEG, 1ppm SPS.....	35
4.1.4	Frequency variation with 400ppm PEG, 2ppm SPS .....	36
4.1.5	Effect of SPS addition.....	39
4.1.6	Effect of reverse time.....	39
4.2	Accelerant in halide bath .....	43
4.2.1	SPS concentration variation in Bromide bath.....	43
4.2.2	MPSA concentration variation in Bromide bath.....	43
4.2.3	SPS concentration variation in Chloride bath.....	44
4.3	Current controlled experiments.....	48
4.3.1	Effect of PEG concentration .....	48
4.3.2	Effect of PEG molecular weight .....	50
4.3.3	SPS concentration variation in 400ppm PEG [6000] .....	56
4.3.4	MPSA concentration variation in 400ppm PEG [6000] .....	56
4.3.5	Cl <sup>-</sup> /Br <sup>-</sup> variation in 400ppm PEG [6000] & 5ppm SPS .....	62
4.4	Cyclic Voltammetry studies of commercial additive systems.....	67
4.4.1	Analysis of Bath I .....	67

4.4.1.1 Accelerant - Fill ratio analysis .....	75
4.4.1.2 Suppressor - Fill ratio analysis.....	77
4.4.1.3 Leveler - Fill ratio analysis .....	84
4.4.2 Analysis of Bath II.....	92
4.4.3 Analysis of Bath III – Current/Potential controlled studies.....	97
4.4.4 Comparison of via filling electrolytes .....	103
<b>V CONCLUSION AND RECOMMENDATIONS</b>	
5.1 Conclusions.....	105
5.2 Recommendations.....	106
NOMENCLATURE .....	107
LITERATURE CITED .....	109

## LIST OF TABLES

TABLE	PAGE
4.1 Characteristic diffusion times and $i/i_L$ – No additives .....	32
4.2 Characteristic diffusion times and $i/i_L$ – Suppressor addition.....	33
4.3 Characteristic diffusion times and $i/i_L$ – Accelerant addition .....	35
4.4 Diffusion times vs. $1/\text{frequency}$ .....	36
4.5 Experimental procedure for Bath III analysis –Suppressor 1ml/L .....	98
4.6 Optimum concentration of additives .....	103

## LIST OF FIGURES

FIGURE	PAGE
1.1 Basic Electrochemical cell.....	3
1.2 Schematic of a rotating disk electrode.....	7
1.3 Image of a superconformally filled via.....	10
1.4 Types of filling.....	11
3.1 PINE Electrochemical cell – AFCELL1.....	22
3.2 PINE Rotating disk electrode.....	23
3.3 Experimental setup.....	24
3.4 Sample outputs for pulse-reverse current deposition from PowerSUITE.....	26
3.5 Interplay of SPS, Cu(I) and O <sub>2</sub> near a planar surface.....	29
3.6 Contrast in current density from model – Cu(I) control.....	29
4.1 Fill ratio vs. frequency – O <sub>2</sub> purging in standard solution with no additives.....	32
4.2 Fill ratio vs. frequency – O <sub>2</sub> purging in standard solution with 400ppm PEG.....	34
4.3 Fill ratio vs. frequency – O <sub>2</sub> purging in 400ppm PEG, 1ppm SPS.....	37

4.4	Fill ratio vs. frequency – O <sub>2</sub> purging in 400ppm PEG, 2ppm SPS .....	38
4.5	Fill ratio vs. frequency- Effect of SPS addition on frequency .....	40
4.6	Fill ratio vs. reverse time - Effect of reverse time .....	41
4.7	Fill ratio vs. reverse potential - Effect of reverse potential.....	42
4.8	Fill ratio vs. SPS concentration - SPS concentration variation in Br <sup>-</sup> bath.....	45
4.9	Fill ratio vs. MPSA concentration - MPSA concentration variation in Br <sup>-</sup> bath ...	46
4.10	Fill ratio vs. SPS concentration - SPS concentration variation in Cl <sup>-</sup> bath.....	47
4.11	Potential difference vs. PEG concentration - Effect of PEG concentration .....	49
4.12	Potential vs. PEG concentration; PEG – 3400MW concentration variation .....	51
4.13	Potential vs. PEG concentration; PEG – 6000MW concentration variation .....	52
4.14	Potential vs. PEG concentration; PEG – 8000MW concentration variation .....	53
4.15	Potential vs. PEG concentration; PEG – 20000MW concentration variation .....	54
4.16	Potential difference vs. PEG concentration - Effect of PEG molecular weight ....	55
4.17	Potential vs. SPS concentration variation in 400ppm PEG [6000].....	57
4.18	Potential difference vs. SPS concentration variation in 400ppm PEG [6000] .....	58
4.19	Potential vs. MPSA concentration variation in 400ppm PEG [6000] .....	59
4.20	Potential difference vs. MPSA variation in 400ppm PEG [6000].....	60

4.21	Fill ratio vs. SPS/MPSA concentration.....	61
4.22	Potential vs. $\text{Cl}^-$ concentration variation in 400ppm PEG [6000] & 5ppm SPS....	63
4.23	Potential difference vs. $\text{Cl}^-$ concentration in 400ppm PEG [6000] & 5ppm .....	64
4.24	Potential vs. $\text{Br}^-$ concentration variation in 400ppm PEG [6000] & 5ppm SPS....	65
4.25	Potential difference vs. $\text{Br}^-$ variation in 400ppm PEG [6000] & 5ppm SPS .....	66
4.26	Current density vs. potential for 10ml/L of Accelerant in Bath I .....	69
4.27	Current density vs. potential for 10ml/L of Accelerant in Bath I-Return scan.....	70
4.28	Current density vs. potential for 15ml/L of Accelerant in Bath I .....	71
4.29	Current density vs. potential for 15ml/L of Accelerant in Bath I – Return scan ..	72
4.30	Current density vs. potential for 20ml/L of Accelerant in Bath I .....	73
4.31	Current density vs. potential for 20ml/L of Accelerant – Return scan .....	74
4.32	Fill ratio vs. measured current at 100rpm .....	76
4.33	Current density vs. potential for 5ml/L of Suppressor in Bath I .....	78
4.34	Current density vs. potential for 5ml/L of Suppressor in Bath I – Return scan.....	79
4.35	Current density vs. potential for 7ml/L of Suppressor in Bath I .....	80
4.36	Current density vs. potential for 7ml/L of Suppressor in Bath I – Return scan.....	81
4.37	Current density vs. potential for 9ml/L of Suppressor in Bath I.....	82



4.38	Fill ratio vs. current measured at 100rpm of the RDE.....	83
4.39	Current density vs. potential for 2.5ml/L of Leveler in Bath I .....	85
4.40	Current density vs. potential for 2.5ml/L of Leveler in Bath I – Return scan .....	86
4.41	Current density vs. potential for 4.5ml/L of Leveler in Bath I .....	87
4.42	Current density vs. potential for 4.5ml/L of Leveler in Bath I – Return scan.....	88
4.43	Current density vs. potential for 6.5ml/L of Leveler in Bath I .....	89
4.44	Current density vs. potential for 6.5ml/L of Leveler in Bath I – Return scan .....	90
4.45	Fill ratio vs. current measured at 100rpm of the RDE.....	91
4.46	Fill ratio vs. current measured at 100rpm – Accelerant in Bath II .....	94
4.47	Fill ratio vs. current measured at 100rpm – Suppressor in Bath II .....	95
4.48	Fill ratio vs. current measured at 100rpm – Leveler in Bath II .....	96
4.49	Fill ratio vs. suppressor concentration - Bath III .....	100
4.50	Fill ratio vs. accelerant concentration - Bath III.....	101
4.51	Fill ratio vs. leveler concentration - Bath III.....	102
4.52	Effectiveness of different additive chemistries.....	104

# ABSTRACT

## STUDY OF ADDITIVES USED IN A COPPER VIA FILLING

### CHEMISTRY

by

Sheik Ansar Usman Ibrahim

University of New Hampshire, September 2009

An experimental study on the effect of additives used in a copper via-filling chemistry is carried out by electroanalytical techniques. These include potential or current pulse reversal deposition and cyclic voltammetry methods. Suppression of electrodeposition caused by polyethylene glycol (PEG) and by a commercial suppressor was examined. Effect of bis-(3-sulfopropyl)-disulfide (SPS) and a combination with the suppressor was also examined. A model based on free accelerant complex formation was used to design the experiments. Contrast in the chemical environment between the bottom and the surface of the vias was simulated on a rotating disk electrode (RDE) by variation of rotation speeds. The currents measured at low and high speeds of RDE simulate the bottom and top of the via respectively. The fill ratio, current at low speed divided by current at high speed, was used as an effective screening tool to compare baths with different additive chemistries.

# CHAPTER 1

## INTRODUCTION

### 1.1 Overview

The development of microelectronics over the past decade has been rapid where the technology is moving towards smaller features and faster devices. An integrated circuit is packaged on a circuit board through interconnect lines. These interconnects thus serve as the route or channel through which all the communication between the chip and the circuit are made. Copper has been widely used in the semiconductor industry and is a key component in the packaging of integrated circuits. Copper has many inherent properties that make it a better choice for interconnect lines than aluminum. Copper has very good resistance to electromigration and lower electrical resistance compared to aluminum, and these properties contribute to a lower RC constant. Copper is being used extensively as an interconnect material as the need for smaller and faster electronics rises.

Interconnects are formed by filling vias and trenches defined by a lithographic mask on a silicon wafer bearing the semiconductor devices. Conventional plating baths contain a source of copper ions like copper(II)sulfate-pentahydrate, an acid like sulfuric acid to reduce the solution resistance as well as chloride ions in ppm concentrations. Plating baths also contain additives like plating-rate suppressing polyether, polyethylene

glycol (PEG) and an accelerant, which is a thiol or an organic sulfonate bearing compound like bis-(3-sulfopropyl)-disulfide (SPS). These additives in combination with chloride ions result in what is termed bottom-up filling. Conformal plating refers to uniform deposition on the walls and the bottom of the features. Conformal plating can result in the formation of seams and voids. Bottom-up or superconformal filling results when, deposition of copper into features fills them without any voids or seams. If the plating rate is lower at the via bottom than it is outside the via, the result is referred to as subconformal filling.

This work is intended to investigate chemistries for bottom up copper electrodeposition for through-silicon vias. Through-silicon vias (TSV) are large (~100 $\mu$ m) channels that extended through the IC chip. The work is also directed to understanding the effect of process parameters on filling effectiveness. Bench scale analysis was done using electroanalytical techniques that include cyclic voltammetry and potential and galvanic pulse reverse deposition.

## **1.2 Electrochemical cell**

A schematic of a three-electrode electrochemical cell is shown in the Figure 1.1. There is a working electrode (WE), a counter electrode (CE) and a reference electrode (RE). The reference electrode maintains an invariant potential and serves for observing, measuring and controlling the potential of the working electrode. The reference electrode used in this work is a saturated calomel electrode (SCE). The working electrode employed for the bench scale electrochemical analysis is a rotating disk electrode (RDE). The active

portion of the rotating disk electrode is a platinum disk. The counter electrode serves the purpose of completing the circuit.

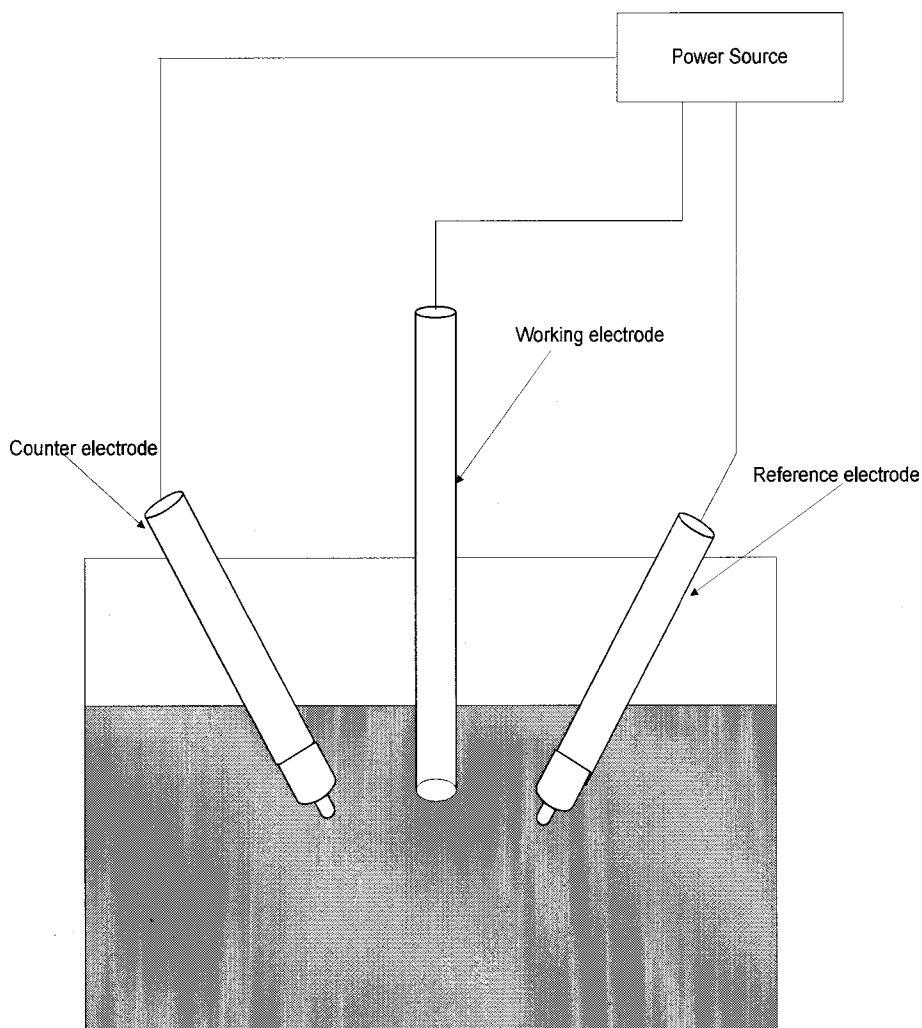


Fig 1.1 Basic electrochemical cell

### 1.3 Electrochemistry

The fundamental purpose of electroanalytical techniques is that they serve in the understanding of the current-potential behavior of the system under study. The process taking place on the working electrode when subjected to potential wave trains is

understood from the current response. These electroanalytical techniques are very useful in understanding the redox reactions taking place in an electrochemical cell. A general redox reaction can be characterized by the following equation:



O and R are the oxidized and the reduced species respectively. The forward reaction is a reduction process where O gains electrons and is reduced to R. The backward reaction is R losing electrons to form O. The rate of loss or gain of electrons is controlled by the potential of the working electrode. A plot of current vs. potential is called a voltammogram. The pattern of a voltammogram depends on the nature of the response to an applied potential and is a characteristic of the working electrode and the solution.

The rate of a reaction is governed by several factors. The reaction rate is sometimes governed by the slowest step in a sequence and that step is termed the rate-determining step (RDS). Factors that determine the rate of electrochemical reactions include transport of electroactive species to the electrode surface and electron transfer at the surface. The reactions whose rates are governed by the transport of electroactive species to the electrode are said to be mass transfer limited processes. Processes controlled by electron transfer are termed kinetically controlled.

#### **1.4 Mass Transport in electrochemical reactions**

There are three modes of material transport in electrochemical reactions: diffusion, convection and migration. Diffusion involves the transport of matter under the influence of a concentration gradient. The driving force for diffusion is concentration gradient and

it continues as long as the gradient remains. Convection occurs when there is a physical movement of the solution containing the electroactive species. Convection can either be forced or natural. Stirring or rotating or even mechanical vibrations of the solution can drive forced convection. Migration is the movement of charged ionic particles under the influence of the electric field. The flux, in  $J$  ( $\text{mol}\cdot\text{cm}^{-2}\cdot\text{s}^{-1}$ ), to the electrode surface is described mathematically by the *Nernst-Planck* equation. The *Nernst-Planck* equation in one dimension is expressed as

$$J(x, t) = -D(\partial C(x, t))/\partial x - zFDC/RT (\partial\varphi(x, t))/\partial x + C(x, t)V(x, t) \quad (2)$$

where  $D$  is the diffusion coefficient ( $\text{cm}^2/\text{s}$ ),  $F$  the Faraday constant ( $96485 \text{ C}\cdot\text{mol}^{-1}$ ),  $R$  the universal gas constant ( $8.314\text{J}\cdot\text{K}^{-1}\cdot\text{mol}^{-1}$ ) and  $T$  the absolute temperature in Kelvin (K). The above equation also contains the terms  $z$ ,  $C$  and  $V$ , which are the equivalents per mol, the concentration and the hydrodynamic velocity in the  $x$ -direction.

The current density is the sum of the fluxes of all charges species weighted by the equivalents per mole,  $i = \sum z_i J_i$ . The current density integrated over the electrode surface  $I = \int_A i \, dA$  is the cell current. The flux equation given by (2) can be complex when all the modes of transport are taking place and determining the current can be complicated as well. Migration effects are often negligible in the presence of supporting electrolyte. Thus the field term in (2) is negligible in comparison with the diffusion and convection terms in very conductive solutions.

The concentrations of the electroactive species are well defined at the beginning of an electrochemical reaction, as they normally equal the concentrations in the bulk solution. Electrochemical reactions are surface reactions and thus the concentration of the component species change at the interfacial region. When the current is applied, there is a

mass transport layer close to the interface where the concentration changes as a function of distance from the electrode surface. The thickness of this layer depends on the hydrodynamic conditions and also the concentration distribution in the solution. The concentration varies within this layer as a result of hydrodynamic conditions and also charge transfer steps occurring during the electrodeposition reaction. Beyond this layer the concentration does not vary and the solution is well mixed. Rotating disk electrodes (RDEs) are often used in understanding and interpreting electrochemical reactions as they generate reproducible and well defined hydrodynamic conditions.

The transport, adsorption and consumption of the additives used in a via filling chemistry are important to control of bottom-up filling. The additives function synergistically to cause bottom-up or superconformal filling of the vias. Electroanalytical analysis is necessary to understand the importance of transport-adsorption of additives in a via-fill process. The additives used include a suppressor that is transport limited, but adsorbs fast, and an accelerant that diffuses rapidly and adsorbs slowly displacing the suppressor, thereby gradually counteracting the effect of the suppressor.

### **1.5 Rotating disk electrode**

The construction of a rotating disk electrode is shown in Figure 1.2. There is an insulated vertical shaft that is connected to a motor, which controls the rotation speed of the disk. The rotating disk is mounted flush onto the end of the shaft. The disk rotates with an angular velocity  $\omega = 2\pi f$ , where  $f$  is the rotation speed in revolutions per second. As a result of the rotation of the disk, the solution close to the disk picks up an outward radial velocity. This draws fresh solution from the bulk to the disk surface.



The relation between the diffusion or mass transport layer thickness  $\delta$  and the rotation speed is given by;

$$\delta = [1.61D^{1/3}v^{1/6}]\omega^{-1/2} \quad (3)$$

The mass-transfer limited current density ( $i_L$ ) is determined by Levich equation,

$$i_L = 0.62nFAD^{2/3}\omega^{1/2}v^{-1/6}C \quad (4)$$

The RDE enables analytical measurements in electrochemical reactions to be highly reproducible and also easy to interpret. The convective nature also results in shorter response times.

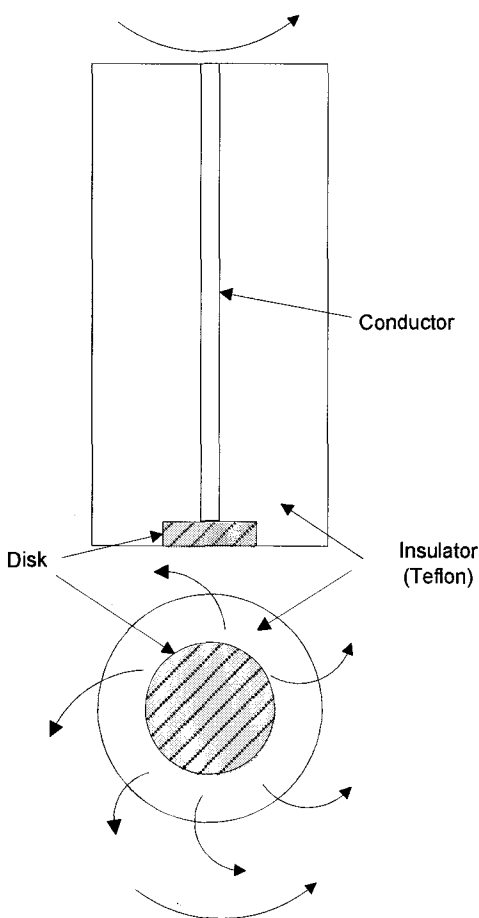


Figure 1.2 Schematic of a Rotating disk electrode

## 1.6 Electrodeposition of copper

Copper is a better interconnect material than vapor deposited aluminum. It has a very low resistivity and when compared with Al,  $\rho_{Cu} = 1.67\mu\Omega\text{cm}$  and  $\rho_{Al} = 2.67\mu\Omega\text{cm}$ . Thus the RC delay is much less with Cu interconnects. Copper has good electromigration resistance. Electromigration can be defined as the gradual movement of the metal atoms due to momentum transfer between the conducting electrons and the diffusing metal atoms. It also has a lower value of D ( $E_a$  for Lattice diffusion = 2.2eV for copper compared to  $E_a = 1.4\text{eV}$  for Al,  $E_a$  for grain boundary diffusion = 0.7-1.2eV for Cu whereas it is 0.4 -0.8eV for Al) [37].

There are physical vapor deposition (PVD) techniques such as sputtering for depositing copper. Their main drawback is that they are not efficient for high aspect-ratio trenches. Chemical vapor deposition (CVD) techniques can also be employed as they result in conformal deposition with excellent coverage in high aspect ratio vias. However, CVD is an expensive process and the deposits are rough. The cost of processing and maintenance is also very high. An effective alternative is electrodeposition. The advantages of electrodeposition are: large grain structure, good step coverage, and good filling capability and compatibility with low-k dielectrics. The grain structure is the determining factor for good electromigration properties of Cu. Copper obtained from CVD has fine grain structure and that from electrodeposition has a columnar structure and hence is more reliable [44].

Damascene plating is considered to be the best technique for the electrodeposition of copper in circuit technology. The substrate that bears a pattern of trenches and vias is made of silicon. Over this substrate is deposited a barrier layer which prevents the

diffusion of copper into the silicon. Over the barrier layer a thin copper seed layer is vapor deposited. Over this seed layer copper is electrodeposited filling the features. The excess copper, or overburden, is then removed by chemical mechanical planarization (CMP).

### **1.7 Types of filling**

The deposition of copper for interconnects requires complete filling without any voids or seams. The presence of voids and seams may result in uneven distribution of current and hence breakdown of the entire electronic circuit. To fill features requires a higher copper deposition rate at the bottom of via than on the top. Via patterns are generally identified by their aspect ratio, which is the ratio of the depth to that of the width of the via. Electrochemical deposition has proved to be the best method for filling high-aspect-ratio vias.

Deposition that occurs at a uniform rate at the walls and the bottom of via and is of equal thickness at all points of the feature is called conformal filling. A conformally filled via results in the presence of a void or seam. Pinching off at the via top, or subconformal filling, occurs when the via opening is closed off by electrodeposited copper in the center before the interlayer is filled. Subconformal filling occurs when there is a considerable decrease of cupric ions inside the feature due to mass-transport limitations. This causes higher currents at more accessible locations outside the via due to significant concentration overpotential. Superconformal filling occurs when the rate of copper electrodeposition is higher at the bottom than at the top.

Electrodeposition of copper into Through-silicon vias (TSV) depends on several parameters which include the dimensions of the via and the diffusion time of cupric ions and the additives. Takahashi and Gross [42] computed a dimensionless diffusion parameter  $\xi_d$  of cupric ions. The diffusion parameter  $\xi_d \approx \frac{L^2}{wD}$ , where L is the dimensional length, w the diameter of the via and D is the diffusivity of cupric ions. A large value of  $\xi_d$  predicts limiting mass transport and subconformal filling. A similar diffusion parameter for additive diffusion can be used to predict bottom-up filling. Deeper the vias, the more difficult it is to fill them uniformly.

Ritzdorf *et al.* [43] conducted filling tests with varying via sizes ranging from 3-80 $\mu\text{m}$  in width and 45-160 $\mu\text{m}$  in depth. With optimized deposition conditions void free filling of all the via dimensions was obtained, but it was more difficult to fill deeper vias. The wider and deeper vias required more plating time.

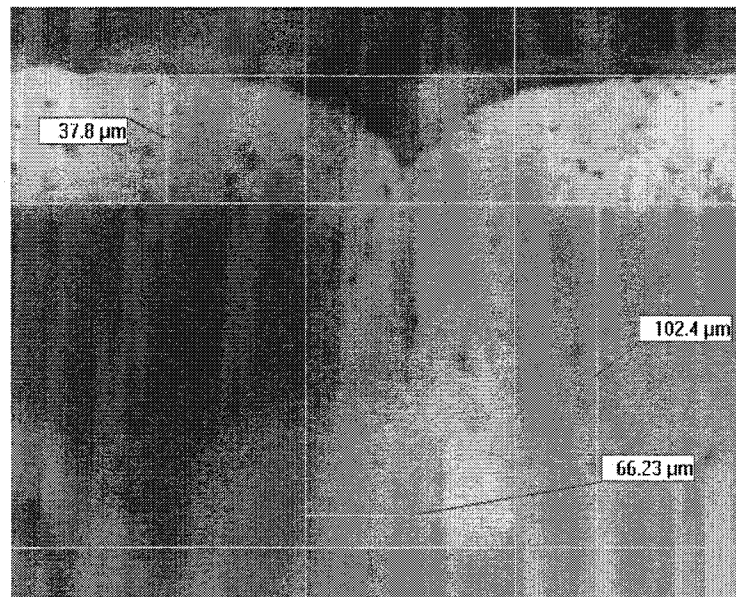


Figure 1.3 Image of a superconformally filled via

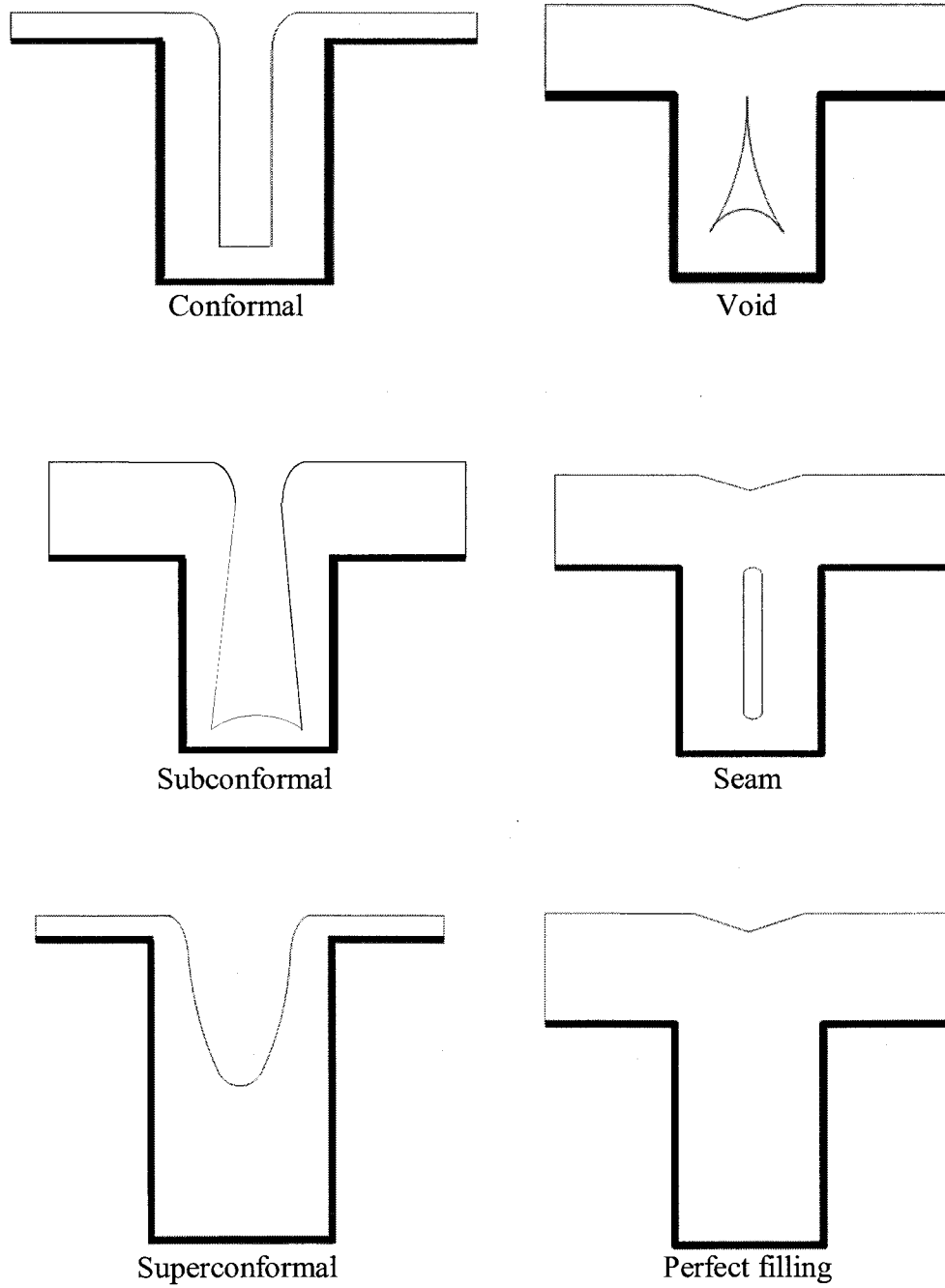


Figure 1.4 Types of filling [36]

## 1.8 Additive systems

Additives in a plating bath determine the nature of the deposit obtained. The additive system used in via plating baths also governs the current distribution in the features. For copper filling process the commonly used additives are a suppressor, an accelerator and a leveler. Control of the additive concentrations in a plating bath is important to obtain bottom-up filling. Process parameters are also important in determining the effectiveness of superfilling in conjunction with appropriate usage of the additive package.

One of the organic additives required for superfilling is the suppressor. The effect of the suppressor is to reduce the deposition rate. A commonly used suppressor is Polyethylene glycol (PEG). The suppression action is more pronounced in the presence of chloride ions [1]. PEG acts by forming an inhibiting layer on the metal surface. Cl<sup>-</sup> forms a coordinated complex with PEG, and the complex is adsorbed on to the surface [18].

The accelerant plays a pivotal role in bottom-up filling. The accelerant counters the suppressor locally and restores a normal current density at points where it reaches the surface. The accelerant most commonly used in via fillings baths is *bis*-(3-sulfopropyl) disulfide (SPS). In some cases 3-mercapto 1-propanesulfonic acid (MPSA) is also used. The true accelerant is probably copper(I)thiolate, formed by reaction with SPS or MPSA. Many authors claim that bottom up filling occurs due to the accumulation of accelerant species at the base of the via by a curvature enhanced accelerant coverage mechanism (CEAC) [25]. However, the model is applicable only to very small features ~ 1 μm.

The leveler is an important additive if filling of the vias is to take place with better finish and lesser overburden. Leveling agents are added to reduce the required grinding and polishing after plating. The leveler is added to promote deposition in recesses and inhibit plating at protrusions. The leveler also acts like an inhibitor and the reaction of the leveler at the cathode is mass transfer controlled. The peaks are areas which are more accessible and there the leveler forms an inhibiting layer, thereby promoting more copper electrodeposition in the recesses [4] [5] [6].

The approach used here to model bottom-up via filling is to exploit the contrast in the reaction-diffusion mechanism at the surface and the bottom of the via. Addition of precursors to the via filling chemistry generates an accelerant which subsequently gets consumed and is responsible for increasing the plating rate. The accelerant generation occurs in a dynamic system. There are several key parameters that control the distribution of the accelerant in the via feature. With pulse-reverse electrodeposition and oxygen bubbling, control of the distribution of accelerant is possible. An immediate objective of this study is to devise a bench-scale screening process that is able to predict the actual filling performance of a given bath and process in wafer plating. This screening would help reduce the reliance on pilot-scale tests for determining the efficiency of a filling chemistry.

## CHAPTER 2

### LITERATURE REVIEW

#### **2.1 Copper plating bath**

Most copper plating baths contain one or more organic additives. Copper plating is done for several end applications, but the area of interest here is that of TSV filling. Typical plating baths for this purpose are made of acidic copper sulfate solutions and small quantities of chloride. They also contain a three component additive system made up of suppressor, an accelerant and a leveler [7], or a two component systems consisting of suppressor and accelerant alone [8]. Typical additives include an organic polyether like polyethylene glycol (PEG) as the suppressor, a sulfur-containing molecule like *bis*-(3-sulfopropyl) disulfide (SPS) as the accelerant and a nitrogen containing molecule like thiourea as leveler. Similar baths containing the same additives have also been employed as industrial baths for fabrication of on-chip copper interconnects [9], [10], and [11].

#### **2.2 Effect of Polyethylene glycol**

Moffat *et al.* [10] showed that a 3 additive system can be used for superfilling of Cu interconnects features. Polyethylene glycol (PEG) is an organic polyether with the



structure  $[(\text{CH}_2\text{-O-CH}_2)_n]$ . Several investigations have shown that PEG alone does not account for the suppression of electrodeposition [8, 14]. Suppression by PEG is believed to be due to its adsorption on the copper surface, where it hinders charge transfer reactions [14]. For PEG to be adsorbed on the copper surface and act as a suppressor, chloride is required as it acts as a bridging ligand between the PEG molecule and the metal [14]. Under certain conditions successful filling has been demonstrated in the presence of PEG and  $\text{Cl}^-$  alone [15].  $\text{Cu}^{2+}$  reduction can be significantly suppressed in the presence PEG and  $\text{Cl}^-$  but the degree of suppression is reduced when PEG alone is present [14, 18]. In the absence of  $\text{Cl}^-$ , little or no PEG adsorbs onto the electrode surface [17, 18].

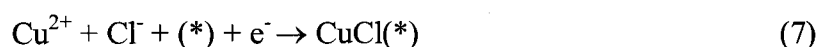
Feng *et al.* [18] suggest the presence of a PEG-Cu-Cl complex on the Cu surface based on surface enhanced Raman Spectroscopy measurements. Doblhofer *et al.* [19] reported, however, that PEG-Cl film formation does not require  $\text{Cu}^{2+}$  or  $\text{Cu}^+$  to be present in the electrolyte. Walker *et al.* [20] also reported similar results. Yokoi *et al.* [14] suggested that PEG formed a coordinated complex with  $\text{Cu}^+$ . The formation of  $\text{Cu}^+(\text{-EO-})_3\cdot\text{H}_2\text{O}$  and  $\text{Cu}^{2+}(\text{-EO-})_4\cdot 2\text{H}_2\text{O}$ - type complexes tend to increase the overpotential in the presence of chloride ions. Reactions in the presence of PEG and  $\text{Cl}^-$  were tabulated by Chen *et al.* [28]. They studied the individual roles of the interaction of PEG and  $\text{Cl}^-$  in a Cu electrodeposition bath from an acidic sulfate solution using Linear Scan Voltammetry (LSV) and Impedance Spectroscopy and concluded that  $\text{Cl}^-$  alone increases the current density of the deposition reaction and PEG alone decreases the current density. In the

presence of both PEG and  $\text{Cl}^-$ , deposition is suppressed due to adsorption of PEG-CuCl and PEG-Cu<sup>+</sup> on the electrode surface.

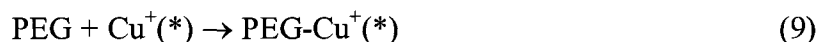
Copper reduction



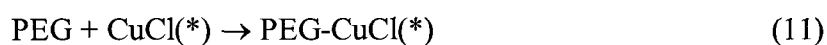
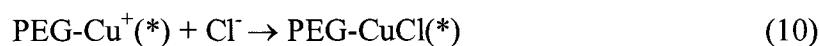
Reaction between cupric and chloride ions



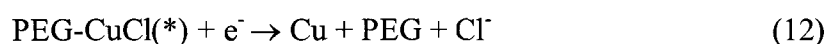
PEG surface adsorption



Surface adsorbed PEG-CuCl complex



Final reduction

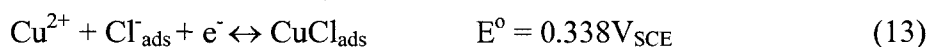


Several important factors contribute to suppression of  $\text{Cu}^{2+}$  reduction. PEG molecular weight, concentration and the electrode potential are important parameters. As PEG concentration increases at fixed concentration of  $\text{Cl}^-$ , suppression increases until a limit is reached. A similar increase in the inhibition capacity is observed when  $\text{Cl}^-$  concentration is increased at a constant PEG concentration. The limiting condition is attributed to the PEG molecules saturating at the electrode surface. The suppression effect of PEG has been observed to be a function of degree of polymerization [14, 16, and

21]. PEG also suppresses the deposition reaction at a lower potential range close to open-circuit potential (OCP). There is a critical potential (-0.550 and -0.650 V MSE) at which the electrode is reactivated and this was observed in the form of hysteresis in voltammograms [14, 17, 38]. Healy *et al.* [16] concluded from Surface Enhanced Raman Spectroscopy that near the OCP, a PEG-Cu<sup>+</sup>-Cl<sup>-</sup> complex was formed and neutral PEG formation occurred at around copper deposition potentials. Pritzker and Garrido studied the formation and disruption of the inhibiting film in the presence of Cl<sup>-</sup> through voltammetry and through multistep chronoamperometry-voltammetry experiments. They attributed the hysteresis during the cathodic scans to the slow restoration of the inhibiting film formed on the electrode surface. Their work also underscored the importance of Cl<sup>-</sup> in regulating the effectiveness of PEG as suppressor.

### 2.3 Effect of chloride

Chloride ions have been reported to have a catalytic action on the copper reduction process and also to influence the orientation, structure and the dynamics of the surface reactions [12, 16]. Studies by Saores *et al.* [12] have shown that presence of Cl<sup>-</sup> ions in a plating bath accelerates the reduction of copper through the formation of a CuCl monolayer. The reaction for CuCl formation from [12]:



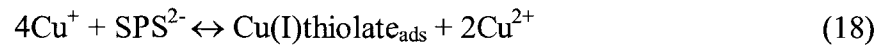
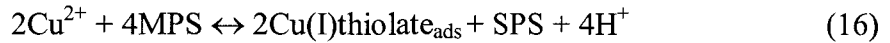
A study of the influence of chloride ions was carried out using cyclic voltammetry and impedance studies by Shao *et al.* [13]. They concluded that variations in the chloride

concentrations can affect the copper reduction reaction causing two competing effects at low and high concentrations of Cl<sup>-</sup> anions.

#### 2.4 Effect of SPS and MPSA

SPS, *bis*-(3-sodiumsulfopropyl) disulfide (Na<sup>+</sup>O<sup>-</sup><sub>3</sub>S(CH<sub>2</sub>)<sub>3</sub>SH)<sub>2</sub>) is often used the accelerator in via filling chemistries [22, 23, 24, 25]. The acceleration effect of Cu electroplating is related to SPS adsorption on the Cu surface in the presence of PEG [26]. SPS by itself is a mild inhibitor. In a via filling chemistry, PEG initially absorbs on the metal surface and slows down the plating rate. SPS then displaces this PEG layer, creating active surface sites for more Cu<sup>2+</sup> reduction. Thus the current density increases as a function of SPS concentration only in the presence of a suppressor.

Reid *et al.* [26] reported the following reactions:



Moffat *et al.* [27] proposed a kinetic model of Cu reduction in the presence of the SPS-PEG-Cl<sup>-</sup> system. From CVS, PD polarization and Electrochemical Impedance

Spectroscopy (EIS) plots. Hung *et al.* [28] concluded that the acceleration effect has a strong correlation to the concentration of SPS. They found that the addition of a small amount of SPS has an inhibiting effect on Cu electrodeposition due to increase in charge transfer resistance. Most studies on MPSA have been focused on verifying its catalytic effects [29, 30]. MPSA is not stable in the electrolyte and undergoes aging by reaction with  $\text{Cu}^{2+}$  ions to form SPS. Kim *et al.* [29] demonstrated the oxidative dimerization of MPSA to SPS by  $\text{Cu}^{2+}$  ions. Similar observations were made by Moffat *et al.* [27] from curves of slow sweep voltammetry between an overnight-aged MPSA electrolyte and SPS electrolyte indicating the oxidation of thiol to form disulfide. Even though MPSA results in filling of vias, it may actually be the reaction product of MPSA with  $\text{Cu}^{2+}$  that produces acceleration. Soo and J. J. Kim [31] studied the dependence of the aging time of the accelerator in superfilling of Cu. They concluded that MPSA was ineffective in the superconformal electrodeposition of Cu and attributed this to the fact that MPSA resulted in  $\text{Cu}^{2+}$  reduction at the trench entrance. A 12h aging time of a MPSA solution was required for achieving superfilling.

## **2.5 Mechanisms of via filling**

Earlier plating models developed by Dukovic *et al.* [32] and West [33] assumed that adsorption of the additives is controlled by diffusive mass-transport while the copper deposition reaction is controlled by interfacial kinetics. With the correct additive concentrations, a higher deposition rate of Cu at the bottom of the via could be achieved. However, these models do not account for the presence of the accelerant. They predict the growth rate variation along the feature caused by diffusion and consumption of the

suppressor alone. Moffat *et al.* [34] evaluated the influence of 3 additives, PEG, MPSA and Cl<sup>-</sup>. They concluded that a synergistic interaction between three species is required for defect-free filling of small vias. Cao *et al.* [35] proposed a model which accounts for the interaction of the suppressor and the accelerant. Studies by Moffat, Josell, and Reid [34, 24, and 26] assume that superfilling is due to local accumulation of accelerant at the bottom of the feature, due to the reduction in the surface area during deposition. This model is applicable to very small vias ( $\sim 1\mu\text{m}$  filled in less than 1 minute). West *et al.* [9] assumes that surface site density varies with deposition rate, while Moffat and Josell *et al.* [34, 24] assume that variation of the accelerator surface concentration depends on local surface curvature, as well as on an empirical form for current density variation with accelerator concentration. The TSV filling of interest in this study pertains to larger dimension high aspect-ratio vias that takes around 3 hours to fill.

## CHAPTER 3

### EXPERIMENTAL

#### **3.1 Introduction**

Experiments were performed to study the effect of additive interaction in the copper via filling chemistry and optimize the concentrations of these additives using electrochemical techniques. These experiments were carried out using a rotating disk electrode (RDE). The RDE has been used extensively to study electrochemical reactions. It creates hydrodynamic conditions for precise control of mass transport.

#### **3.2 Experimental apparatus and instrumentation**

##### **3.2.1 Experimental cell**

A multi-necked cell was used as a standard for running the electrochemical reactions. A 5-neck AFCELL1/AFCELL2 125ml glass cell (PINE) was used. Such a setup is very useful when carrying out experiments with a rotating electrode as the working electrode. In the 5 neck cell, the central neck has a configuration (24/40) for the glass joint and the

rest of the necks are of (14/20) dimensions. The larger central neck allows the RDE to enter the cell. The other openings are available for the reference electrode, counter electrode, gas purging and thermometry. The cell has also the advantage of holding the counter electrode and the reference electrode in place in the cell, at distance very close to the working electrode, in order to eliminate the uncompensated solution resistance between the working electrode and the reference electrode. The electrodes were inserted into the 14/20 necks of AFCELL using an Isolation tube AFUBE with a frit.



Figure 3.1 PINE Electrochemical cell - AFCELL1

### 3.2.2 Electrodes

The reference electrode was a single junction Saturated Calomel Electrode (SCE)-AFREF1. Potassium chloride (4M) was used as the filling solution for the reference electrode. All the potentials in the experimental findings and conclusions are reported with respect to SCE. The counter electrode used was a thin foil of copper.



A platinum PINE rotating disk electrode was used as the working electrode. The RDE shaft was connected to the modulated speed rotator (PINE Model - AF MSR<sub>X</sub>), to control the rotation speed of the RDE. The electrodes are connected to the rotator through 2 pairs of carbon-silver brush contacts.

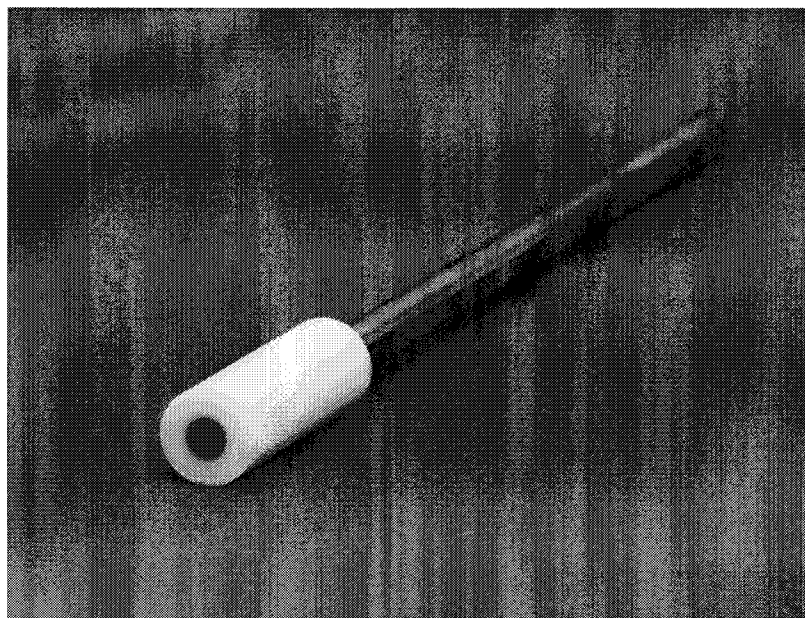


Figure 3.2 PINE Rotating disk electrode

### 3.2.3 Potentiostat

The study of most electrochemical reactions requires a potentiostat for either measuring or controlling the potential at the working electrode - electrolyte interface. The potentiostat used here was a Princeton Applied Research - Ametek<sup>®</sup> (PARSTAT<sup>®</sup> 2273). The complete experimental setup is shown in the Figure 3.3.

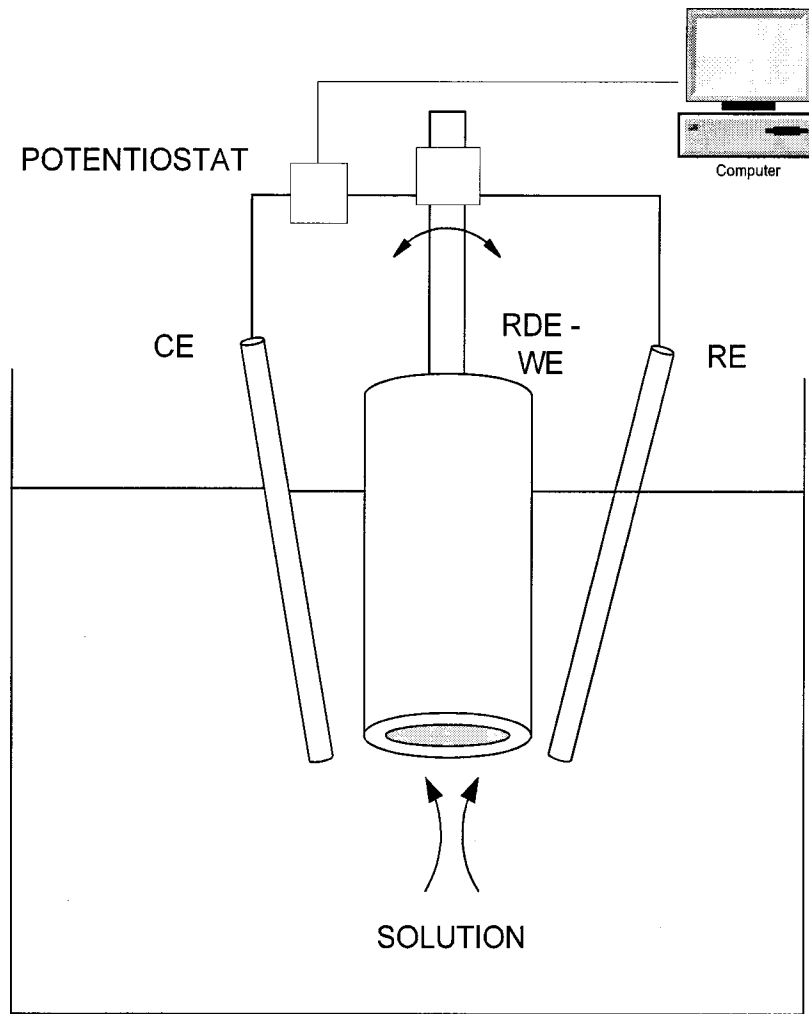


Figure 3.3 Experimental setup

CE – Counter electrode, WE – Working electrode, RE – Reference electrode

### 3.2.4 Polishing tool

The wafer segments that were electrodeposited with copper are broken into smaller segments for analysis of the nature and type of via filling. The polishing of the segment cross-section is important for getting a better resolution of the image under analysis. The

polishing was done on a Struers<sup>®</sup> mechanical polishing tool – Rotopol 11<sup>®</sup>. SiC 1000 and 800 grit papers were used for grinding. Final polishing was done with PPEO solution – oil and water based polishing solution.

### **3.2.5 Chemical reagents**

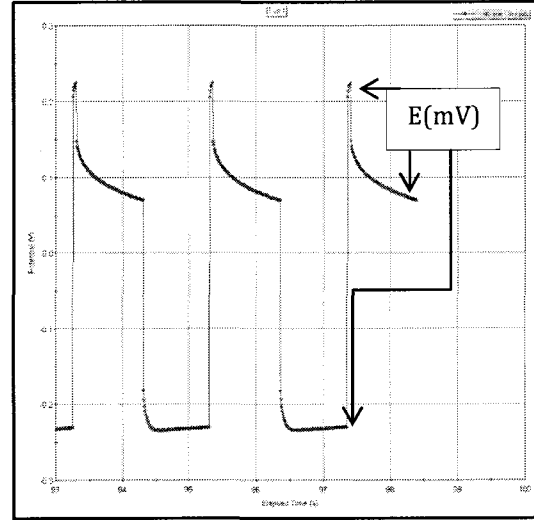
The base copper sulfate solution was prepared using hydrated cupric sulfate crystals of molecular weight 249.68 (J. T. Baker, Acros Organic, and Sigma Aldrich). The additives used in the bath include SPS, PEG and chloride and concentrated sulfuric acid. Polyethylene glycol of several molecular weights was used: PEG 3400 (Aldrich), PEG 6000 (EMD), PEG 8000 (J. T. Baker) and PEG 20000 (J. T. Baker). The source of chloride ions in solution was sodium chloride crystals of molecular weight 58.44 (J. T. Baker). Concentrated sulfuric acid (J. T. Baker, 96.6 %) and concentrated nitric acid (VWR) was used. Ultrapure water (Millipore<sup>®</sup> Q ultrafilter) was used to make up all the solutions.

### **3.2.6 Computer software and hardware**

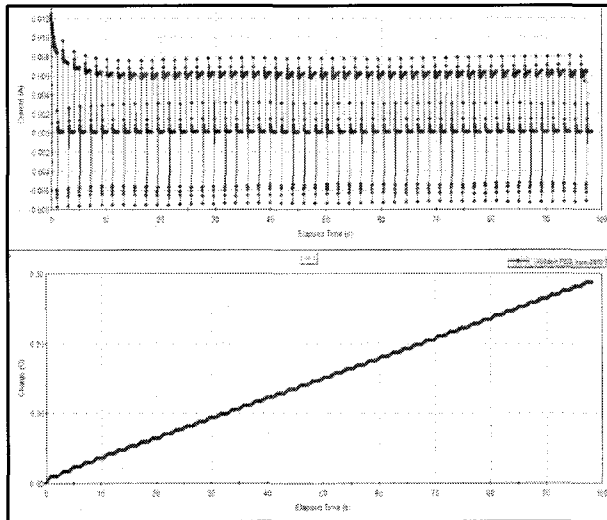
All the electrochemical analysis of the plating baths were done using the software, PowerSUITE<sup>®</sup>, an electrochemical software which allows data analysis for cyclic voltammetry, chronoamperometry and chronopotentiometry. PowerSUITE<sup>®</sup> comprises of several modules and the ones that were used include PowerPULSE, PowerCV, PowerCORR, PowerSINE and PowerSTEP. All the experiments are performed by applying the desired set of waveforms from the PC to the cell through the potentiostat. The user end is the PC and the software (PowerSUITE) allows different waveforms to be applied.



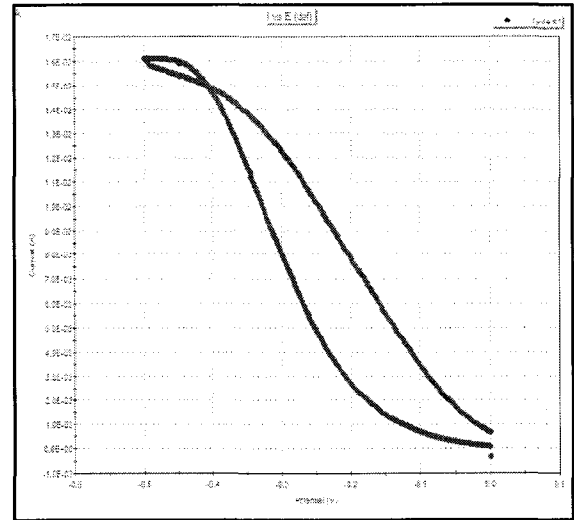
(a) Sample Potential vs. time output



(b) Potentials measured at the end of the cycle



(c) Complete current vs. time cycle



(d) Sample CV

Figure 3.4 Sample outputs for pulse-reverse-current deposition from PowerSUITE

### 3.3 Model

Several models for bottom-up filling of vias have been proposed. The bottom up filling process takes place in the as a result of competitive adsorption-desorption phenomena taking place in the bottom of the via. The objective is to produce more rapid copper deposition on the bottom of the via than on the surface of the via.

The source of  $\text{Cu}^{2+}$  ions is the copper sulfate solution. On applying a negative potential to the working electrode,  $\text{Cu}^{2+}$  gains 2 electrons to give Cu metal. The copper reduction is a 2-step process. Reactions (23) and (24) both are single electron transfer steps. In these reactions, (23) is the slower and rate determining step.



Bottom-up filling is a result of the additive interactions and is important to understand their interplay in the plating bath. Additives that can be used to produce bottom up filling include SPS, PEG and  $\text{Cl}^-$ . PEG molecules along with  $\text{Cl}^-$  produce an inhibiting layer. The accelerator reverses the suppressing effect of PEG and restores a high rate of deposition. SPS probably acts an accelerating agent when it reacts with Cu(I). So to produce filling, the concentration of Cu(I) should be higher at the bottom than at top of the via.

The distribution of current within a via is simulated by using a rotating disk electrode. The rotating disk is rotated at low and high speeds to simulate the bottom and surface of the via respectively. Cu(I), Cu(II) and  $\text{O}_2$  are considered to be very important

for successful engineering of bottom-up filling. In the bulk of the solution the  $O_2$  concentration is saturated and any Cu(I) present is oxidized to Cu(II). Hence, at the wafer surface, the Cu(I) concentration is suppressed. Inside the via, there exists a higher concentration of Cu(I).

A planar RDE subjected to forward and reverse pulses, the forward pulse causes the reduction reaction to proceed. The reverse pulse generates Cu(I). The concentration of Cu(I) reaches a maximum and falls again during the OFF time. During the off time the  $O_2$  tends to consume the Cu(I). The RDE is subjected to 2 speeds of high and low rpm. During the higher speed of rotation of the RDE, the consumption rate of Cu(I) is higher compared to the slow speed of rotation of the RDE. Thus the stronger agitation simulates conditions outside the via i.e. on the surface of the via and the low speeds of the RDE, the bottom of the via. The currents are measured at high and low speeds of the RDE are used to compute the Fill ratio which is defined as the ratio of the current measured at low speed of the RDE (via bottom) to that measured at high speed of the RDE (via surface). Chemistries with Fill ratio  $> 1$  would result in bottom-up filling. The higher the value of Fill ratio, the greater is the chance that the via-filling chemistry would result in bottom-up filling.

$$\text{Fill ratio} = \frac{\text{Current measured at low speed of the RDE (via bottom)}}{\text{Current measured at high speed of the RDE (via surface)}}$$

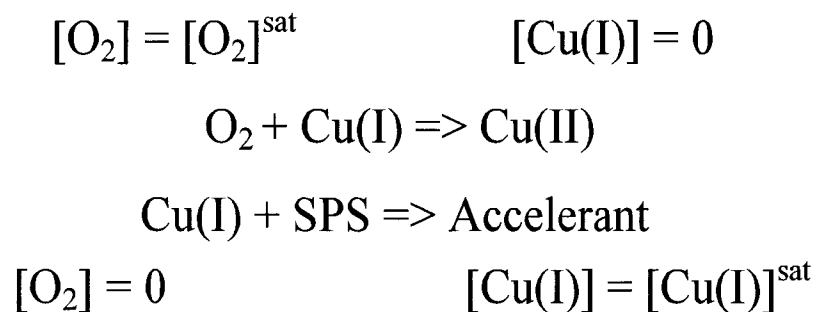


Figure 3.5 Interplay of SPS, Cu(I) and O<sub>2</sub> near a planar surface

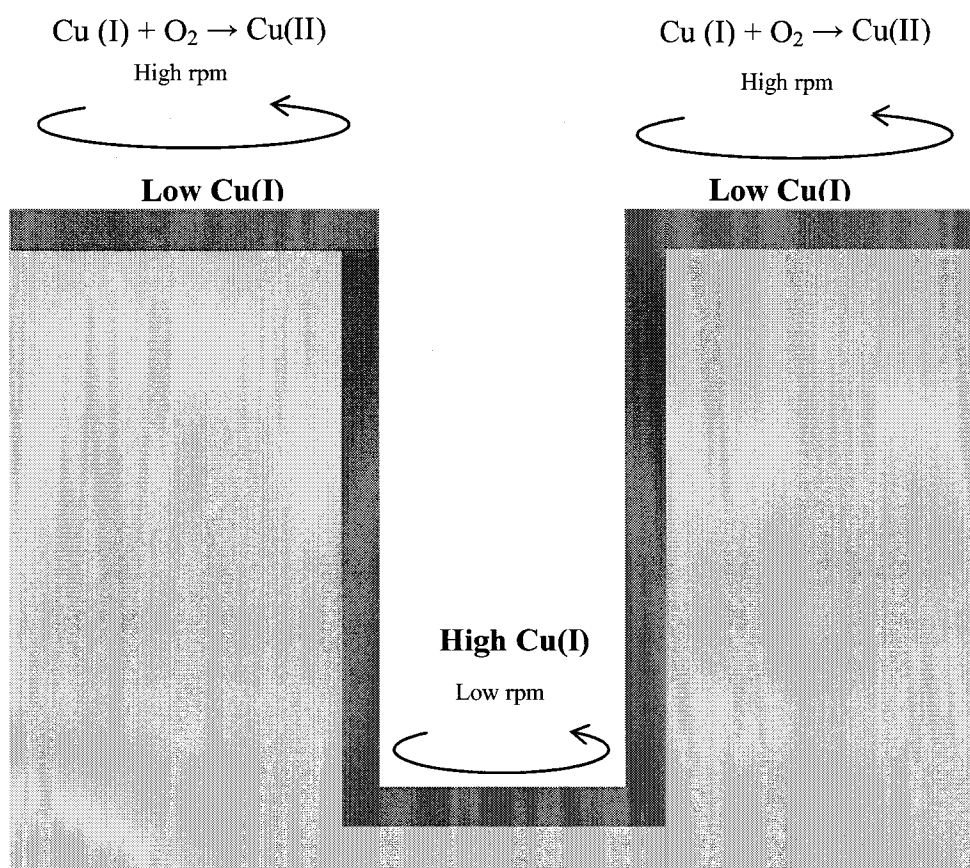


Figure 3.6 Contrast in current density from model – Cu(I) control

## CHAPTER 4

### RESULTS AND DISCUSSION

#### 4.1 Effect of frequency

PEG-SPS-Cl<sup>-</sup> as well as a commercial suppressor-accelerant combination in a standard solution (0.6M CuSO<sub>4</sub>, 1.8M H<sub>2</sub>SO<sub>4</sub> and 50ppm Cl<sup>-</sup>) was used to study the effect of frequency in pulse-reverse plating for bottom-up filling. The frequency of a plating cycle is measured in Hertz (Hz). A Potential-Pulse reverse (PPR) experiment was carried out with continuous O<sub>2</sub> purge. The ON time was varied as multiples of 2x100ms, reverse (REV) time as multiples of 2x10ms and the OFF time as multiples of 2x100ms. A potential pulse amplitude of (-300/150/0mV) ON/REV/OFF potential was applied. The currents were measured at RDE speeds of 36, 110 and 1800rpm. The Pt disk surface of the RDE was stripped after each run by immersion in HNO<sub>3</sub> and ultrapure water in the ratio 3:1 followed by rinsing. The ratio of the currents measured at lower speed of rotation to that at higher speed, the Fill ratio, was calculated at the end of each run.



#### 4.1.1 Frequency variation with no additives

The standard solution with no additives was analyzed first. Figure 4.1 shows a plot of Fill ratio vs. frequency. The fill ratios of both ( $I_{36}/I_{1800}$ ) and ( $I_{110}/I_{1800}$ ) were below unity. This shows that chemistry with no additives will not produce bottom-up filling. Increasing the frequency does increase the fill ratio, but higher frequencies in such chemistry would still result in sub-conformal plating because the ratio is very much less than unity. This implies higher currents and correspondingly thicker copper deposits on the surface of the via than on the bottom of the via.

Mass transfer of  $\text{Cu}^{2+}$  is important in successfully modeling the bottom-up via filling mechanism. In the absence of additives in copper plating solution there is a tertiary current distribution in the system, meaning that the current distribution is controlled by mass transfer. The mass transfer limiting current density on the RDE,  $i_L$ , was calculated with Levich's equation and the ratio of the  $i/i_{L,\text{rpm}}$  was computed. A value of one indicates complete control by mass transfer. A value less than 0.3 indicate that mass transfer is not controlling. The boundary layer thickness ( $\delta$ ) was also determined at different RDE speeds. The via surface simulated by high RDE speeds and the via bottom by low RDE speeds were used to calculate the characteristic diffusion time  $\tau$ , where  $\tau_s$  corresponds to diffusion time to the surface and  $\tau_v$  to the via bottom. The calculated values for 100/10/100ms wave-train are tabulated below in Table 4.1.

Table 4.1 : Characteristic diffusion times and  $i/i_L$  – No additives

RDE speed	$i_L$ (mA)	$(i/i_{L,rpm})$	$\delta$ (cm)	$\tau_s$ (s)	1/frequency(s)
36	139.8777	0.0599	0.0068	0.0465	0.205
110	244.5082	0.0392	0.0039	$\tau_s$ (s)	
1800	989.0845	0.0120	0.0010	2.30259	

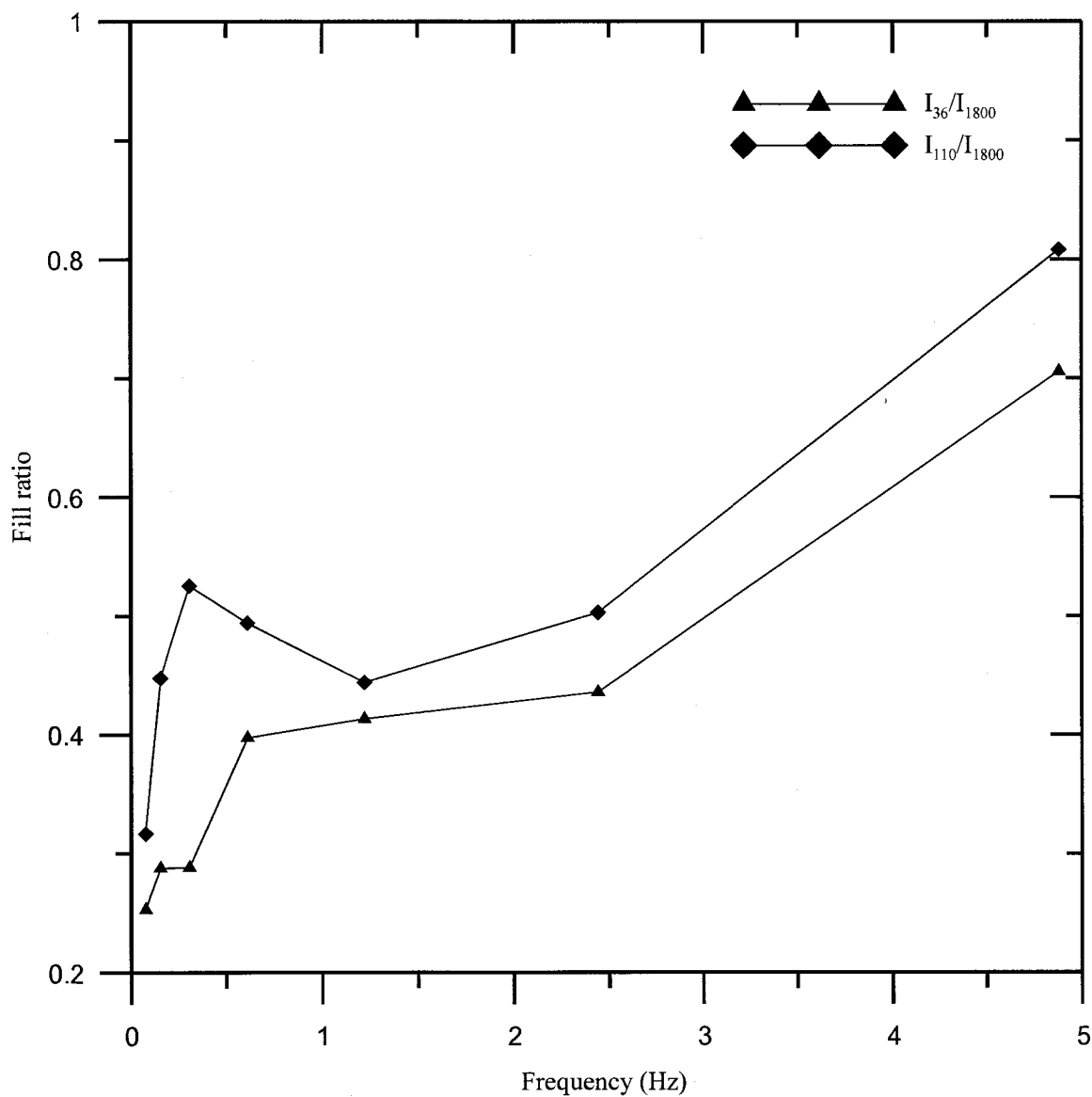


Figure 4.1 Fill ratio vs. frequency -  $O_2$  purging in standard solution with no additives.

#### 4.1.2 Effect of suppressor

The standard solution was then analyzed for the effect of suppressor alone without any accelerant. A pulse-reverse deposition experiment was carried out. A fill ratio analysis was done with the measured currents at RDE speeds of 36, 110 and 1800 rpm. A plot of the calculated Fill ratio vs. the frequency is shown in Figure 4.2. The trends of both Fill ratios,  $(I_{36}/I_{1800})$  and  $(I_{110}/I_{1800})$ , show a higher filling ability at low frequency which falls with increasing frequency and then rises again at higher frequencies.

The suppressor initially acts to slow down the plating rate on the disk. In the presence of suppressor alone, the kinetic resistance is large and mass transfer is no longer controlling. Hence there is a secondary current distribution due to slow electrode kinetics. Although there is an increase and decrease in fill ratio with increasing frequency, it still remains under unity, and hence presence of PEG alone would not produce bottom-up filling. The boundary layer thickness and  $\tau$  are determined. The ratio  $i/i_{L, rpm}$  was calculated for different frequencies at different RDE speeds. The values for 100/10/100ms wave-train in the presence of PEG alone is tabulated in Table 4.2.

Table 4.2 : Characteristic diffusion time and  $i/i_L$  – Suppressor addition

RDE speed	$i_L$ (mA)	$(i/i_{L, rpm})$	$\delta$ (cm)	$\tau_s$ (s)	1/frequency(s)
36	139.8777	0.0663	0.0068	0.0465	0.205
110	244.5082	0.0349	0.0039	$\tau_v$ (s)	
1800	989.0845	0.0104	0.0010	2.30259	

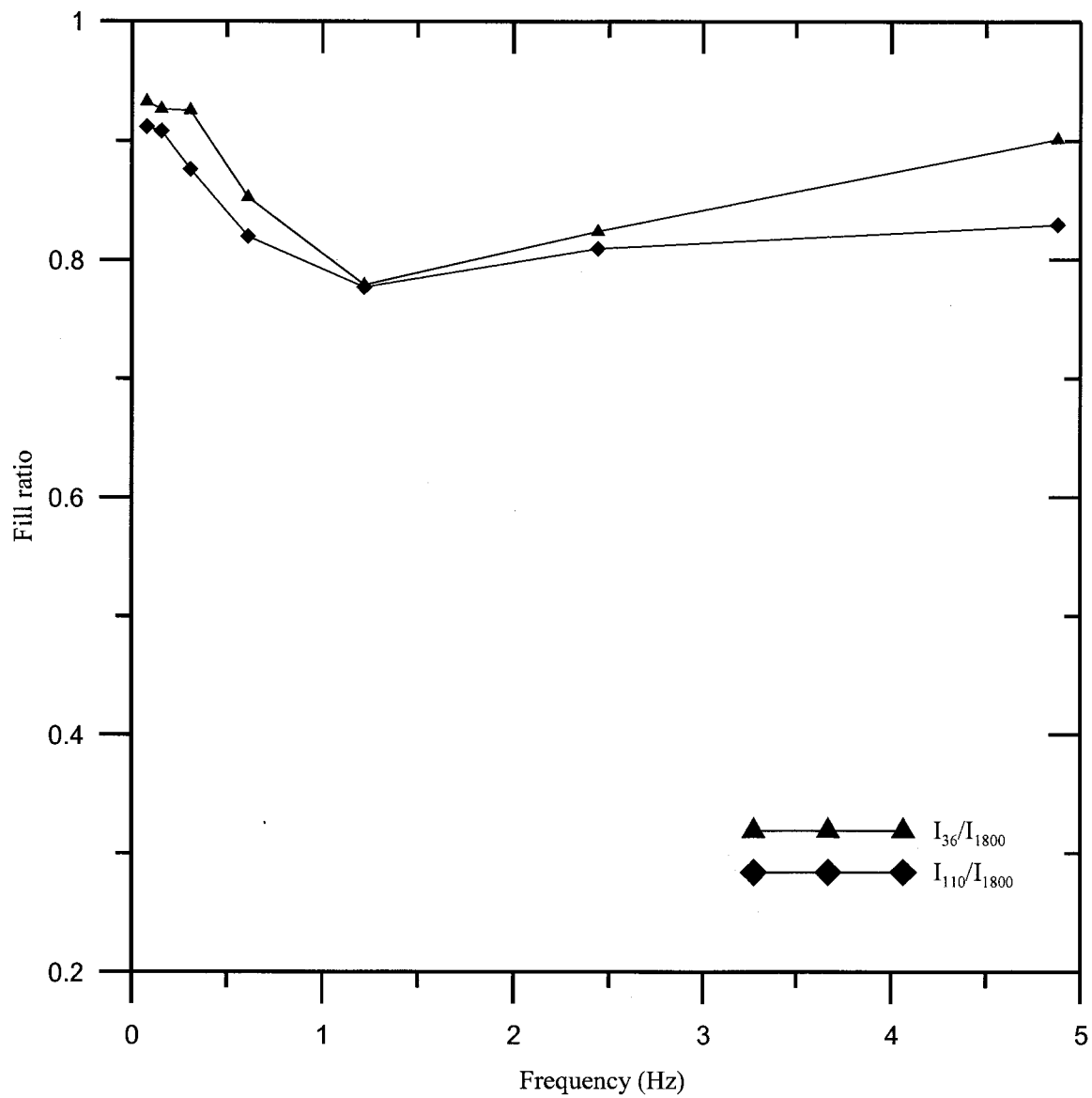


Figure 4.2 Fill ratio vs. frequency - O<sub>2</sub> purging in standard solution with 400ppm PEG

### 4.1.3 Frequency variation with 400ppm PEG, 1ppm SPS

The effect of adding the accelerant SPS to the standard solution containing PEG and  $\text{Cl}^-$  was investigated with a fill ratio analysis. The solution contained 400ppm of PEG and 1ppm SPS. A pulse-reverse wave train with varying frequencies was applied. Currents at RDE speeds of 36, 110 and 1800 rpm were measured. From the measured currents, the fill ratio was calculated and a plot of Fill ratio vs. the frequency was constructed. The plot of Fill ratio vs. frequency for 1ppm SPS in standard solution with  $\text{O}_2$  purging is shown in the Figure 4.3.

The plot in Figure 4.3 shows ratios ( $I_{36}/I_{1800}$ ) and ( $I_{110}/I_{1800}$ ) much greater than one. This validates the requirement of the presence of both PEG and SPS in a  $\text{Cl}^-$  containing acidic sulfate bath. Frequency  $< 1\text{Hz}$  has a strong effect on the reactive/mass transfer mechanism in the production and consumption of the free accelerant. Further increase in frequency does not affect the fill ratio. The Levich equation was used to calculate the limiting current density for different RDE speeds. The boundary layer thickness was calculated from  $\delta = [1.61D^{1/3}\nu^{1/6}]\omega^{-1/2}$ , where  $D$  is the diffusion coefficient,  $\nu$  the kinematic viscosity and  $\omega$  is the angular velocity. The characteristic diffusion time  $\tau$  is defined as ratio of  $\delta^2/4D$ , i.e.  $\tau = \delta^2/4D$ . The time required for the ions to diffuse to the surface and bottom of the via are calculated at high and low speeds of the RDE.

Table 4.3 : Characteristic diffusion time and  $i/i_L$  – Accelerant addition

RDE speed	$i_L$ (mA)	$(i/i_{L, \text{rpm}})$	$\delta$ (cm)	$\tau_s$ (s)	1/frequency (s)
36	139.8776	0.2594	0.0068	0.0465	0.205
110	244.5082	0.1521	0.0039	$\tau_v$ (s)	
1800	989.0845	0.0299	0.0010	2.30259	

For different frequencies, characteristic diffusion times to the surface and the bottom of the via are calculated. From these measurements, values of 1/frequency between  $\tau_v$  and  $\tau_s$  would be best for via filling (Table 4.4). From this table, cycle 800/40/800ms would result in best filling results as 1/Frequency = 1.64s and lies in between  $\tau_s$  and  $\tau_v$ .

Table 4.4 Diffusion times vs. 1/frequency

Wave train ON/REV/OFF (ms)	1/Frequency (s)	$\tau_s$ (s)	$\tau_v$ (s)
100/5/100	0.205	0.046052	2.302597
200/10/200	0.41		
400/20/400	0.82		
800/40/800	1.64		
1600/80/1600	3.28		
3200/160/3200	6.56		
6400/320/6400	13.12		

#### 4.1.4 Frequency variation with 400ppm PEG, 2ppm SPS

The effect of varying the pulse wave trains with 2ppm of SPS added to the standard solution containing 400ppm of PEG was analyzed. A PPR with varying wave-train times was carried out and the currents were measured at RDE speeds of 36, 110 and 1800rpm.

The plot in the Figure 4.4 of Fill ratio vs. frequency shows the fill ratio is higher at lower frequency and tends to decrease as the frequency is increased. The fill ratios obtained in the presence of 2ppm SPS are higher than that obtained in a bath containing 1ppm SPS (§4.1.3). Higher concentrations of SPS have better filling capability. The presence of SPS in a plating chemistry is necessary and its concentration is to be optimized in for best bottom-up filling results.

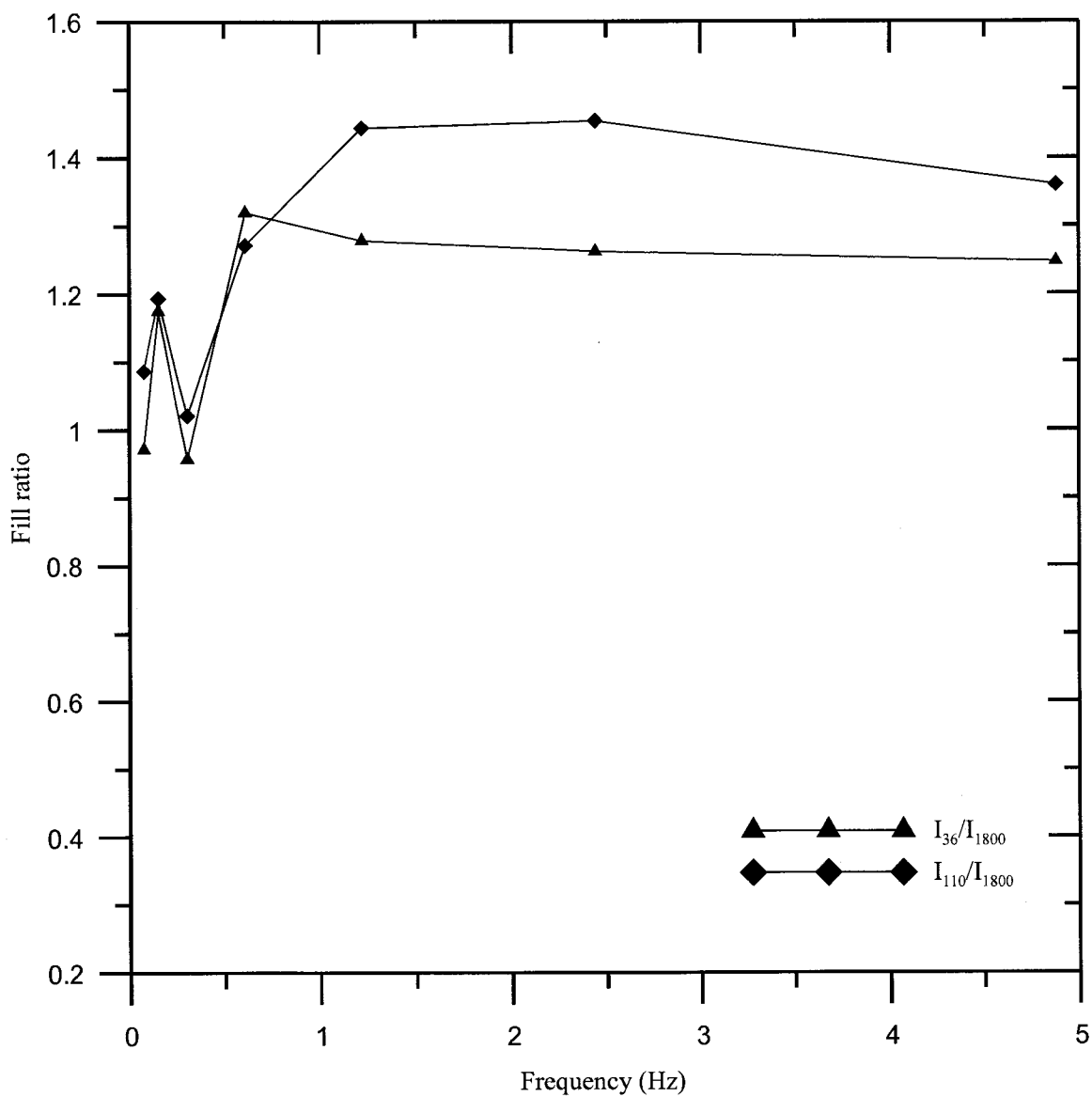


Figure 4.3 Fill ratio vs. frequency - O<sub>2</sub> purging in 400ppm PEG, 1ppm SPS

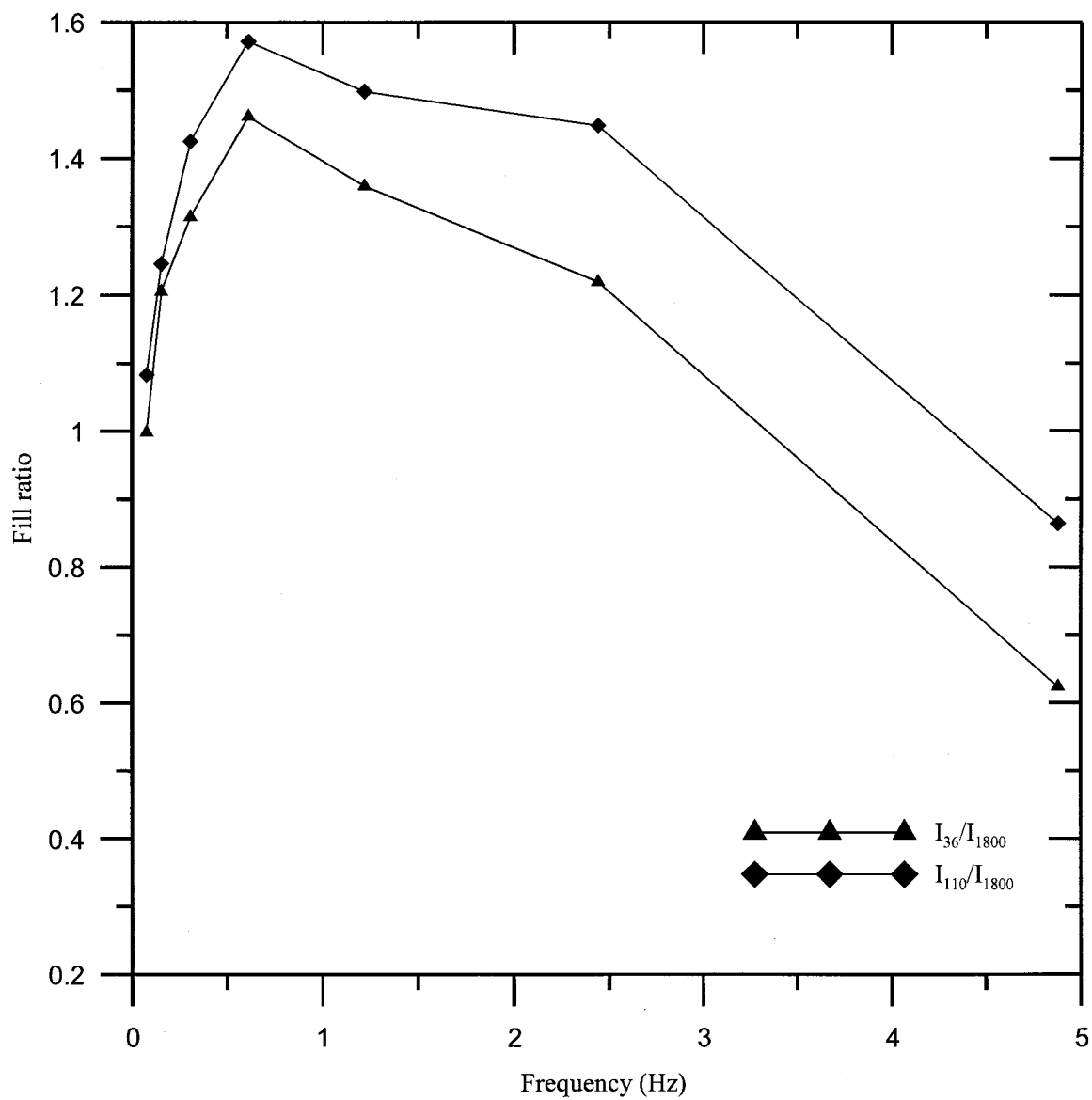


Figure 4.4 Fill ratio vs. frequency - O<sub>2</sub> purging in 400ppm PEG, 2ppm SPS



#### **4.1.5 Effect of SPS addition**

The trends for four different chemistries with no additives, no SPS, 1ppm SPS and 2ppm SPS in an acidic copper sulfate bath are shown in Figure 4.5. The fill ratio is highest for a plating bath containing 2ppm SPS. The frequency range for the best filling chemistry lies at lower frequencies. From the Figure 4.5, the higher the SPS concentration, the higher is the current at lower RDE rotation speed. This is obvious from the fill ratio measurements at different SPS concentrations. Operating in the range below 0.7Hz gives the highest fill ratio for each of the compositions. Operation of the pulse-reverse cycle with a wave-train of 800/40/800 ms should give the best filling.

#### **4.1.6 Effect of Reverse time**

The standard solution with 400ppm PEG and 2ppm of SPS was used to analyze the effect of the reverse pulse. The optimized ON/REV/OFF wave-train for the above solution was found to be 800/40/800 ms, when the ON and OFF times were held constant. The reverse time in the pulse wave train was varied in steps of 40ms from 40 to 160ms. The fill ratio is highest for a wave train with 120ms of REV time, i.e. for 800/120/800 ms wave train.

The effect of varying the potential of the reverse pulse was also studied as shown in the Figure 4.7. The standard potential initially used was -300/150/0mV. The potential wave train has an ON potential of -300 mV and OFF potential of 0 mV. Both the ON and OFF potentials were held constant. The REV potential was varied in steps of 50mV from 100mV to 250mV. From the plot of Fill ratio vs. the reverse potential, the fill ratio is higher at higher reverse potential. The reverse pulse generates Cu(I) and hence higher fill ratios were observed. The observation is in agreement with the model.

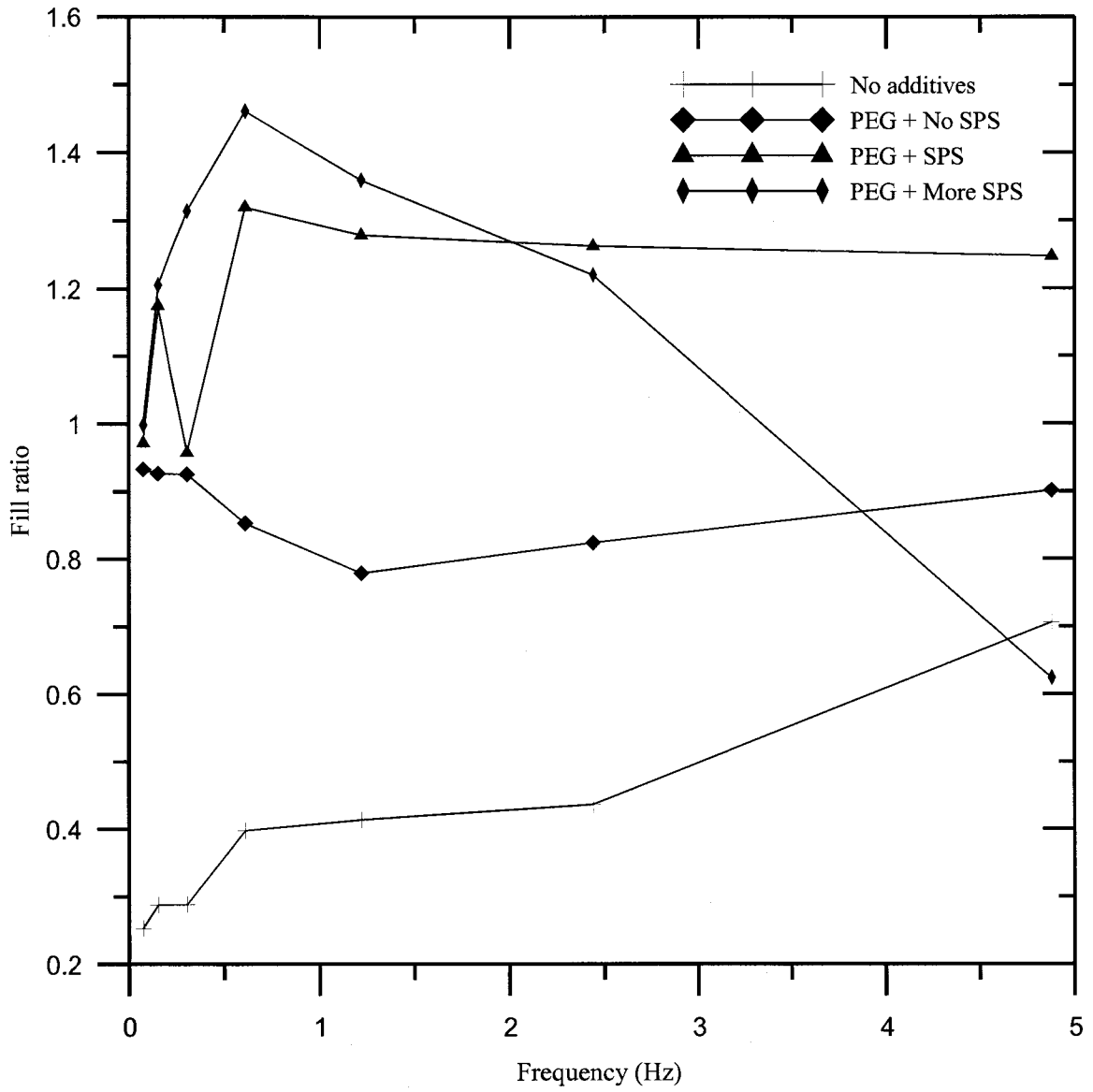


Figure 4.5 Fill ratio vs. frequency- Effect of SPS addition on frequency

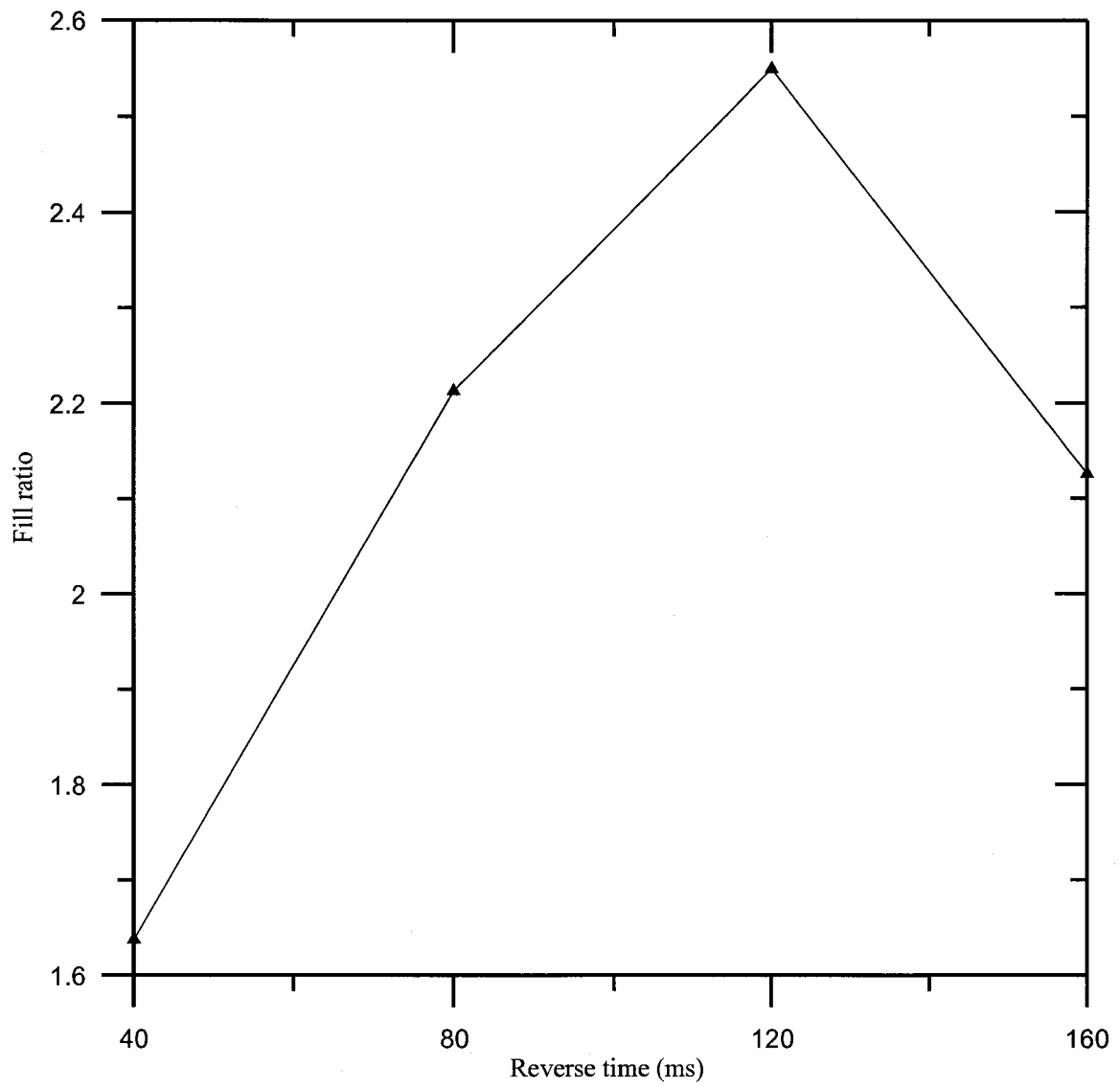


Figure 4.6 Fill ratio vs. reverse time - Effect of reverse time

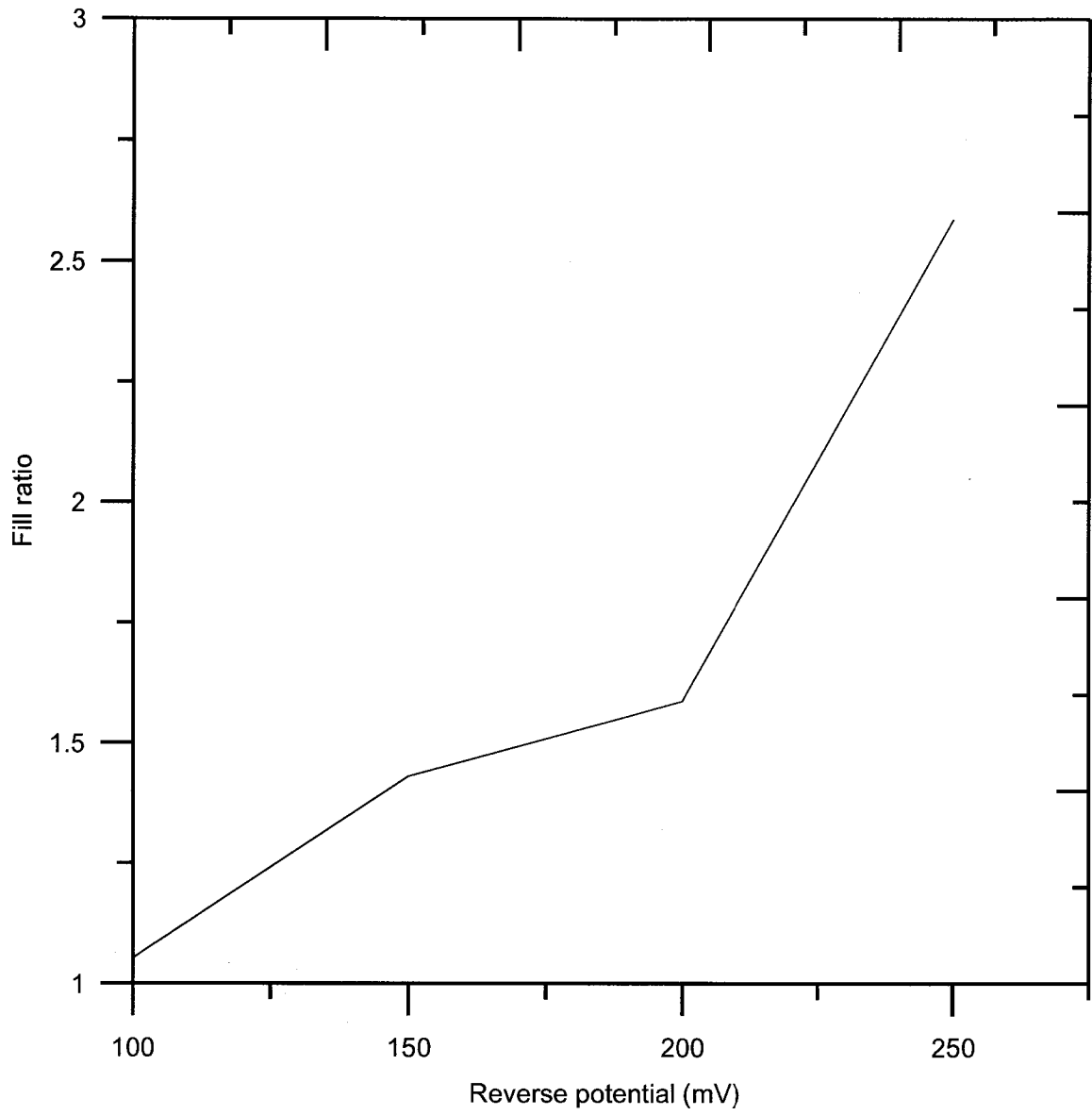


Figure 4.7 Fill ratio vs. reverse potential - Effect of reverse potential

## **4.2 Accelerant in halide bath**

SPS and MPSA act as accelerants in via filling chemistry. The effect of varying the concentrations of each of these accelerants in chloride and bromide baths was studied. A standard 2 liter solution containing 0.6M  $\text{CuSO}_4 \cdot 5\text{H}_2\text{O}$  and 1.8M  $\text{H}_2\text{SO}_4$  was made up with ultrapure water. The solution contained 400ppm of PEG. The halide concentration was fixed at 50ppm. Fill ratio analysis for various concentrations of the accelerants was performed.

### **4.2.1 SPS concentration variation in Bromide bath:**

The source of bromide ions was Potassium Bromide. A potential pulse-reverse wave-train of -400/200/0mV for a period of 400/20/400ms was applied. The SPS concentration was varied from 1ppm to 10ppm. The current for each concentration of SPS was measured at RDE speeds of 40, 160 and 2560rpm. From the measured currents, fill ratios of  $I_{40}/I_{2560}$  and  $I_{160}/I_{2560}$  were calculated.

Figure 4.8 shows a plot of fill ratio vs. SPS concentration. Fill ratios  $I_{40}/I_{2560}$  and  $I_{160}/I_{2560}$  are less than unity. Via filling with such a bath may result in sub-conformal plating with a defect. Replacement of chloride with bromide does not improve the fill ratio.

### **4.2.2 MPSA concentration variation in Bromide bath:**

The efficiency of MPSA in a bromide bath was studied. Potassium bromide was used to prepare 50ppm of  $\text{Br}^-$  in the standard electrolyte. A pulse-reverse wave train of -150/100/0mV for 400/20/400ms of ON/REV/OFF was applied. The MPSA concentration

was varied from 1 to 10ppm and the currents were measured at 40, 160 and 2560rpm of the RDE. Fill ratios of  $I_{40}/I_{2560}$  and  $I_{160}/I_{2560}$  were calculated.

Figure 4.9 shows fill ratio vs. MPSA concentration. It can be observed that the fill ratio  $I_{160}/I_{2560}$  has a higher value at the same MPSA concentration than  $I_{40}/I_{2560}$ . But the ratios were still below unity. It can be concluded from the above analysis that the thio-group in a bromide bath would not result in defect free filling of the via.

#### **4.2.3 SPS concentration variation in Chloride bath:**

The effect of SPS in a standard copper sulfate bath containing chloride was studied. 50ppm of chloride ions was added to the electrolyte. A potential pulse-reversal experiment of -250/150/0mV for 400/20/400ms was run. Currents were measured at RDE speeds of 40, 160 and 2560rpm for each concentration of SPS. Fill ratios  $I_{40}/I_{2560}$  and  $I_{160}/I_{2560}$  were calculated and a plot of fill ratio vs. SPS concentration was constructed.

Figure 4.10 shows the plot of fill ratio vs. the SPS concentration. There is a very large contrast in the fill ratio observed with chloride and bromide addition (Figure 4.8) to the standard electrolyte. Chloride produces a much better fill ratio. The Fill ratio  $I_{160}/I_{2560}$  is similar in trend to  $I_{40}/I_{2560}$  but with higher values. The ratios observed for  $I_{40}/I_{2560}$  are much smaller than  $I_{160}/I_{2560}$ . The fill ratio increases with increasing SPS up to about 4ppm. No further improvement occurs at higher concentrations.

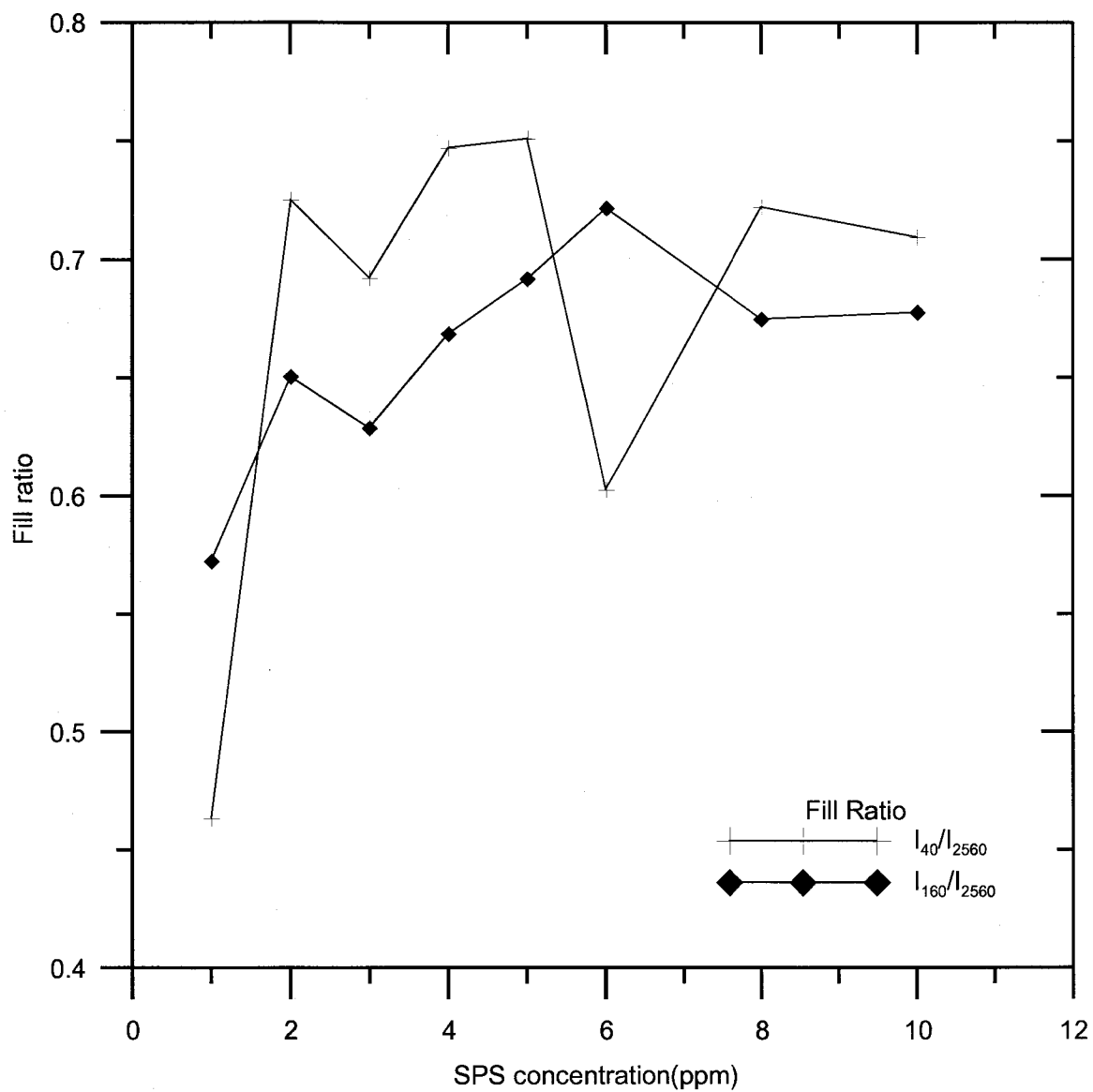


Figure 4.8 Fill ratio vs. SPS concentration - SPS concentration variation in  $Br^-$  bath

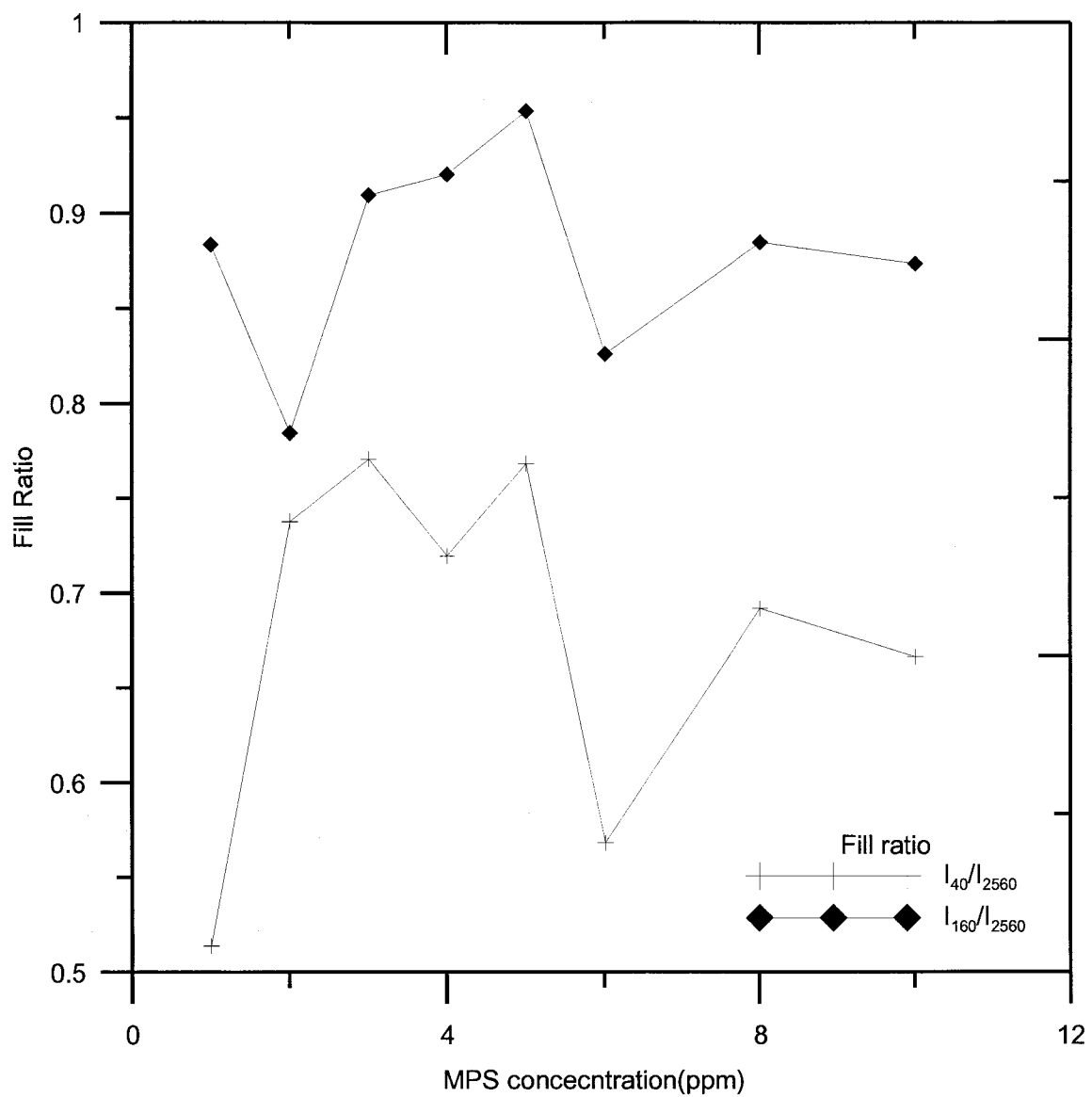


Figure 4.9 Fill ratio vs. MPSA concentration - MPSA concentration variation in Br<sup>-</sup> bath



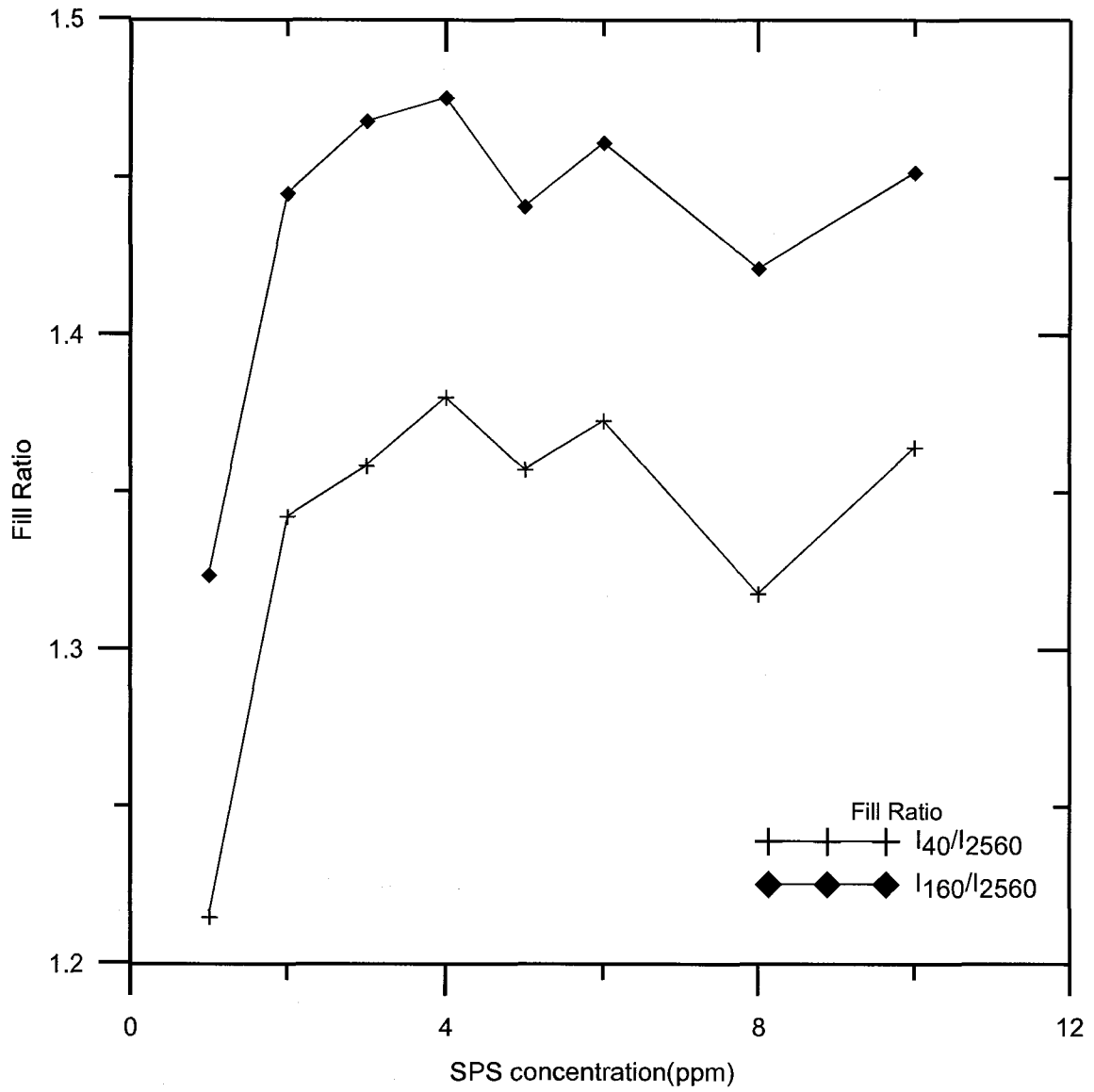


Figure 4.10 Fill ratio vs. SPS concentration; SPS concentration variation in Cl<sup>-</sup> bath

### **4.3 Current controlled experiments**

Current pulse-reversal studies were used to understand the effect of each of the additives. The magnitude of deviation of the electrode potential from the equilibrium value is defined as the overpotential. The difference in the potentials at fixed currents and different speeds predicts the contrast in plating rate at the bottom versus the top of the via.

A copper sulfate standard solution with 0.6M  $\text{CuSO}_4 \cdot 5\text{H}_2\text{O}$  and 1.8M  $\text{H}_2\text{SO}_4$  with 50ppm chloride and 4ppm SPS was prepared. Current wave-trains were applied and the potentials were recorded at RDE speeds of 40, 160, 640 and 2560rpm. The potential difference at different speeds was used to evaluate the efficiency of the additive system. A higher overpotential indicates more strongly inhibited deposition.

#### **4.3.1 Effect of PEG concentration**

The concentration of PEG was varied with concentrations of all the other additives held constant. A galvanic pulse of +7/-14/0mA with duration of 1000/50/1000ms was applied at several RDE speeds. The potential of the RDE was recorded.

The plot of difference in potential recorded at 160 and 1560 rpm of the RDE vs. the change in the concentration of the PEG is shown in Figure 4.11. From the plot there is no considerable change in the potential difference at different concentrations of PEG, higher than 100ppm and this could be due to the saturation of the surface by  $\text{PEG} > 100\text{ppm}$ .

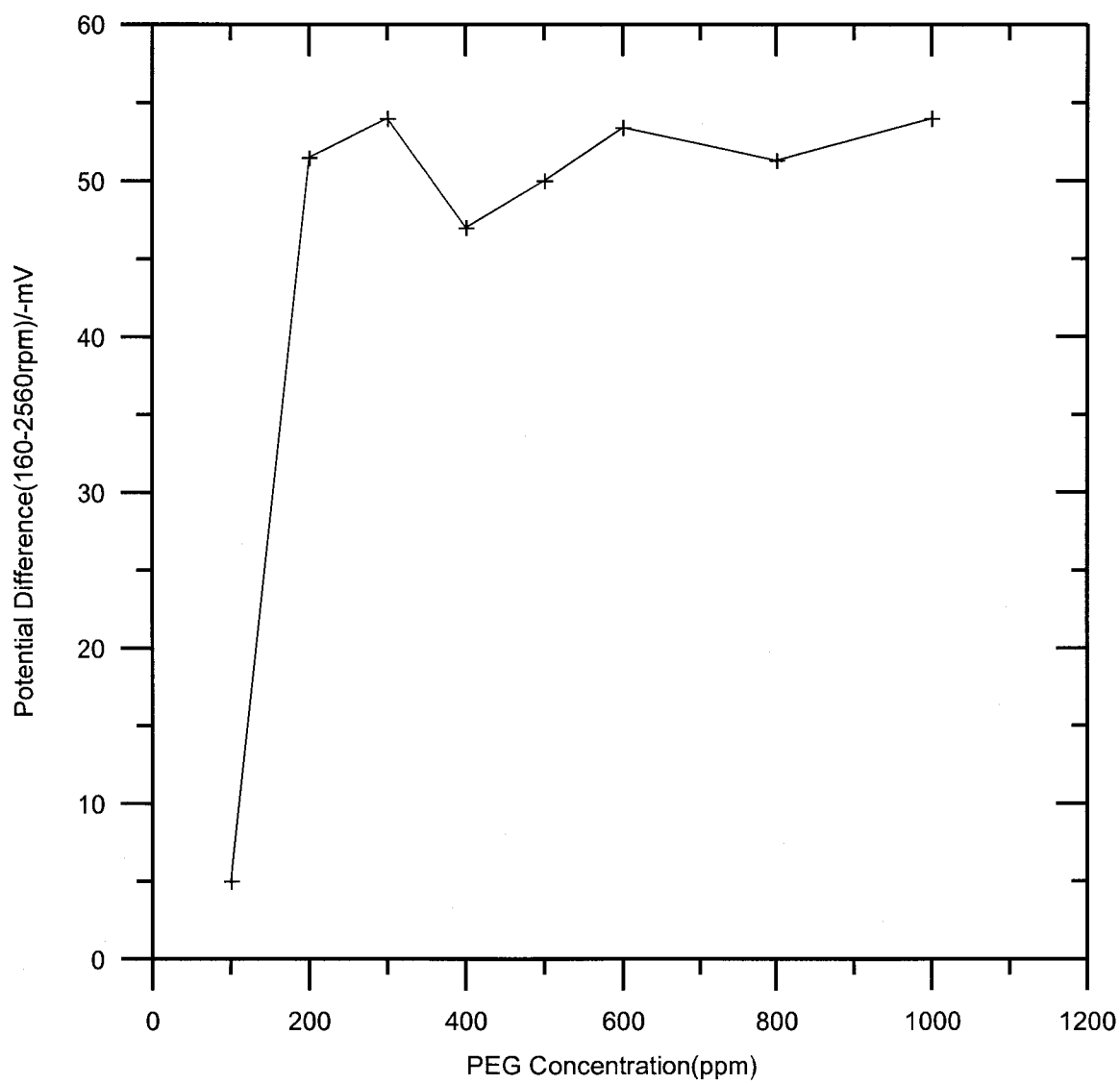


Figure 4.11 Potential difference vs. PEG concentration - Effect of PEG concentration

### 4.3.2 Effect of PEG molecular weight

The dependence of fill ratio on the molecular weight of PEG was studied. The molecular weights of PEG compared were 3400, 6000, 8000 and 20000. The concentration of PEG was varied for each of the molecular weights in steps of 100ppm. The potential was recorded at different speeds of the RDE. Finally a plot of difference in potential measured at 2 speeds of the RDE vs. PEG concentration was made for all the PEG molecular weights.

The higher the difference in measured potentials at 2 different speeds (low and high), the better is the filling capability of the chemistry analyzed. Plots of potential vs. the PEG concentration were made for each of the molecular weights considered. These are shown in Figure 4.12, 4.13, 4.14 and 4.15 for PEG of molecular weight 3400, 6000, 8000 and 20000g.mol<sup>-1</sup> respectively.

The potential curve obtained for 160 rpm has the least negative potential for PEG of all molecular weights. The difference in potential from each of the plots is highest for that between 160rpm and 2560rpm. The plot of the difference in potential vs. the concentration gives an idea of the optimum molecular weight of PEG that has to be used in a via filling chemistry in order to get bottom-up filling.

The difference in potential is calculated at the same concentration of PEG for different molecular weights. A plot comparing all the molecular weights of PEG considered is shown in Figure 4.16. From Figure 4.16, the optimum molecular weight of PEG should be in between 6000 – 8000g.mol<sup>-1</sup>. These molecular weights have the largest difference in potentials.

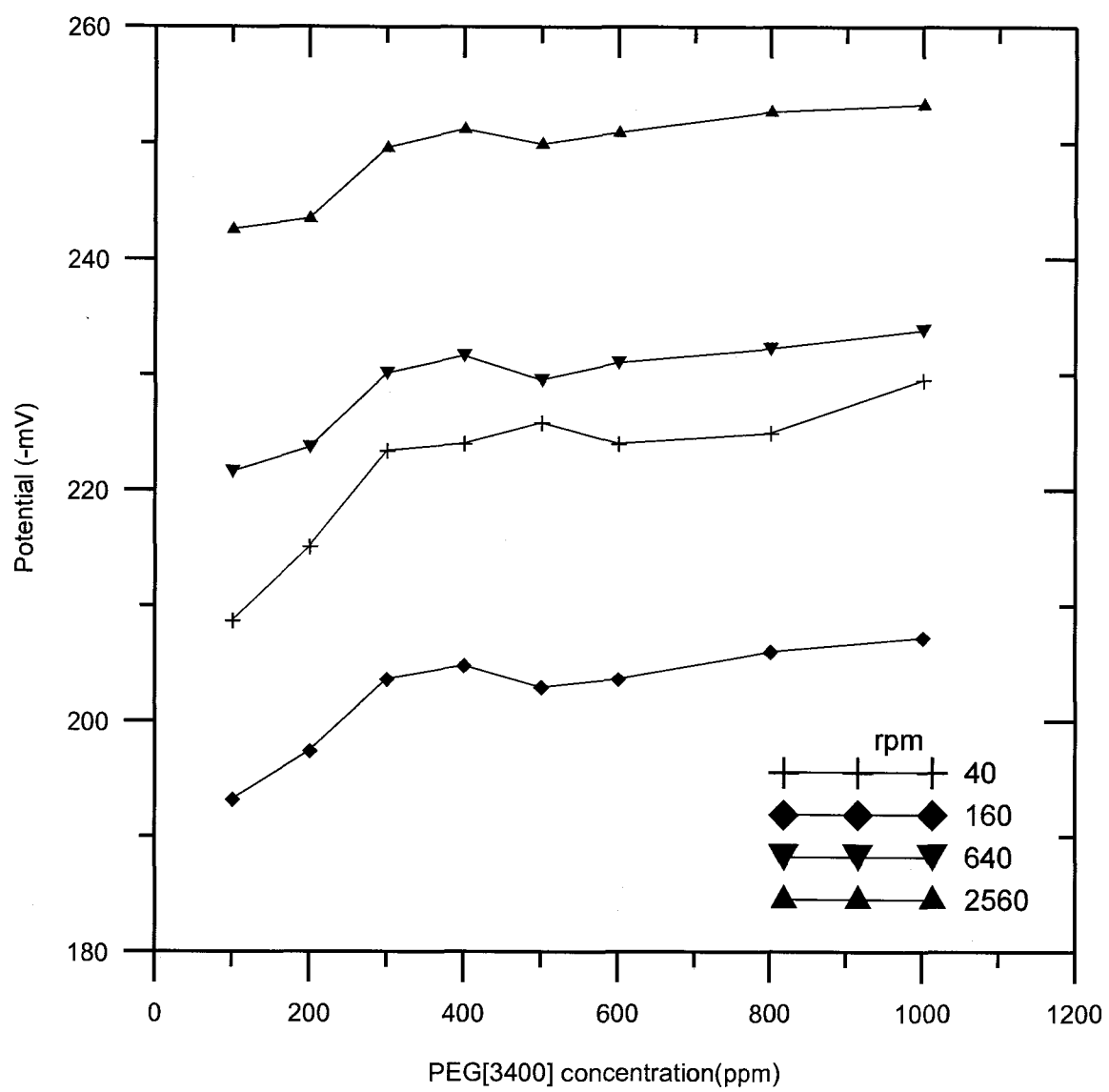


Figure 4.12 Potential vs. PEG concentration; PEG – 3400MW concentration variation

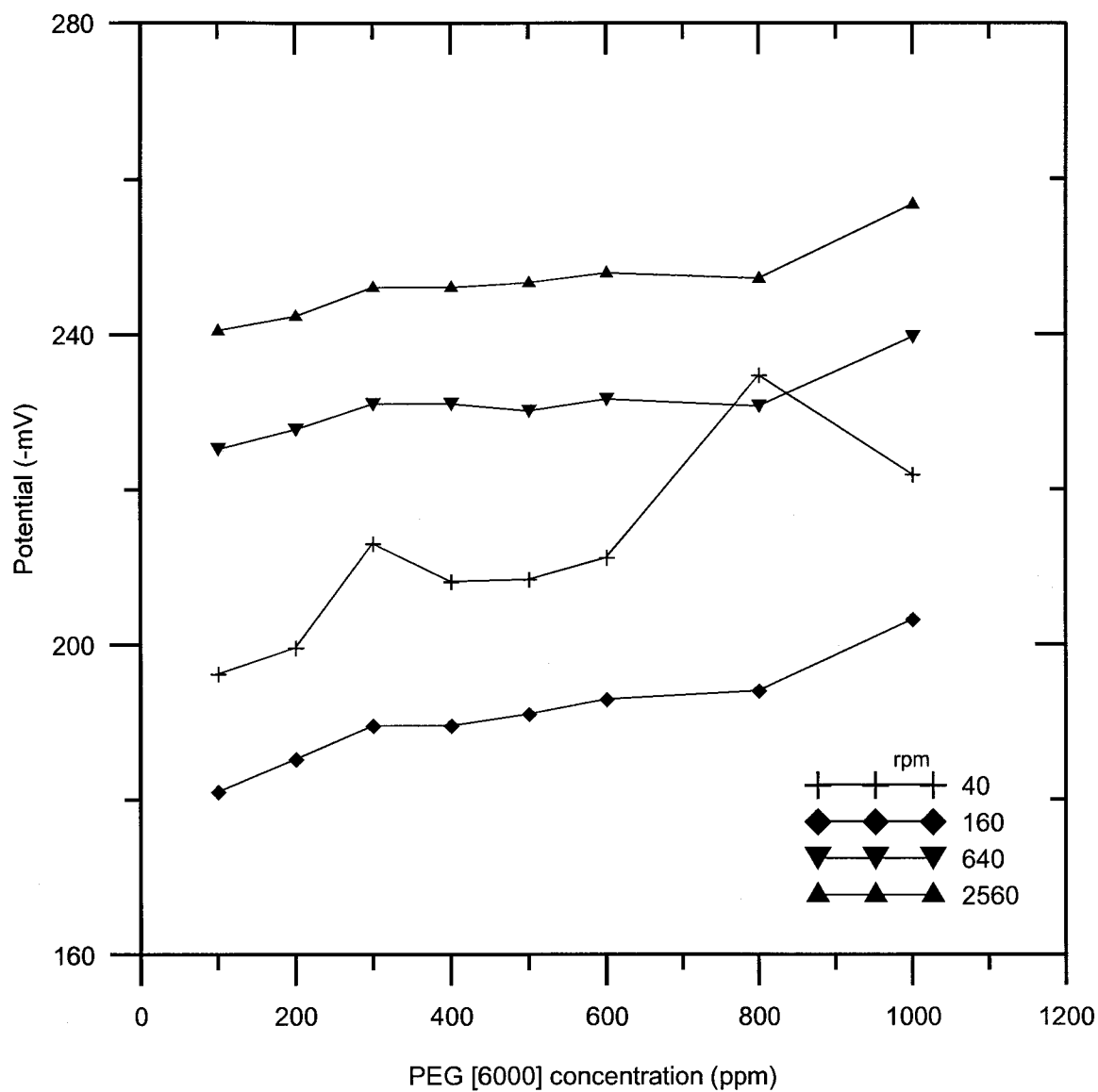


Figure 4.13 Potential vs. PEG concentration; PEG – 6000MW concentration variation

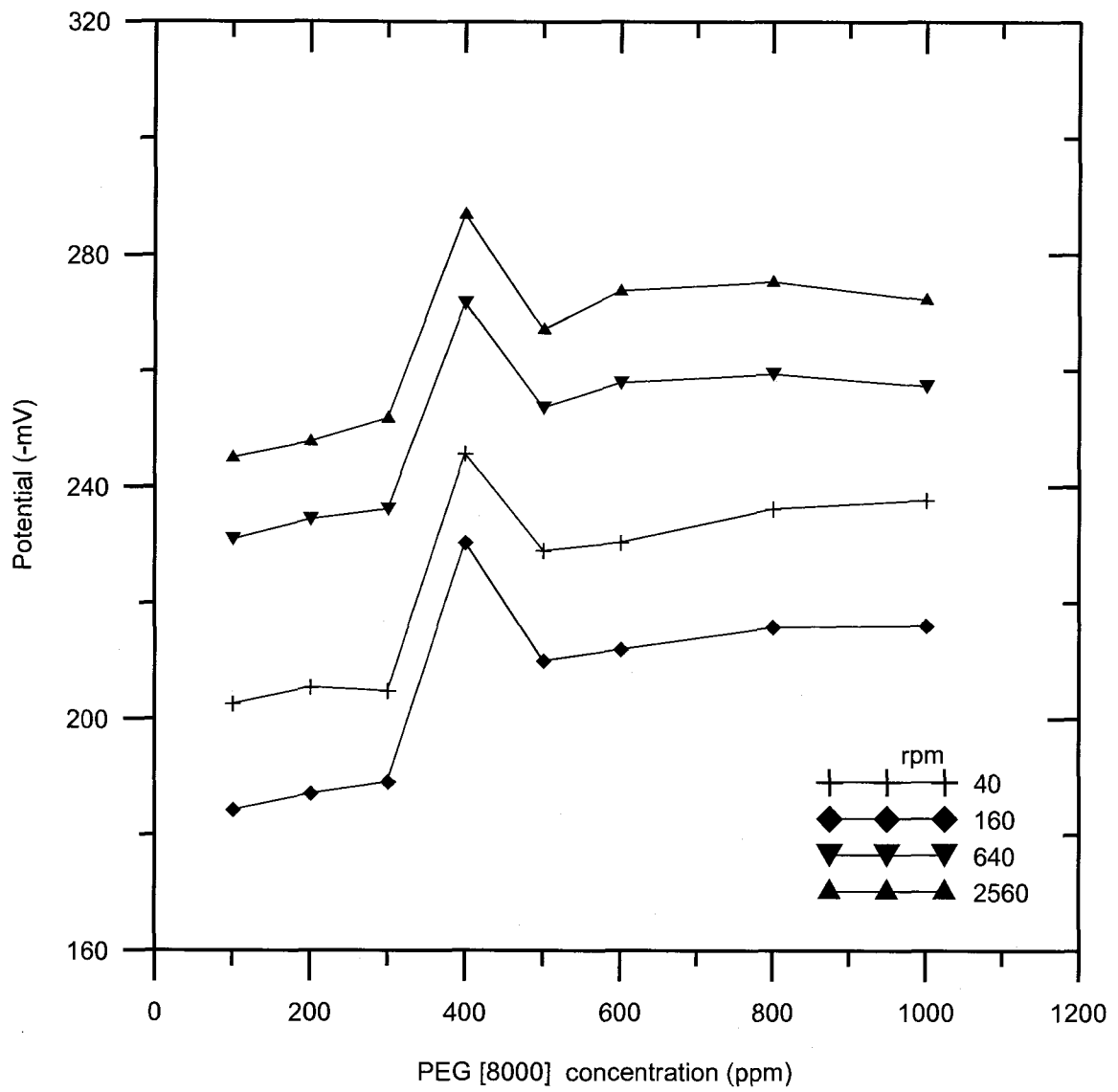


Figure 4.14 Potential vs. PEG concentration; PEG – 8000MW concentration variation

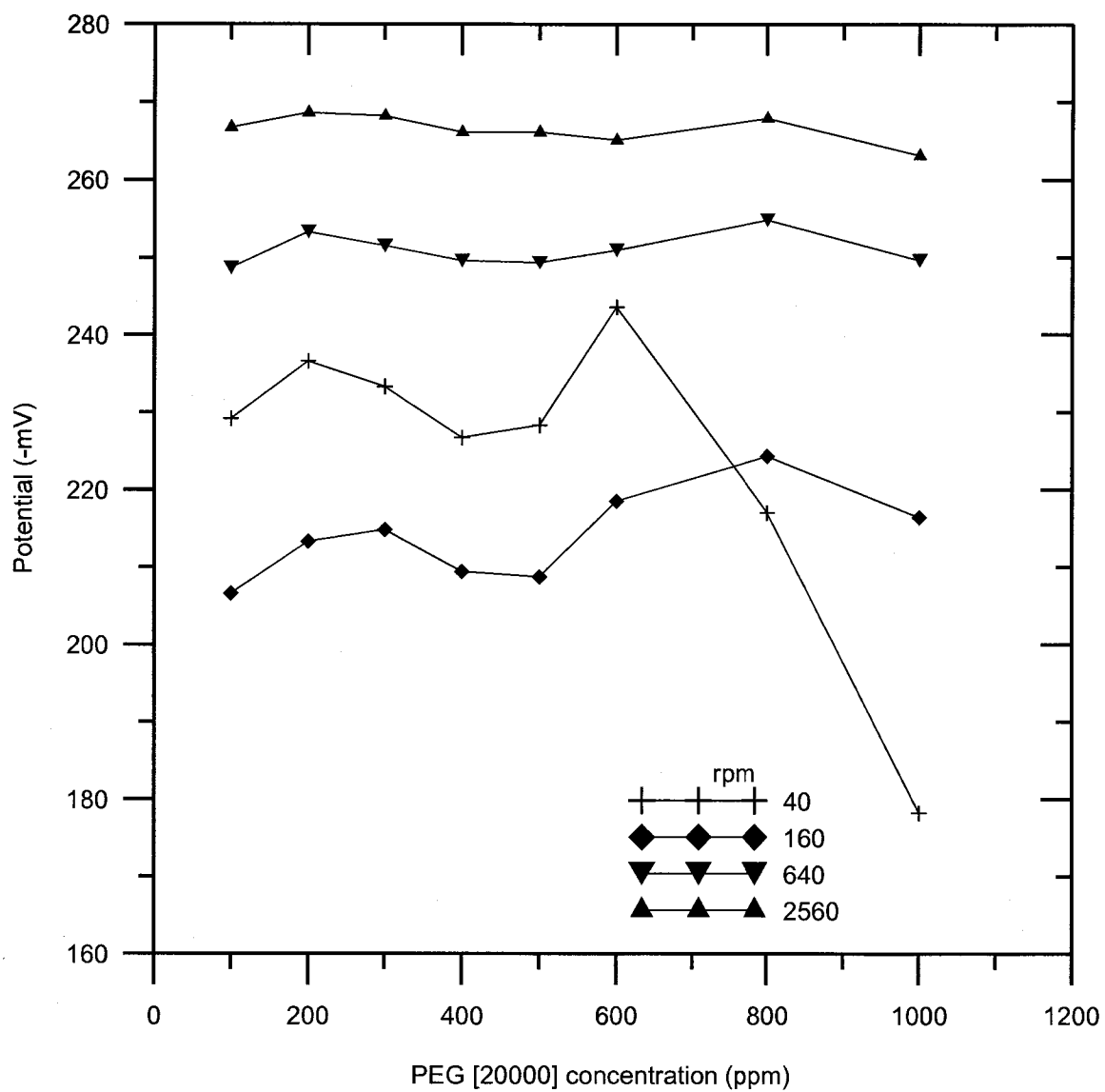


Figure 4.15 Potential vs. PEG concentration; PEG – 20000MW concentration variation



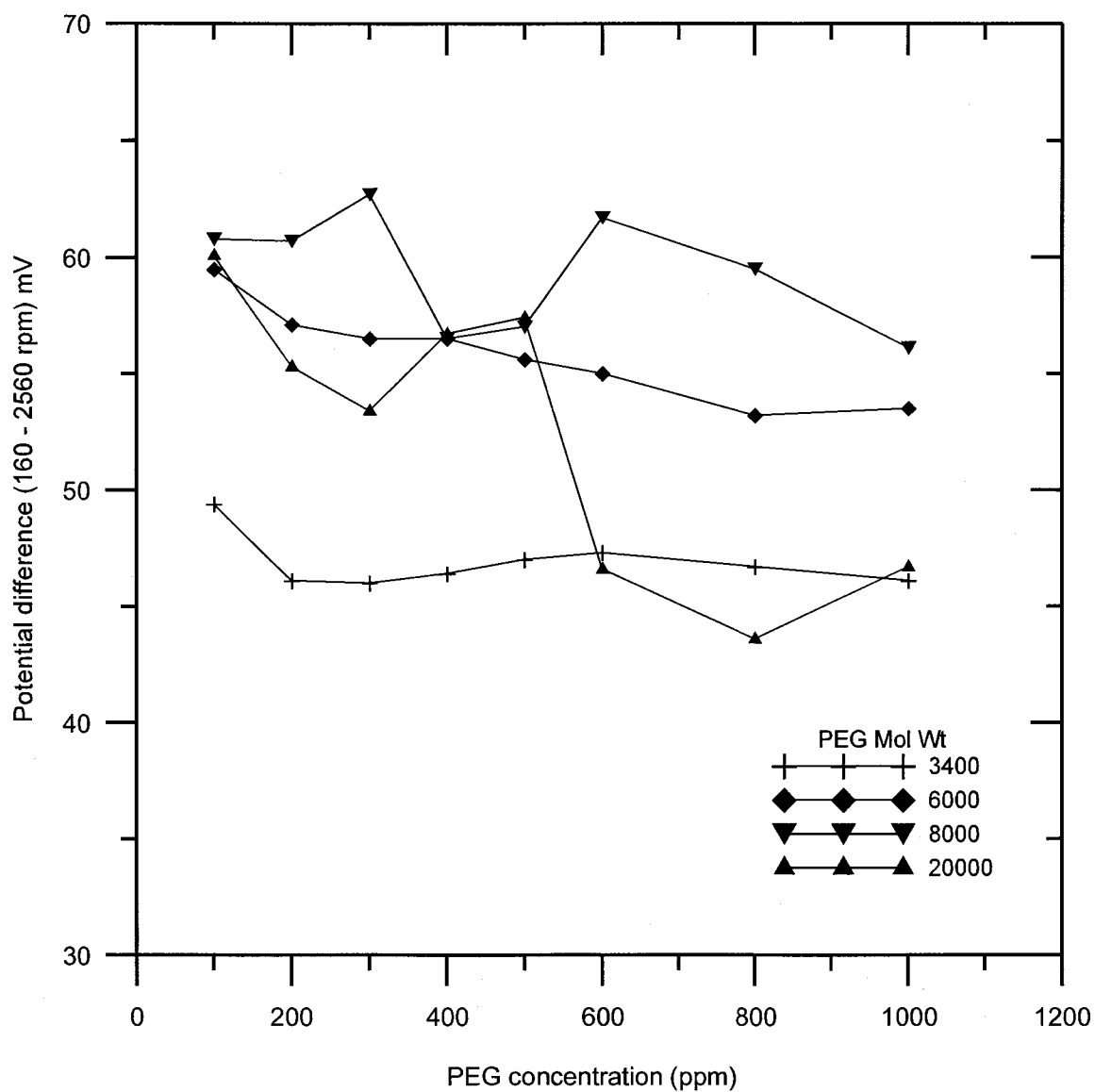


Figure 4.16 Potential difference vs. PEG concentration- Effect of PEG molecular weight

#### **4.3.3 SPS concentration variation at 400ppm PEG [6000]**

At fixed molecular weight of PEG, the optimum concentration of SPS was studied. The base solution containing 400ppm of PEG was subjected to a galvanic wave train with the same set of parameters as previously but with varying concentration of SPS. The potentials were recorded at RDE speeds of 40, 160, 640 and 2560rpm. The plot of the measured potential in  $-mV$  vs. the SPS concentration for different RDE speeds was made. This is shown in Figure 4.17. The largest contrast in potential was observed between 160rpm and 2560rpm. Hence the potential difference vs. SPS concentration was constructed by accounting the difference in potential between 160rpm and 2560rpm for different concentrations of SPS.

A plot of the difference in the potentials measured at 160rpm and 2560rpm of the RDE vs. SPS concentration is made and is shown in Figure 4.18. From figure 4.18, SPS concentration in the range of 5ppm – 6ppm would be an optimum for achieving filling results in the plating chemistry with 400ppm PEG, 50ppm  $Cl^-$ . Increasing the concentration of SPS beyond 6ppm would have no effect on filling.

#### **4.3.4 MPSA concentration variation in 400ppm PEG [6000]**

The procedure described in §4.3.3 was applied to study the effect of MPSA. A plot of the potential difference vs. MPSA concentration is shown in the Figure 4.20. A higher MPSA concentration would be required for obtaining bottom-up filling. The difference in potentials observed for SPS is much higher than that of MPSA. Hence SPS would be a preferred choice with the standard chemistry of 400ppm PEG [6000], 50ppm  $Cl^-$ .

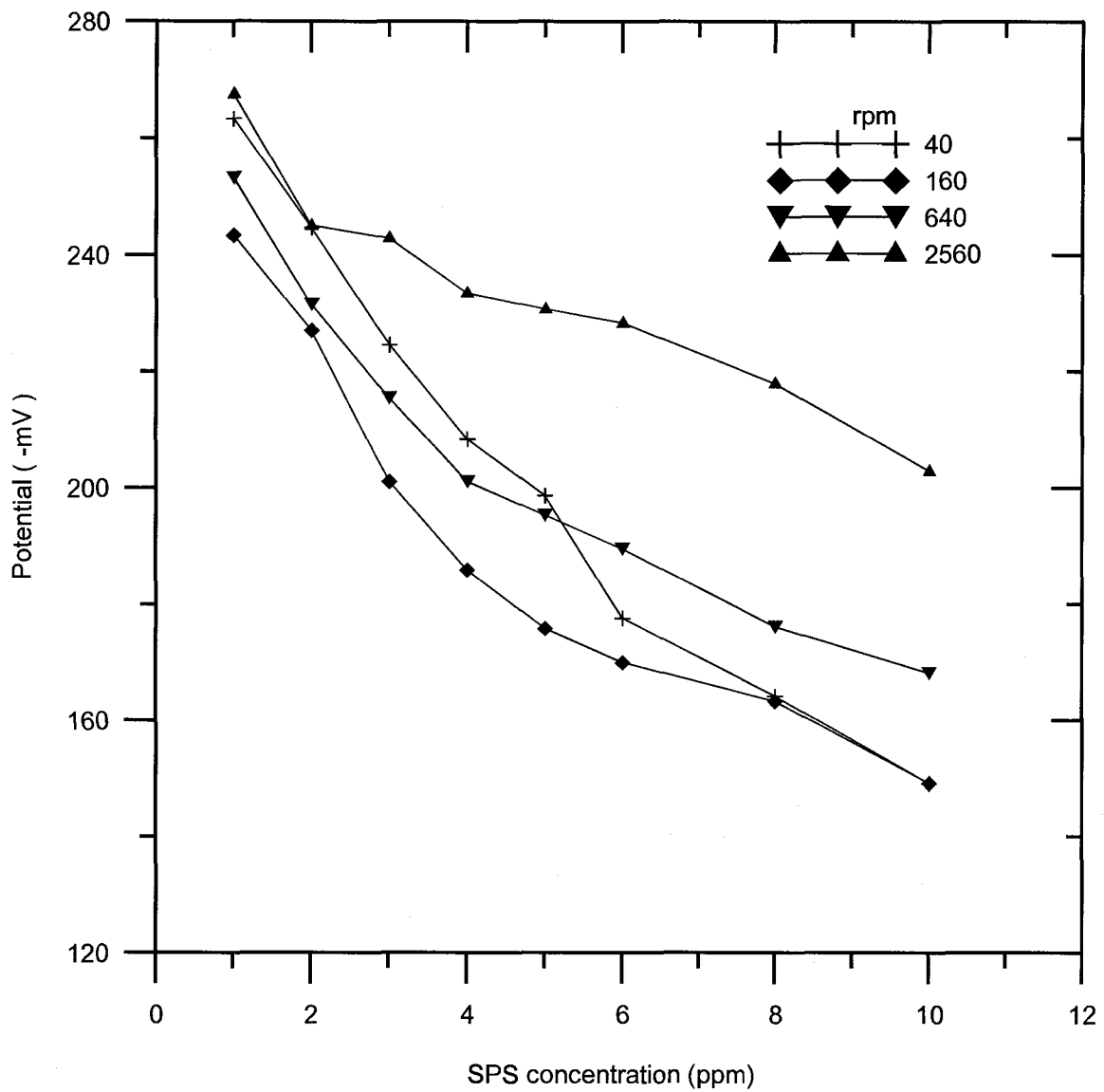


Figure 4.17 Potential vs. SPS concentration variation in 400ppm PEG [6000]

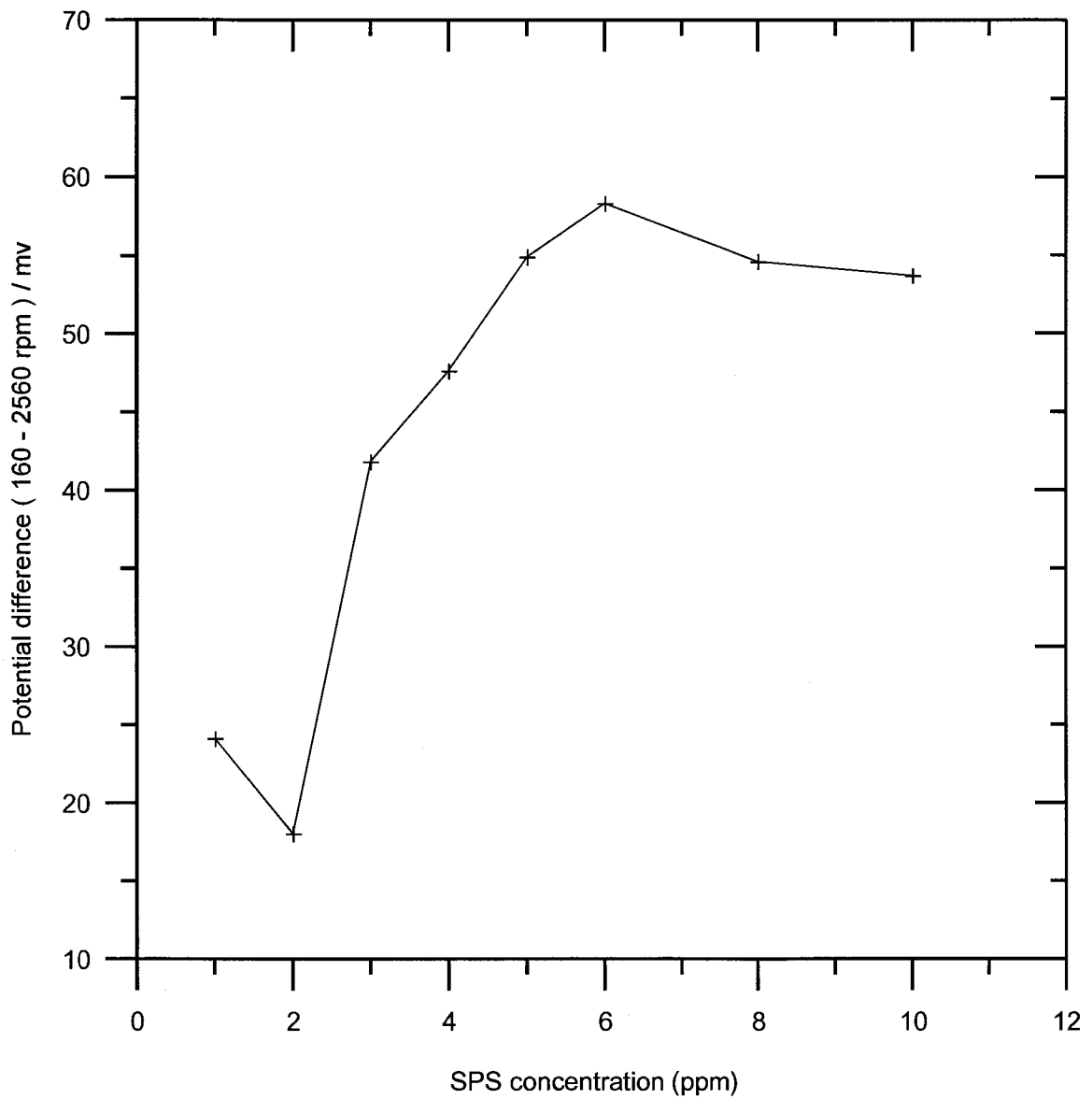


Figure 4.18 Potential difference vs. SPS concentration variation in 400ppm PEG [6000]

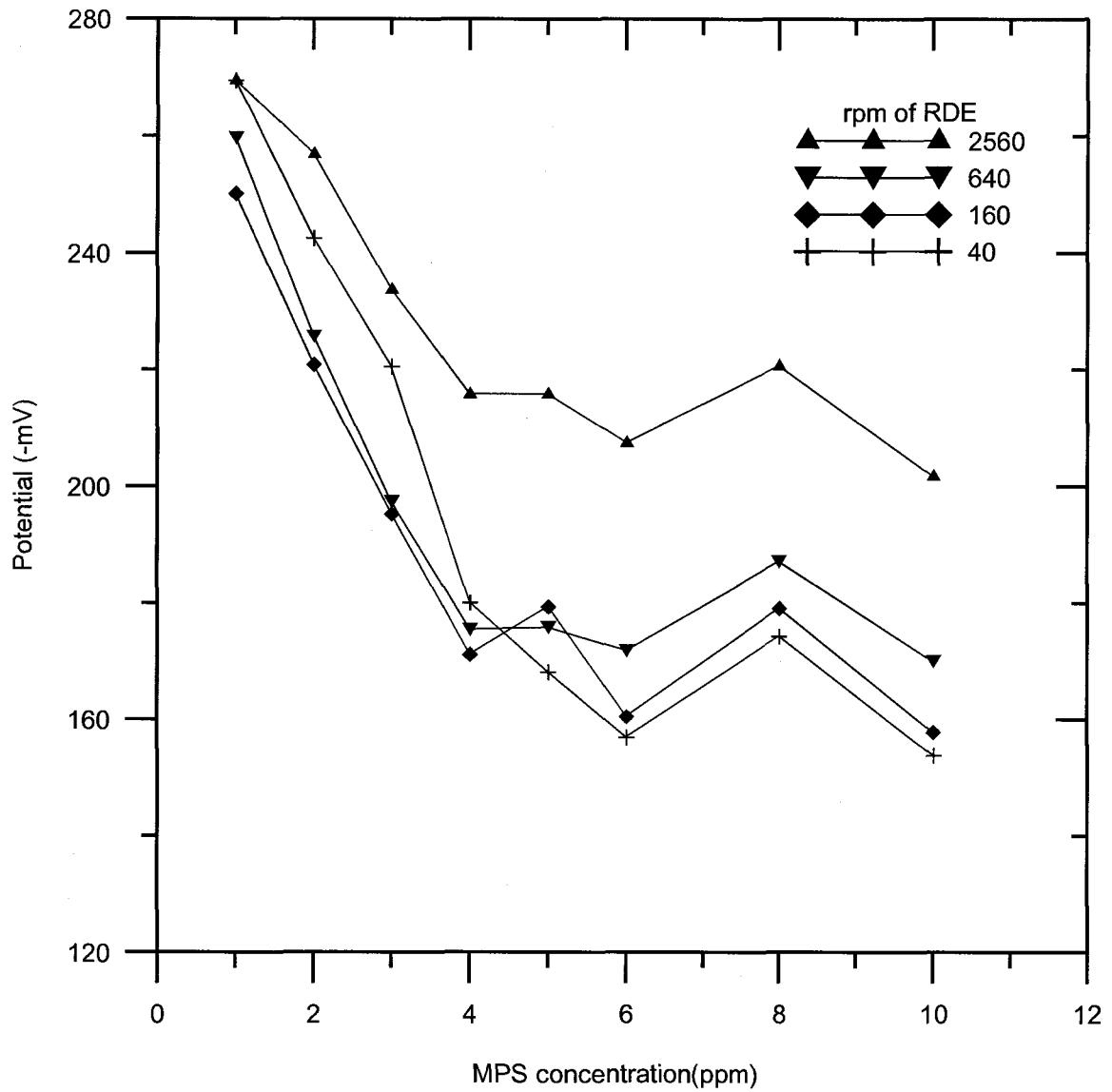


Figure 4.19 Potential vs. MPSA concentration variation in 400ppm PEG [6000]

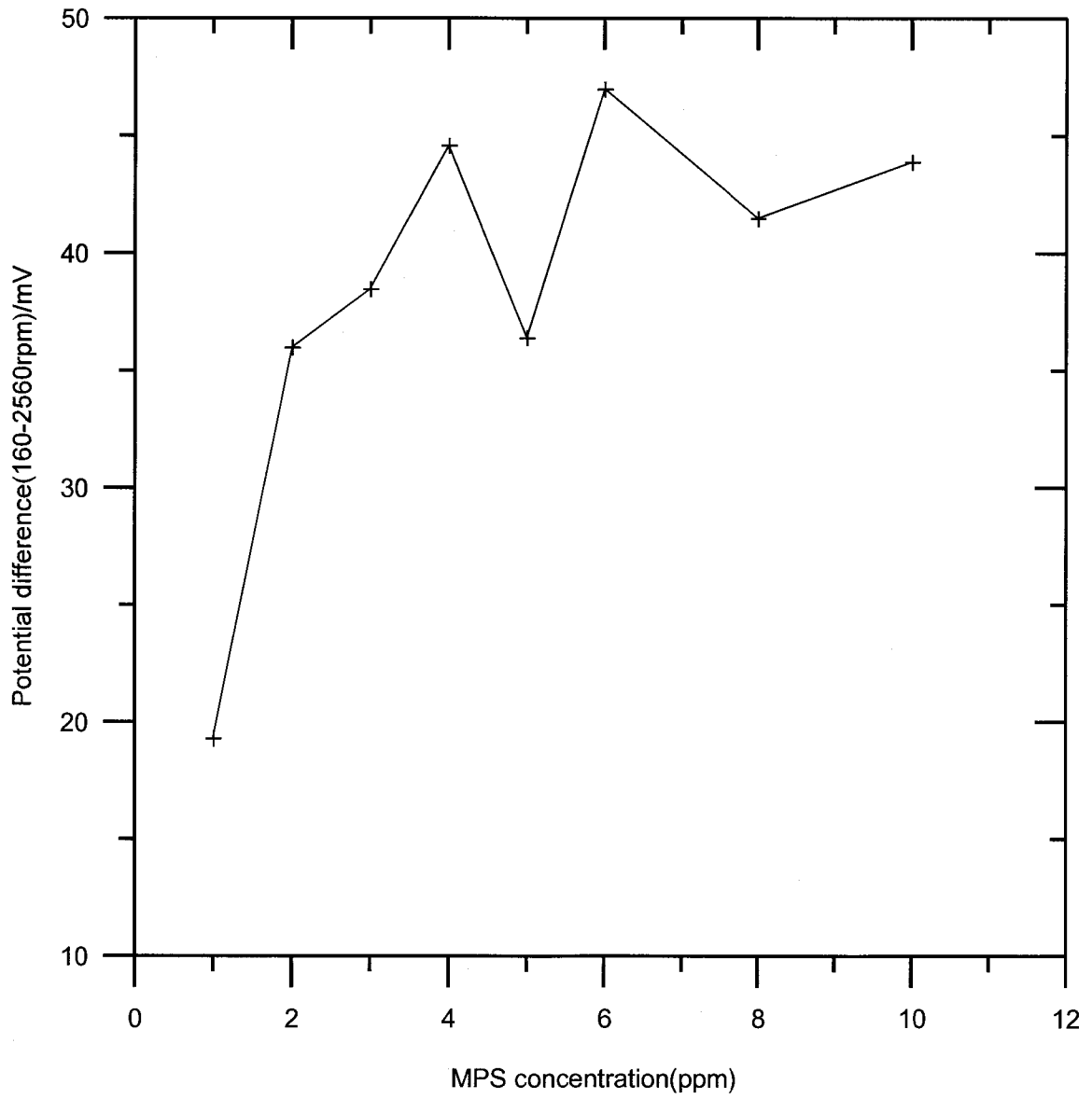


Figure 4.20 Potential difference vs. MPSA variation in 400ppm PEG [6000]

A fill ratio analysis was done for varying concentrations of MPSA and SPS in a solution containing 400ppm PEG and 50ppm Cl<sup>-</sup>. A pulse-reverse potential wave-train was applied and the currents were measured at different RDE speeds. The ratio of currents  $I_{40}/I_{2560}$  and  $I_{160}/I_{2560}$  were computed. From the Figure 4.21, SPS gives the highest fill ratio at a concentration 3 ~ 4ppm and MPSA at ~ 5ppm.

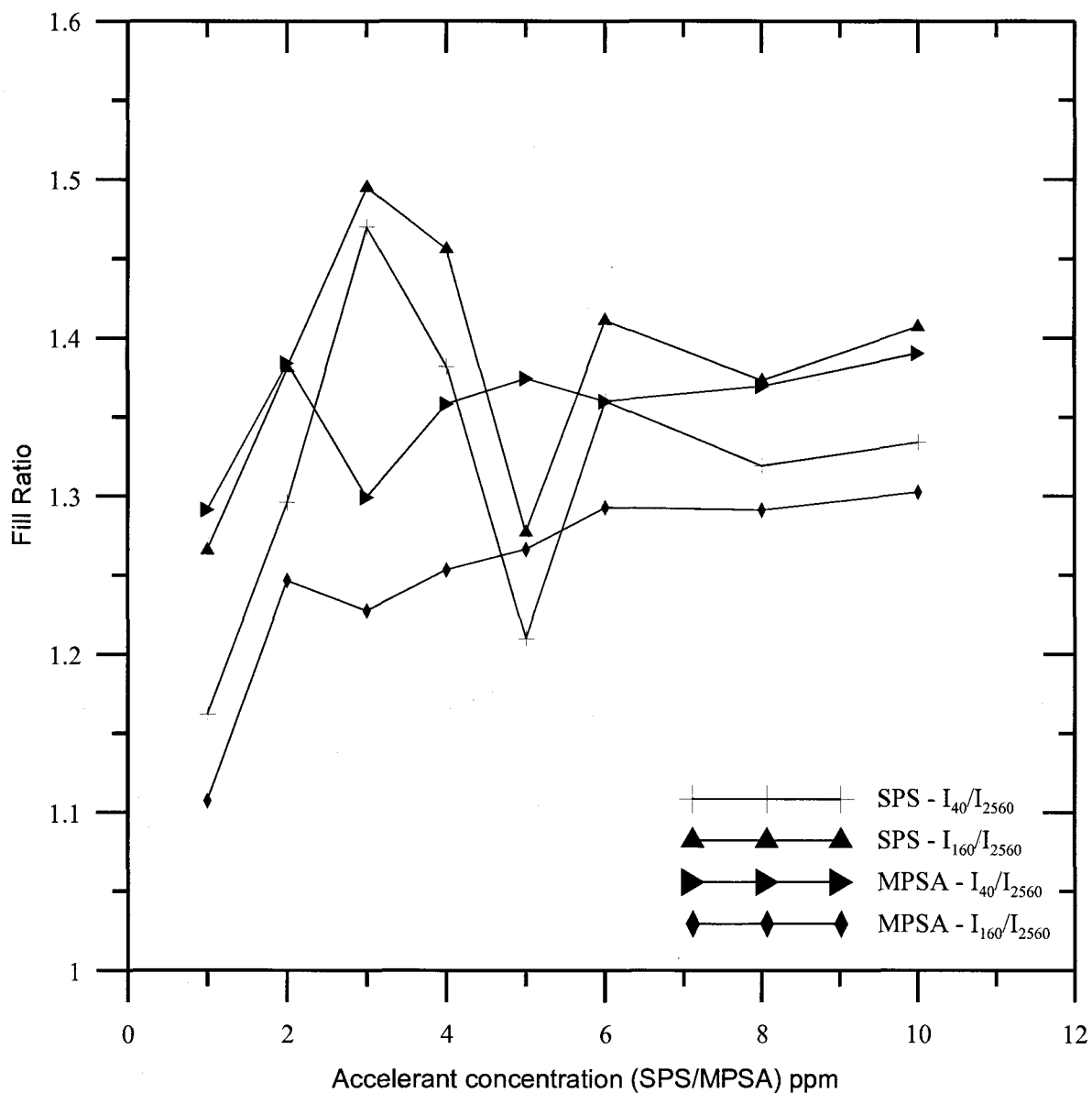


Figure 4.21 Fill ratio vs. SPS/MPSA concentration

#### **4.3.5 $\text{Cl}^-/\text{Br}^-$ variation in 400ppm PEG [6000] & 5ppm SPS**

The effect of  $\text{Cl}^-$  concentration with 400ppm of suppressor and 5ppm of accelerant was studied. The plot of potential difference vs.  $\text{Cl}^-$  concentration is shown in Figure 4.23. From this plot, the potential difference decreases as the concentration of  $\text{Cl}^-$  increases. With an increase in concentration of  $\text{Cl}^-$  beyond 50ppm, the potential difference falls drastically. A similar study was also extended to determine the optimum concentration of  $\text{Br}^-$  ions in the same via filling bath. The galvanic pulse was applied at different speeds of the RDE at varying concentrations of the  $\text{Br}^-$ . The difference in potential at 160 and 2560rpm was recorded and Figure 4.25 was constructed.



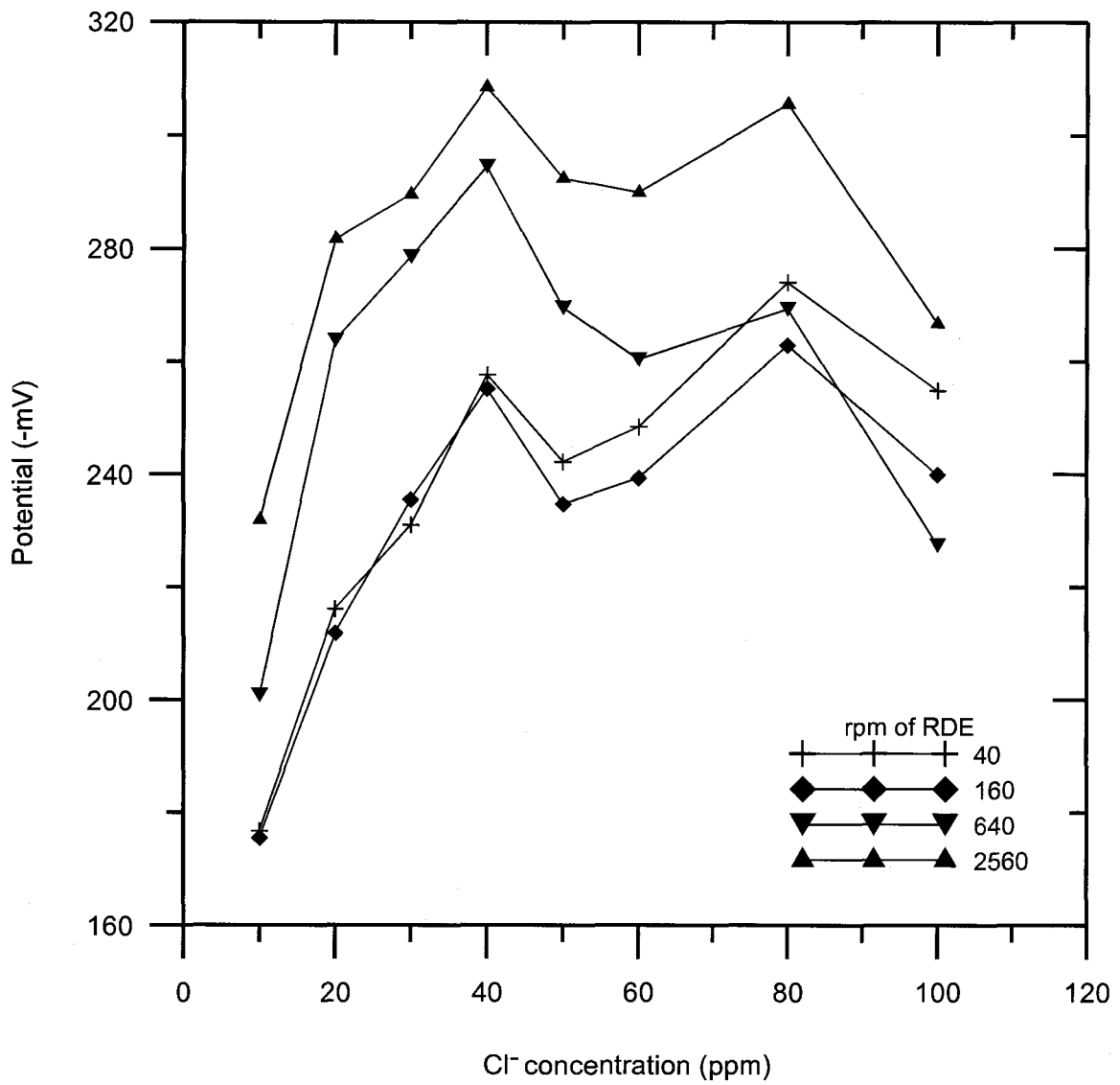


Figure 4.22 Potential vs. Cl<sup>-</sup> concentration variation in 400ppm PEG [6000] & 5ppm SPS

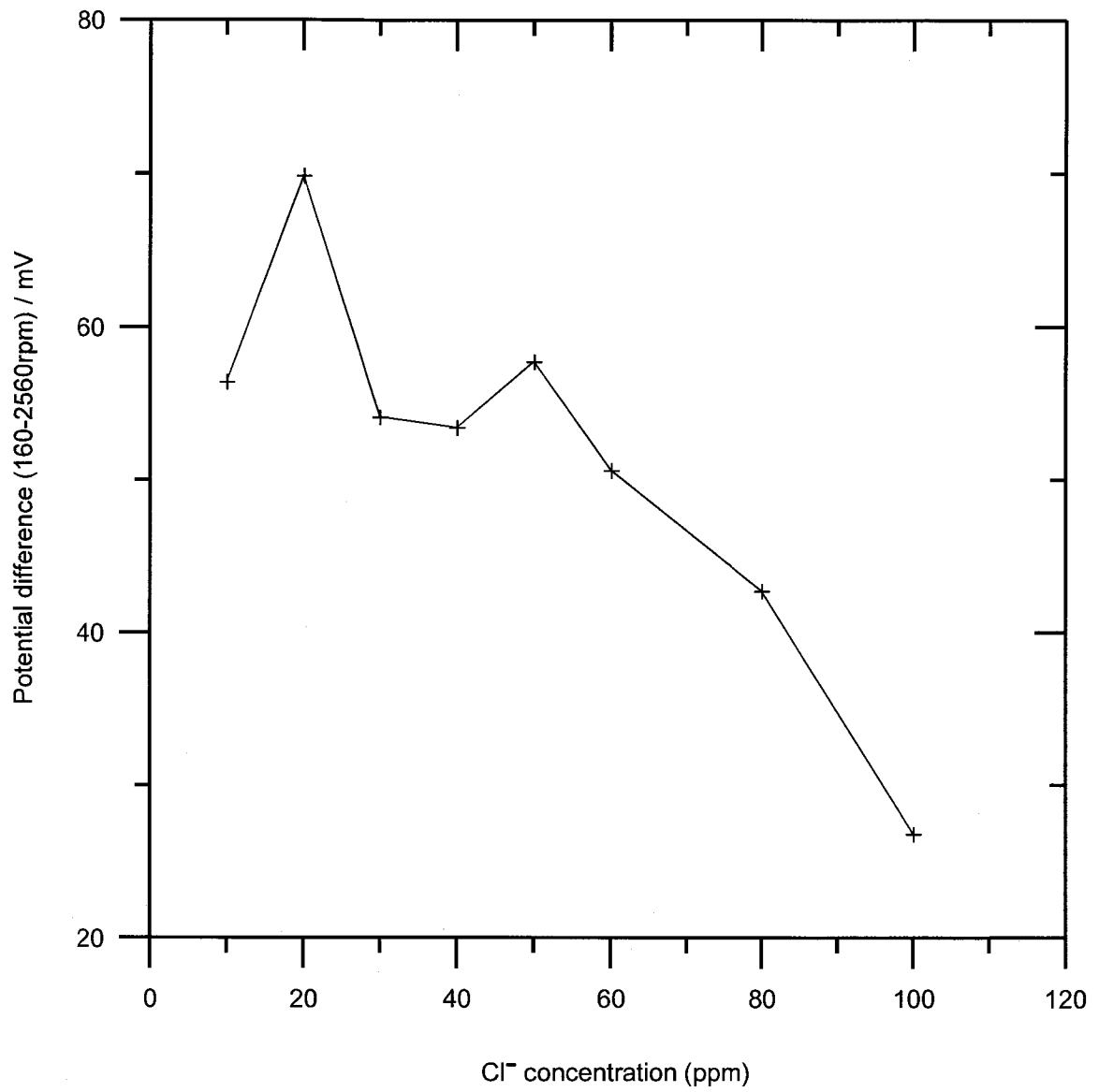


Figure 4.23 Potential difference vs. Cl<sup>-</sup> concentration in 400ppm PEG [6000] & 5ppm SPS

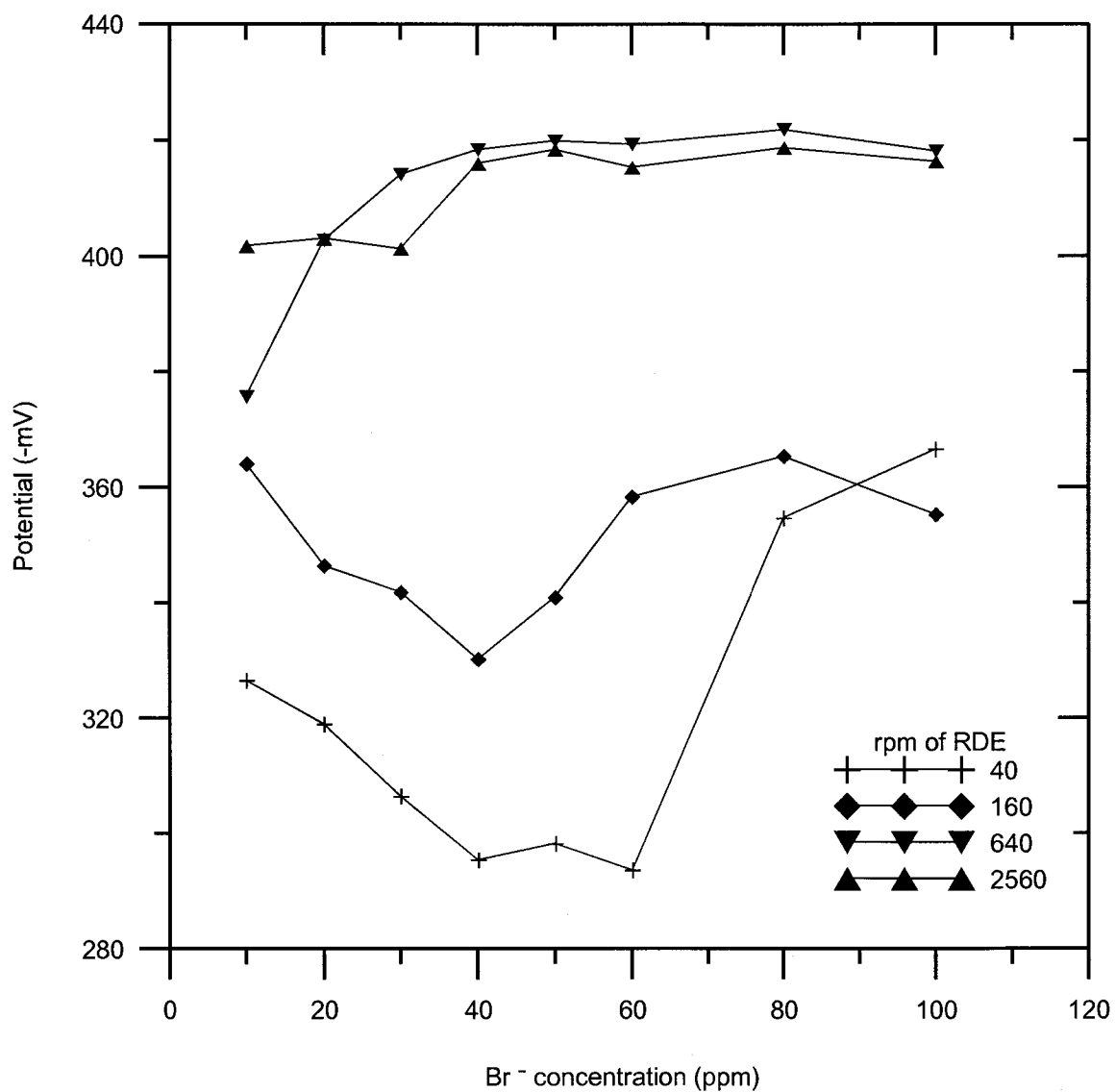


Figure 4.24 Potential vs. Br<sup>-</sup> concentration variation in 400ppm PEG [6000] & 5ppm SPS

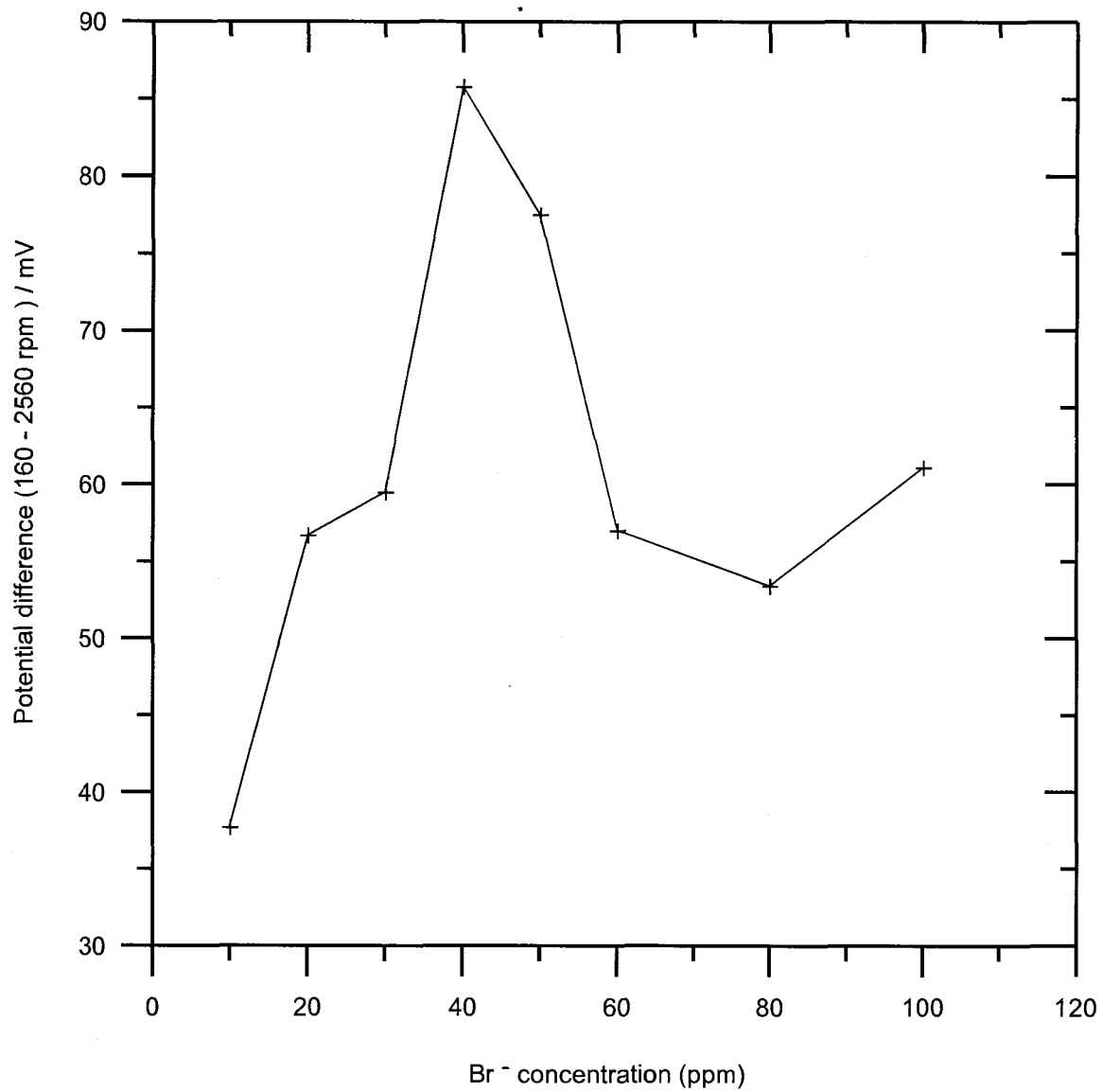


Figure 4.25 Potential difference vs. Br<sup>-</sup> variation in 400ppm PEG [6000] & 5ppm SPS

#### **4.4 Cyclic Voltammetry studies of commercial additive systems**

Cyclic voltammetry (CV) serves as an alternative electroanalytical technique for screening the filling efficiency of different copper via filling baths. The experiments were performed with a rotating disk electrode. The analysis of the solutions was done using a linear CV method. The potential was scanned at 5mV/s between the set potentials of 200mV and -600mV. Two scans were performed for each experimental condition. The RDE was rotated at 100 and 1600 rpm. The first scan was done at 100 rpm. At the end of the first scan the speed was stepped up to 1600 rpm, and the second scan was performed.

The scan measurements were performed with a EcoChemie potentiostat. A 250ml 3-neck cell was used. The working electrode was a Pt RDE (Pine). A saturated calomel electrode was used as the reference electrode. The speed of the RDE was modulated using a Pine ASR. Concentrated sulfuric acid and chloride were present in the base copper sulfate solution. Three additive systems in the base solution (Rohm & Haas) were used in the analysis. Each of these three systems had a different accelerant, suppressor and leveler. These three systems are named Bath I, Bath II and Bath III.

##### **4.4.1 Analysis of Bath I**

Bath I was subject to linear sweep cyclic voltammetry measurements. Bath I has 3 additives, which are accelerant, suppressor and a leveler. A plot of current vs. potential was made from the current density measured during the potential sweep from 200mV to -600mV. The solid line is the current measured at 100rpm of the RDE and the dashed line at 1600rpm. In this run, the concentration of the accelerant was 10ml/L.

The limiting current ( $i_L$ ) densities from Figure 4.26 were around  $2.1\text{mA}/\text{cm}^2$  and  $3.1\text{mA}/\text{cm}^2$  at 100rpm and 1600rpm respectively. The data points corresponding to the return portion of the scan were plotted. The solid line corresponds to currents measured at 100rpm and the dashed line to 1600rpm. The contrast in the return scans at different RDE speeds is utilized to predict the filling nature of different chemistries. The plot provides a visual understanding of filling performance of the bath. If the return scans at both speeds overlap, then using such a bath would not result in a good fill. Similar plots were made with 15ml/L and 20ml/L of accelerant. The reverse scans for 10ml/l, 15ml/l and 20ml/l of accelerant are shown in Figure 4.27, 4.29 and Figure 4.31 respectively.

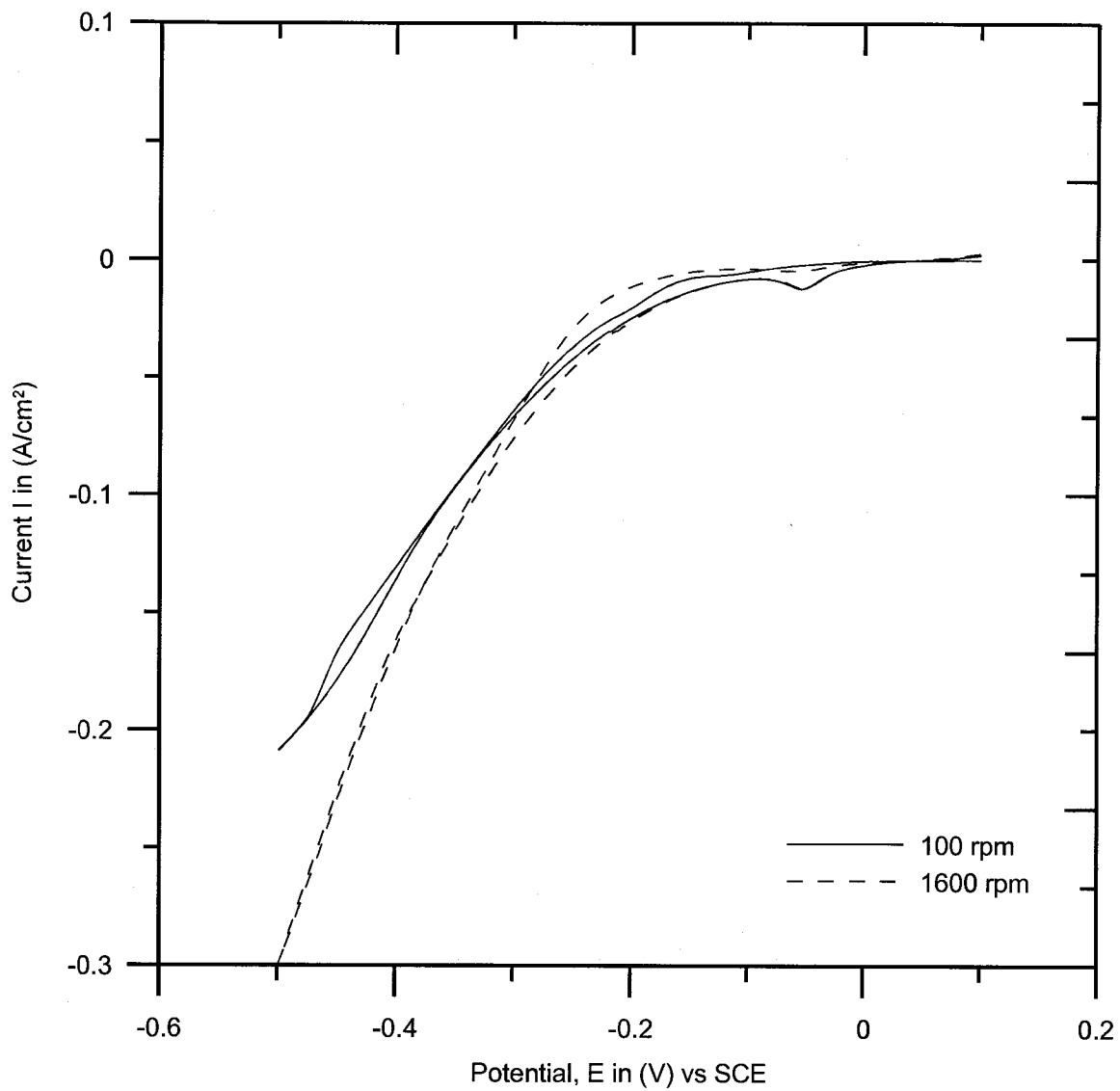


Figure 4.26 Current density vs. potential for 10ml/L of Accelerant in Bath I

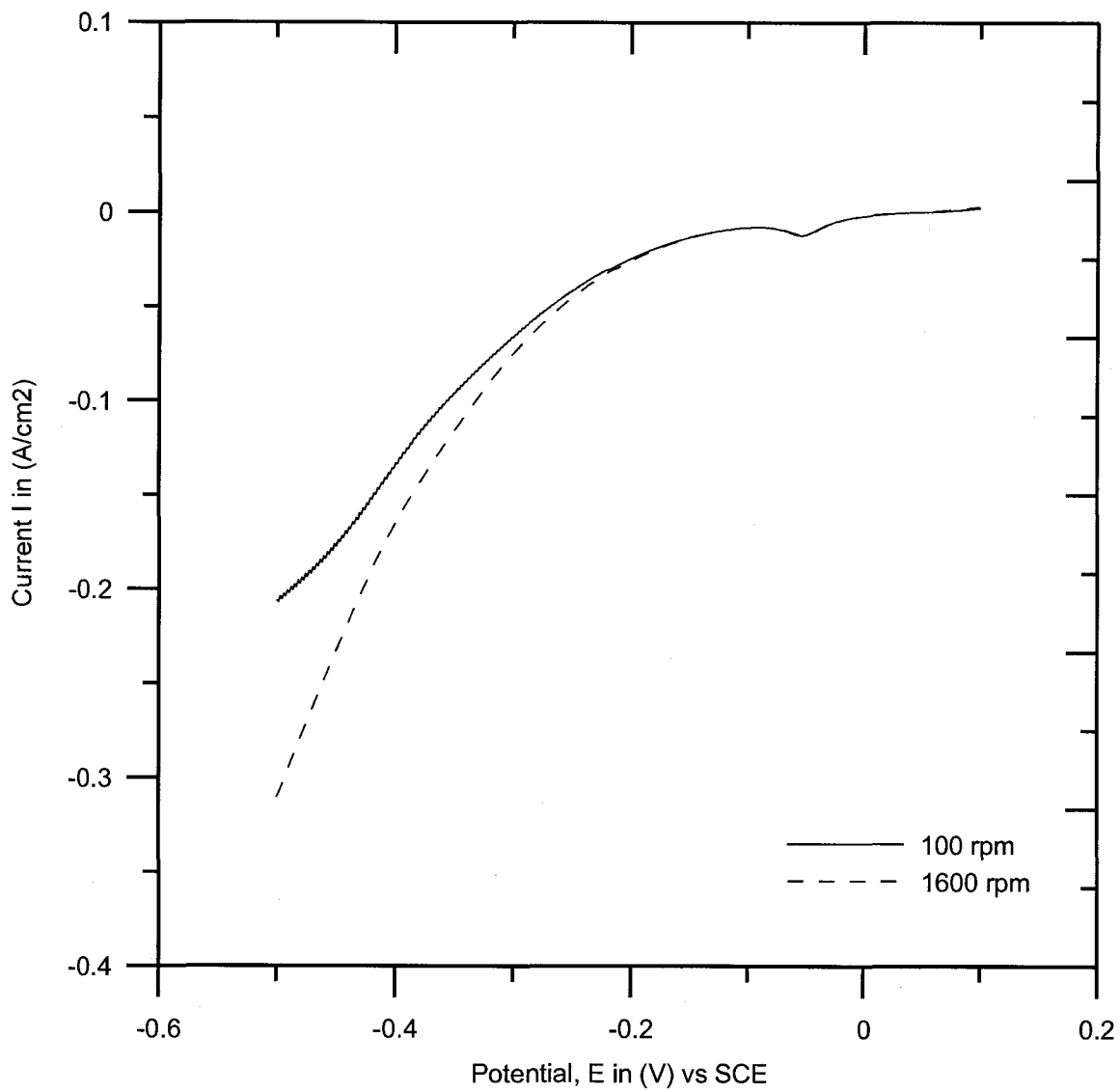


Figure 4.27 Current density vs. potential for 10ml/L of Accelerant in Bath I-Return scan



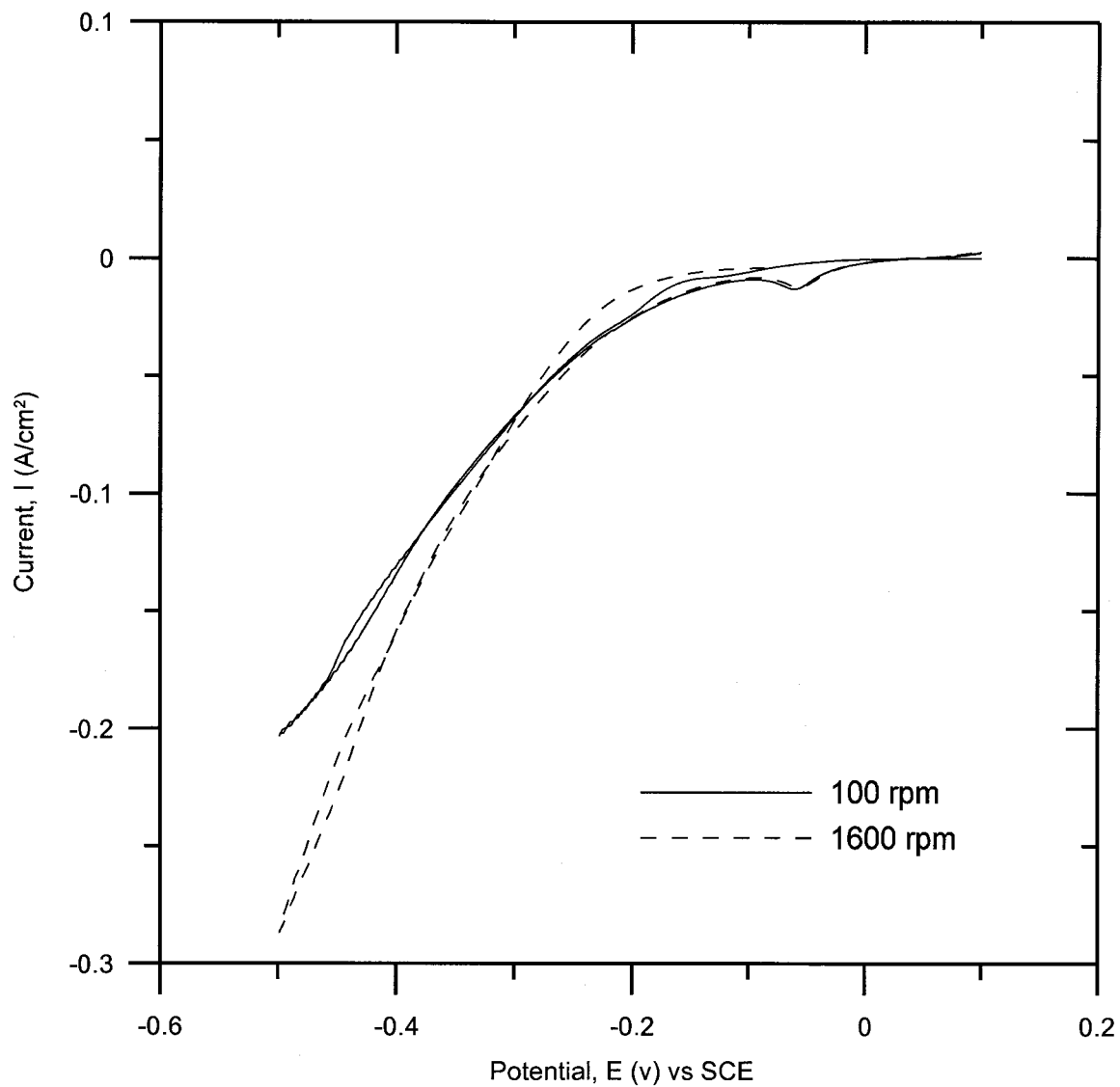


Figure 4.28 Current density vs. potential for 15ml/L of Accelerant in Bath I

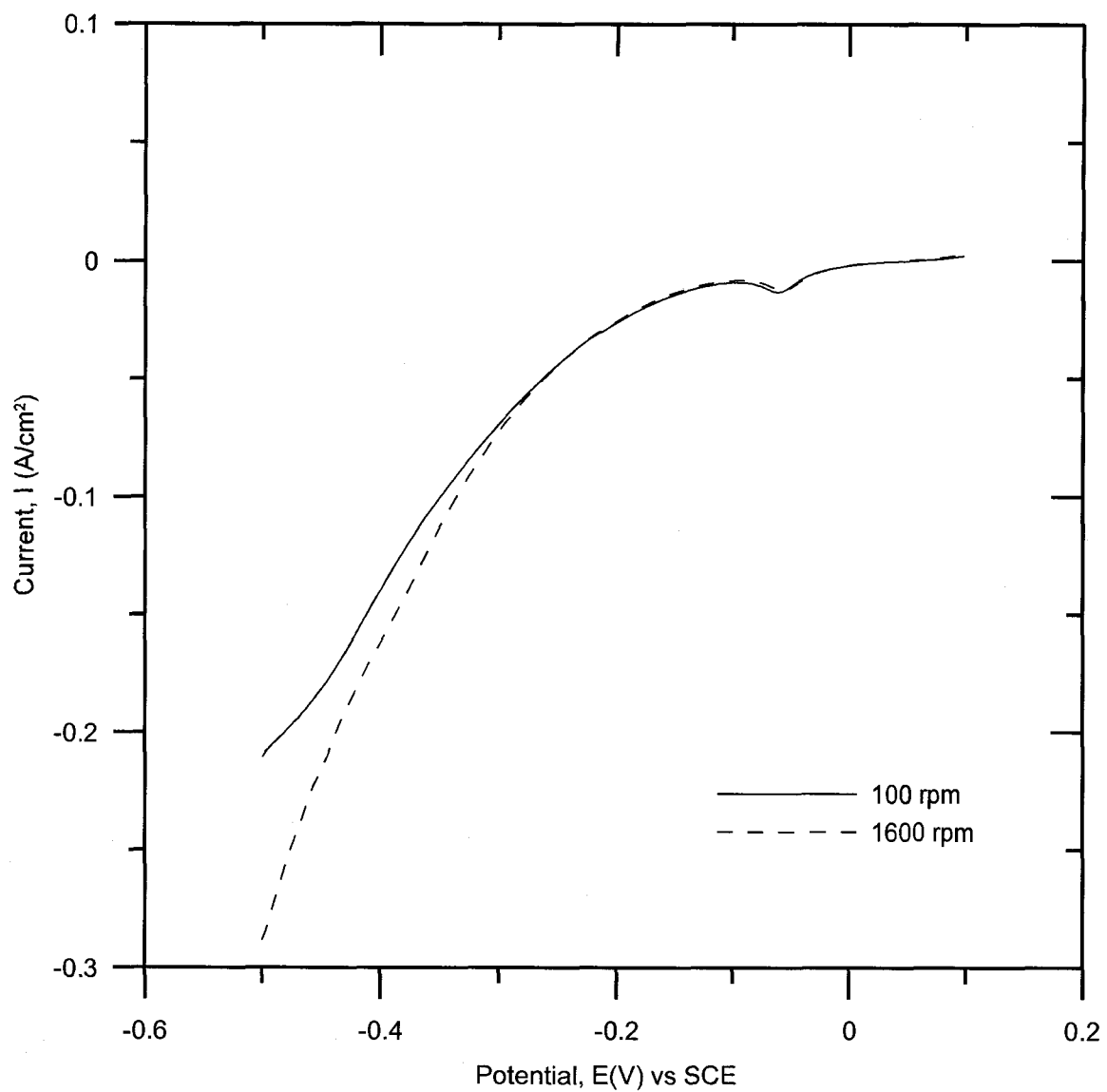


Figure 4.29 Current density vs. potential for 15ml/L of Accelerant in Bath I—Return scan

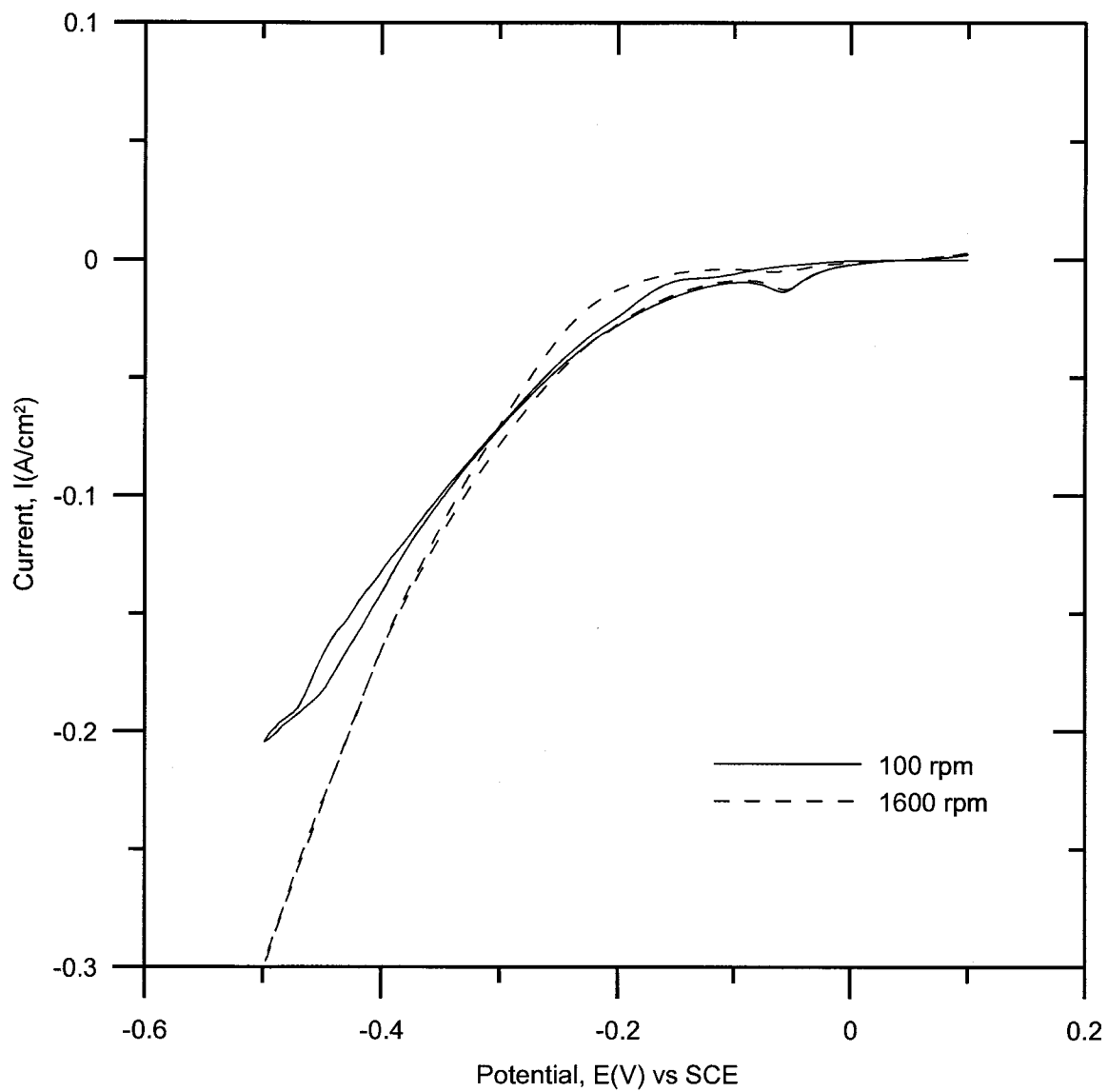


Figure 4.30 Current density vs. potential for 20ml/L of Accelerant in Bath I

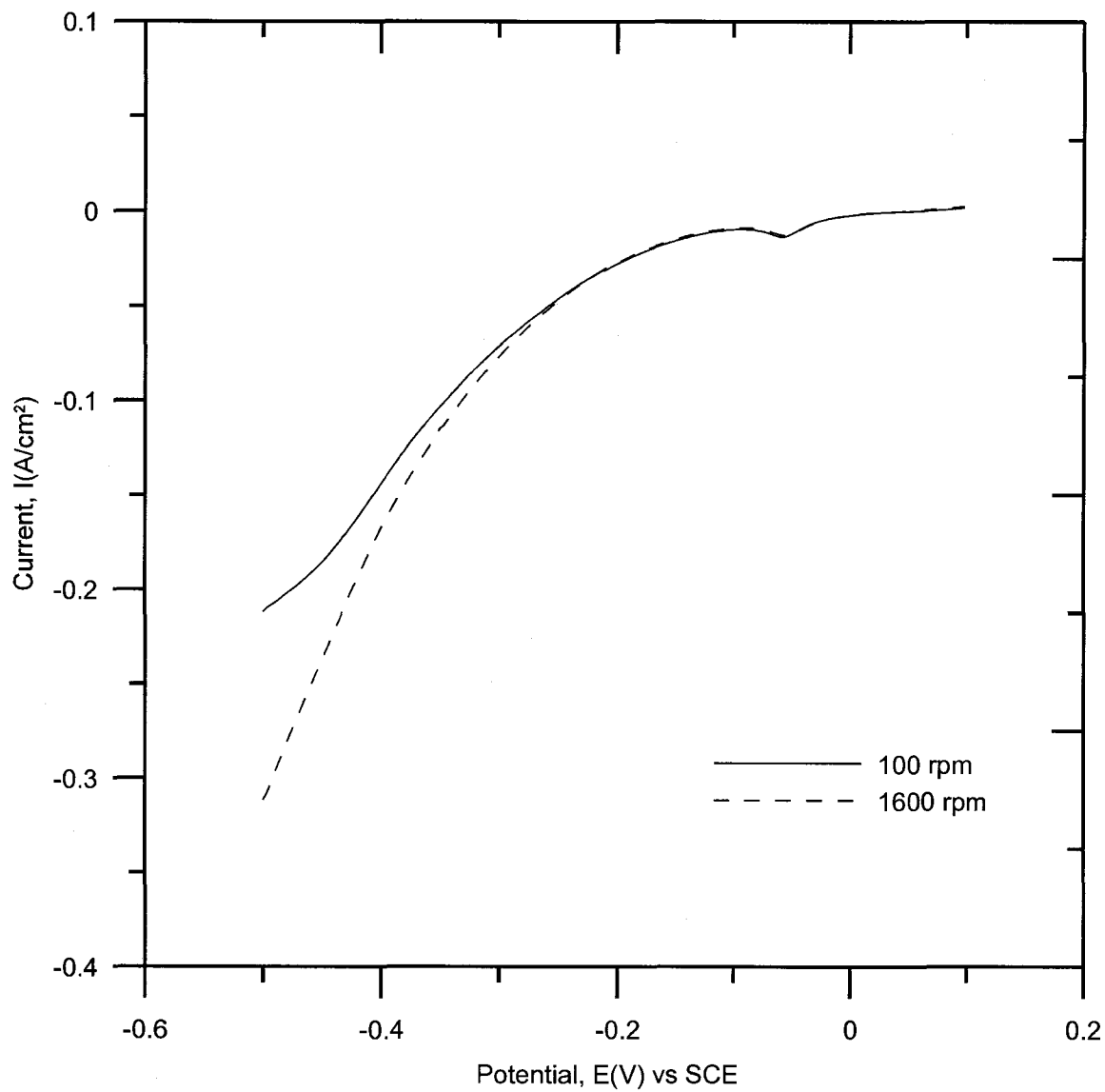


Figure 4.31 Current density vs. potential for 20ml/L of Accelerant—Return scan

#### 4.4.1.1 Accelerant - Fill ratio analysis

The return scan data points of the current density were utilized in determining the fill ratio as a function of the applied potential. Fill ratio measurements obtained for 10ml/L, 15ml/L and 20ml/L of accelerant were plotted against the current measured at 100rpm. Higher current at the bottom of the via is desired for bottom-up filling. In a bath with the optimized concentrations of the additives, the X-axis would help in determining the optimum operating current density.

The fill ratio for this bath is very close to unity and would not be suitable for via filling. From the Figure 4.32, the best accelerant concentration for Bath I is 15ml/L. Accelerant concentration of 20ml/L also has a fill ratio close to that of 15ml/L. The current density at which the maximum fill ratio is obtained is  $0.018\text{A}/\text{cm}^2$ . A higher operating current density is always sought in order to fill the via at a faster rate. The current density is almost the same for all three concentrations of the accelerant.

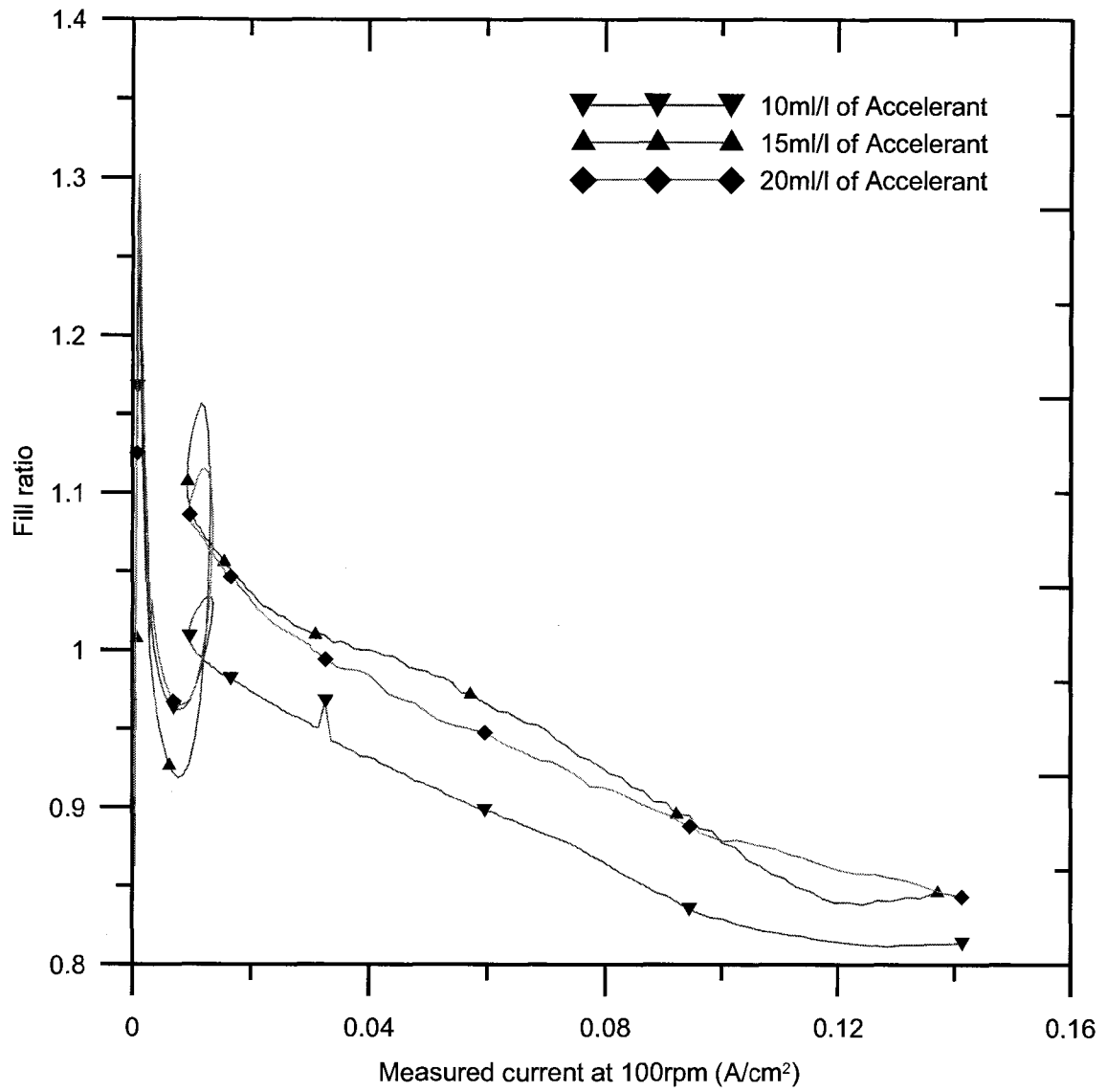


Figure 4.32 Fill ratio vs. measured current at 100rpm

#### 4.4.1.2 Suppressor – Fill ratio analysis

The optimum concentration of the suppressor was determined by CV analysis. The different concentrations analyzed were 5ml/L, 7ml/L and 9ml/L of the suppressor in the base copper via filling electrolyte.

The solid lines in the plots represent the current measured at 100rpm and the dotted lines represent the currents measured at 1600rpm. The 2 scans at 100rpm and 1600rpm are shown in the Figure 4.33. The plot containing the reverse scan data points only is shown in Figure 4.34. The  $i_L$  for 5ml/L at 100rpm and 1600rpm was around  $0.21\text{A}/\text{cm}^2$  and  $0.31\text{A}/\text{cm}^2$  respectively.

Similar current vs. potential plots were constructed for 7ml/L and 9ml/L of the suppressor. The complete scans at 5mV/s for suppressor concentrations of 7ml/L and 9ml/l are shown in Figure 4.35 and Figure 4.37 respectively. The limiting current densities for these concentrations of the suppressor are approximately  $0.2\text{A}/\text{cm}^2$  and  $0.3\text{A}/\text{cm}^2$ . The optimum concentration of the suppressor is determined from the fill ratio measurements from the return scans.

The current density recorded during the reverse potential sweep was utilized in calculating the fill or the Fill ratio. The currents corresponding to potentials close to 0mV and further on till 200mV are neglected, as the currents data points tend to overlap and are irrelevant for fill ratio analysis. From Figure 4.38, suppressor concentration of 5ml/L has the highest fill ratio. However the fill ratio obtained for all concentrations of the suppressor were not very high. The operating current density from the plot would be less than  $0.02\text{A}/\text{cm}^2$  when Bath I is used with a suppressor concentration of 5ml/L to get the highest filling performance.

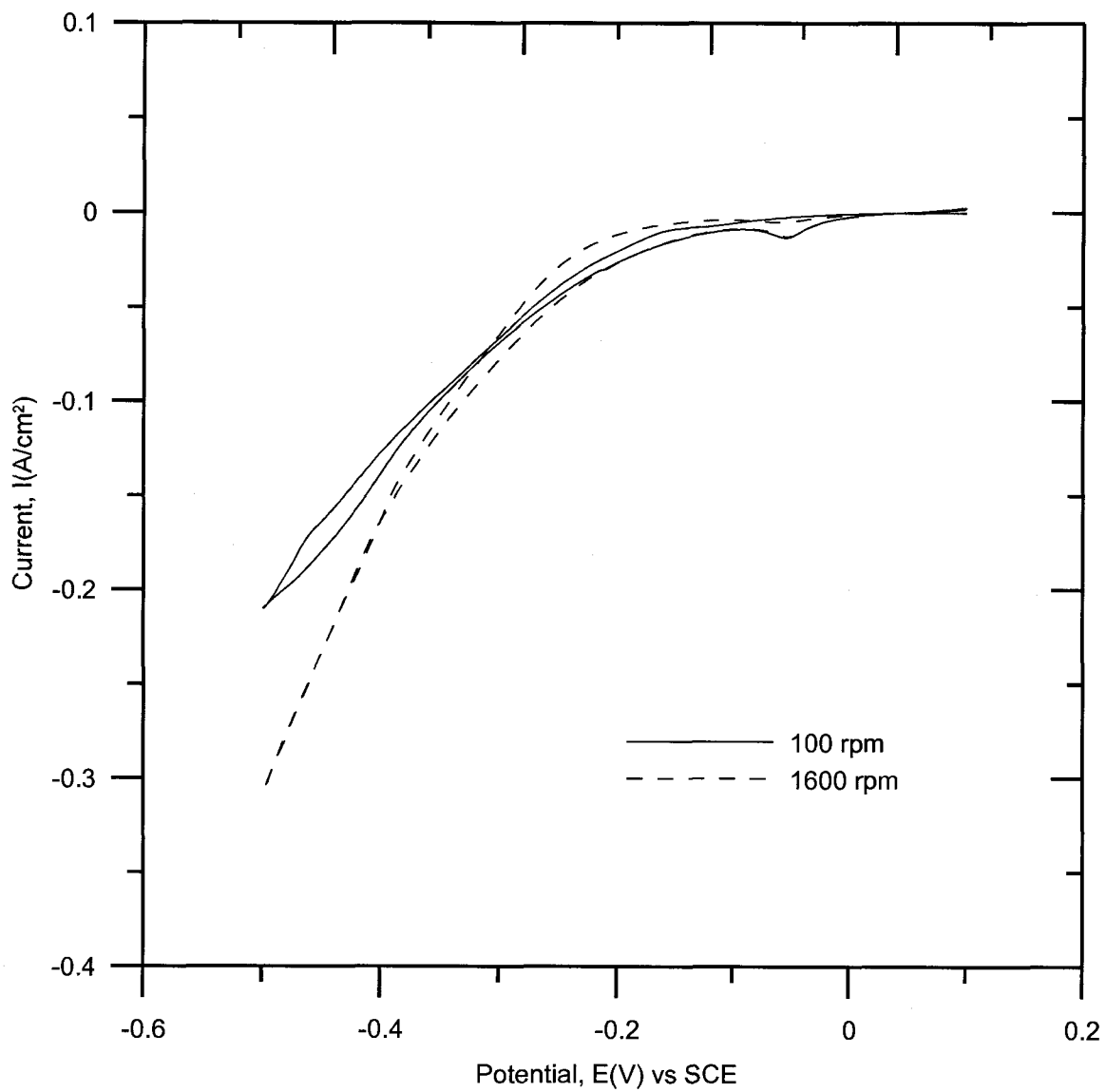


Figure 4.33 Current density vs. potential for 5ml/L of Suppressor in Bath I



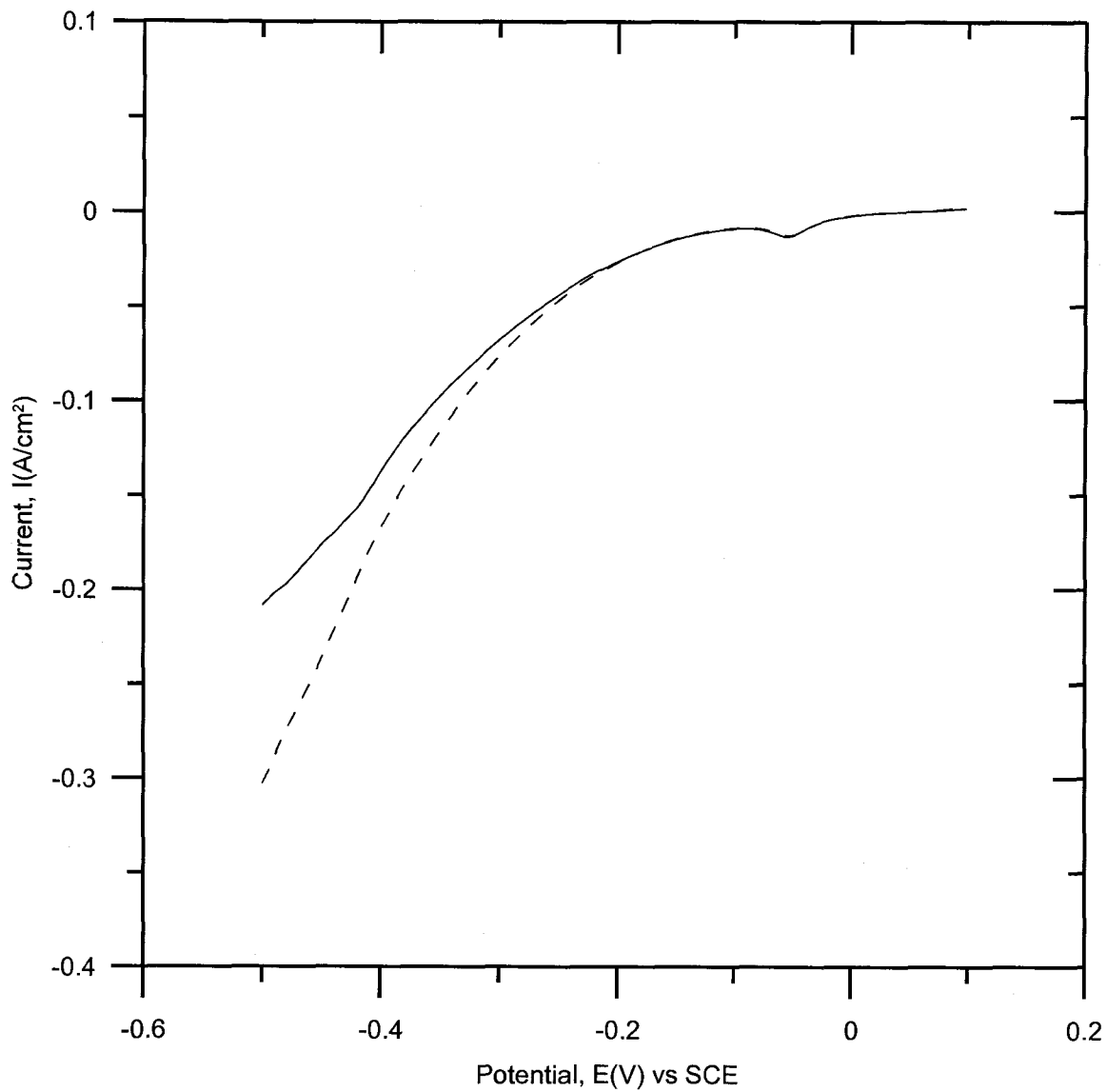


Figure 4.34 Current density vs. potential for 5ml/L of Suppressor in Bath I – Return scan

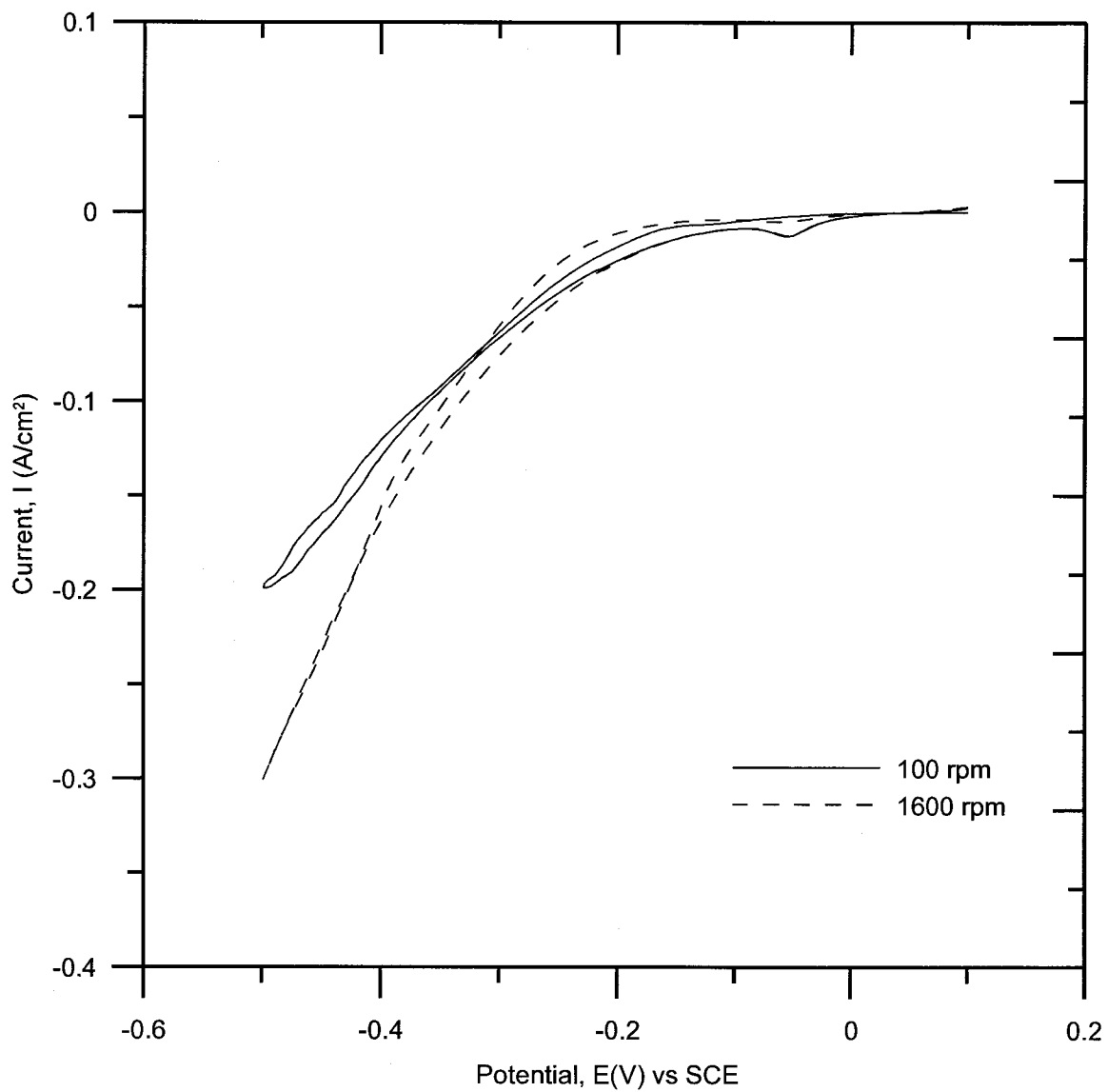


Figure 4.35 Current density vs. potential for 7ml/L of Suppressor in Bath I

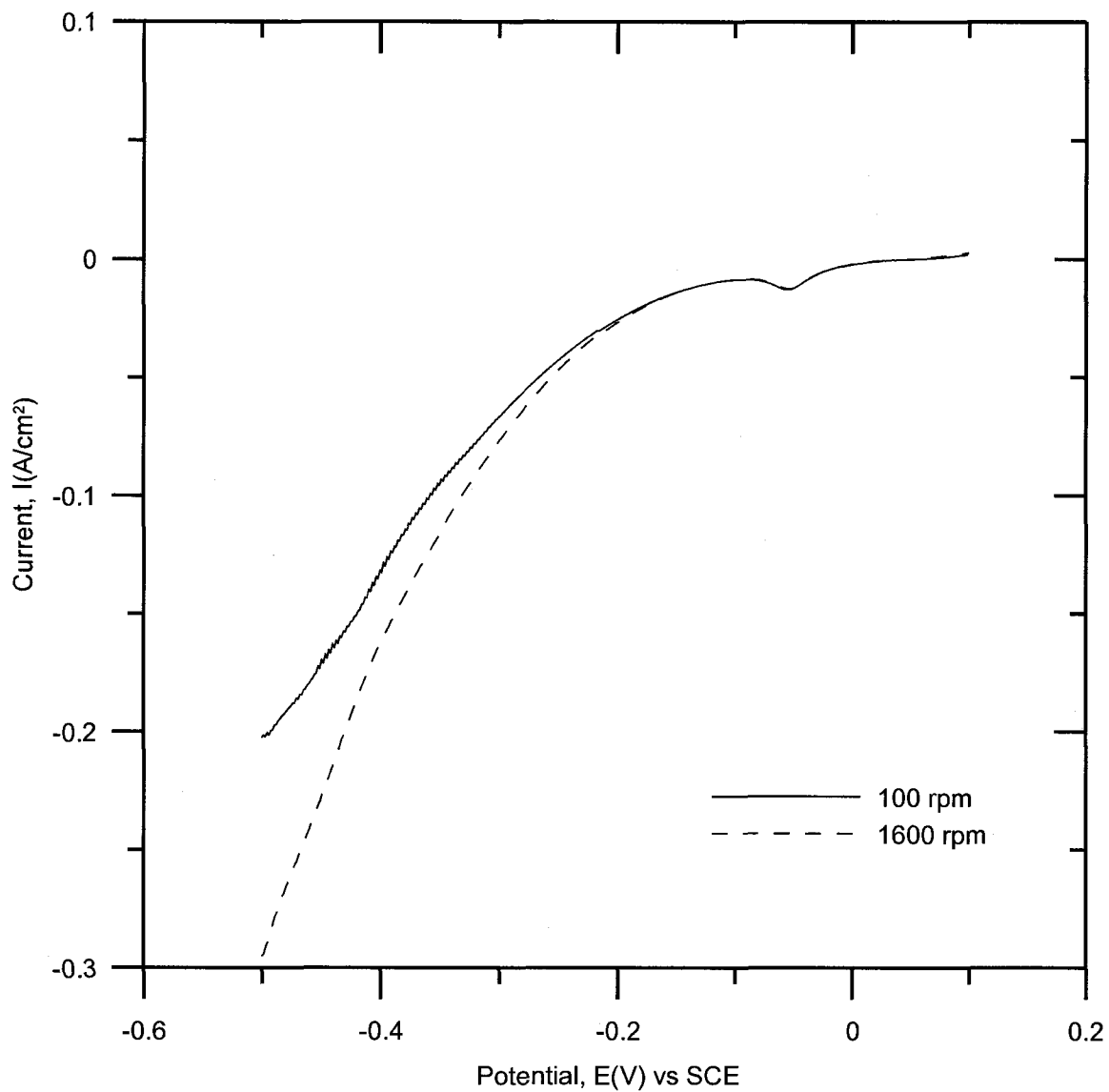


Figure 4.36 Current density vs. potential for 7ml/L of Suppressor in Bath I – Return scan

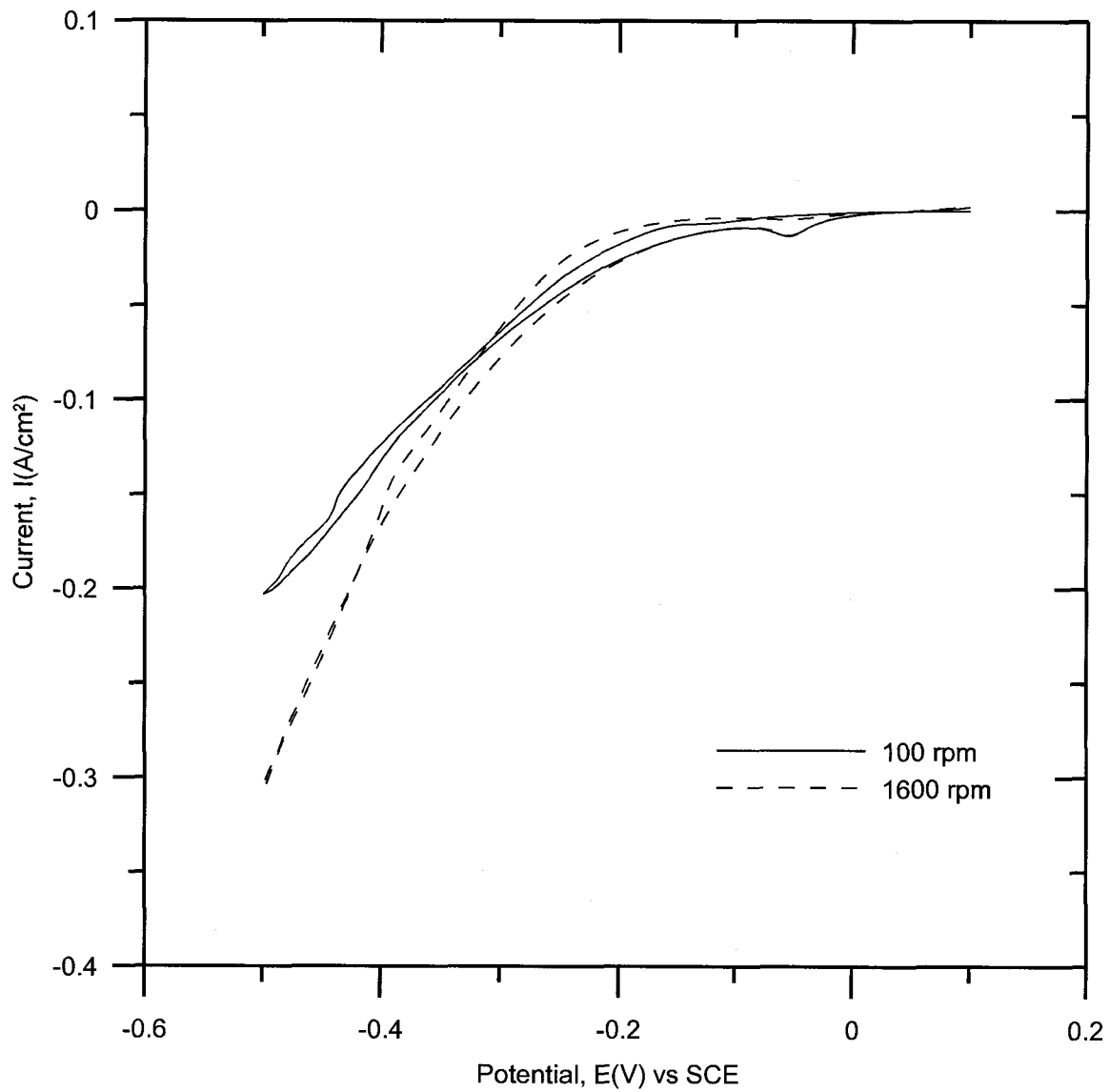


Figure 4.37 Current density vs. potential for 9ml/L of Suppressor in Bath I

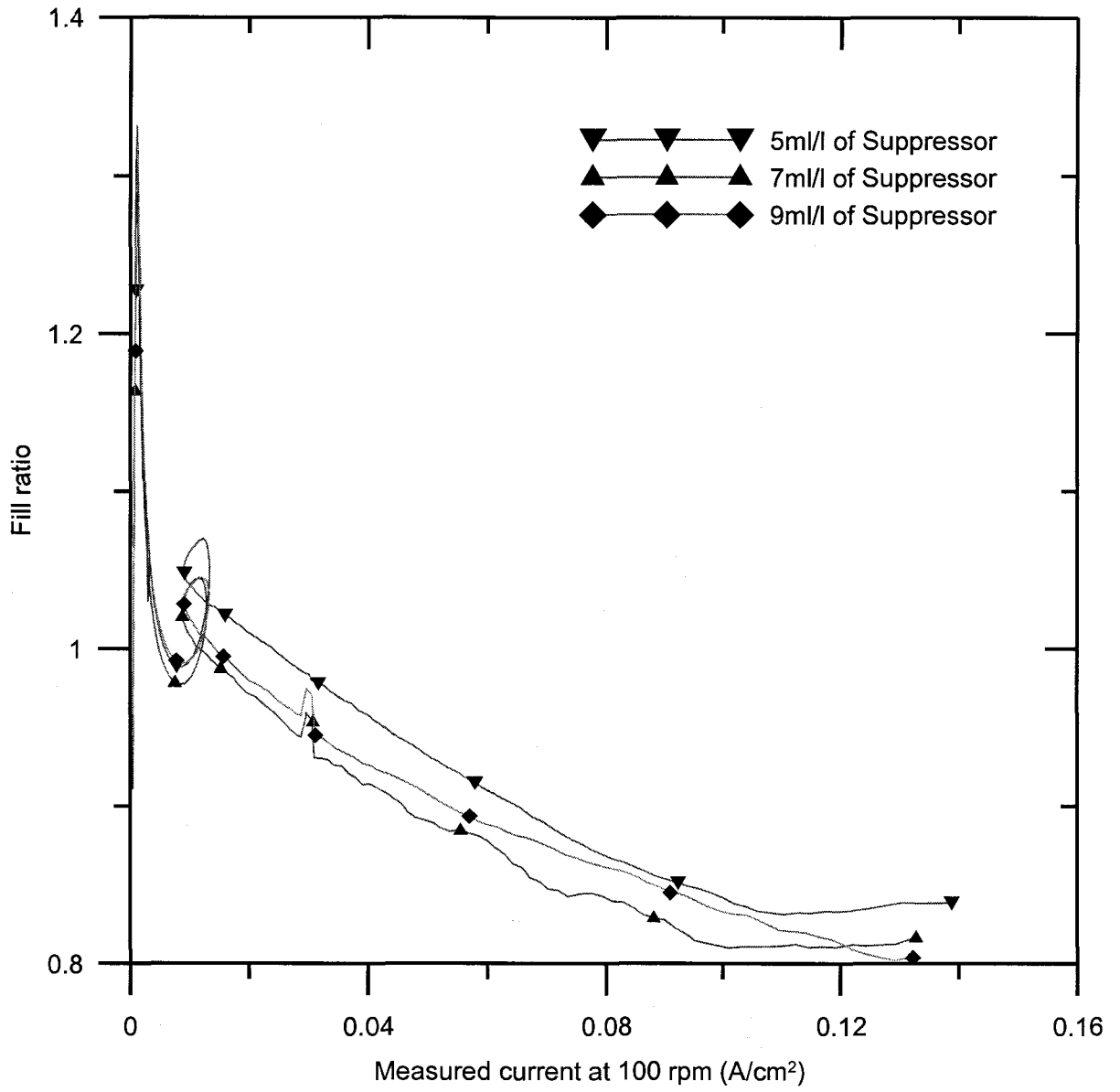


Figure 4.38 Fill ratio vs. current measured at 100rpm of the RDE

#### 4.4.1.3 Leveler – Fill ratio analysis

CV analysis of a copper via filling chemistry with varying concentrations leveler was performed. The leveler concentrations were 2.5ml/L, 4.5ml/L and 6.5ml/L in the standard solution. The plot in Figure 4.39 shows the forward and the return scan for 2.5ml/L of the leveler. The  $i_L$  is around 0.029A/cm<sup>2</sup> and 0.042A/cm<sup>2</sup> at 100rpm and 1600rpm. Similar CV experiments were carried out with a fresh Pt RDE in copper via filling electrolyte with 4.5ml/l and 6.5ml/l of leveler respectively. The plot of the return scan data is shown in Figure 4.42 and Figure 4.44 for 4.5ml/L and 6.5ml/L of leveler respectively. A small increase in the  $i_L$  up to 4.5A/cm<sup>2</sup> is observed for these concentrations at 1600rpm.

The fill ratio plot is constructed from the return scan data. The ratio of the currents measured at 100rpm and 1600rpm of the RDE is plotted against the currents measured at 100rpm of the RDE. From the fill ratio plot in Figure 4.45, 2.5ml/L of leveler has the highest fill ratio. Bath I has better filling capacity at lower concentrations of bath additives. The operating current density for Bath I is less than 0.02A/cm<sup>2</sup>. At this current density, the highest fill ratio was observed but it was not large enough. The bath with the best fill ratio was then used for copper via filling process on a pilot scale.

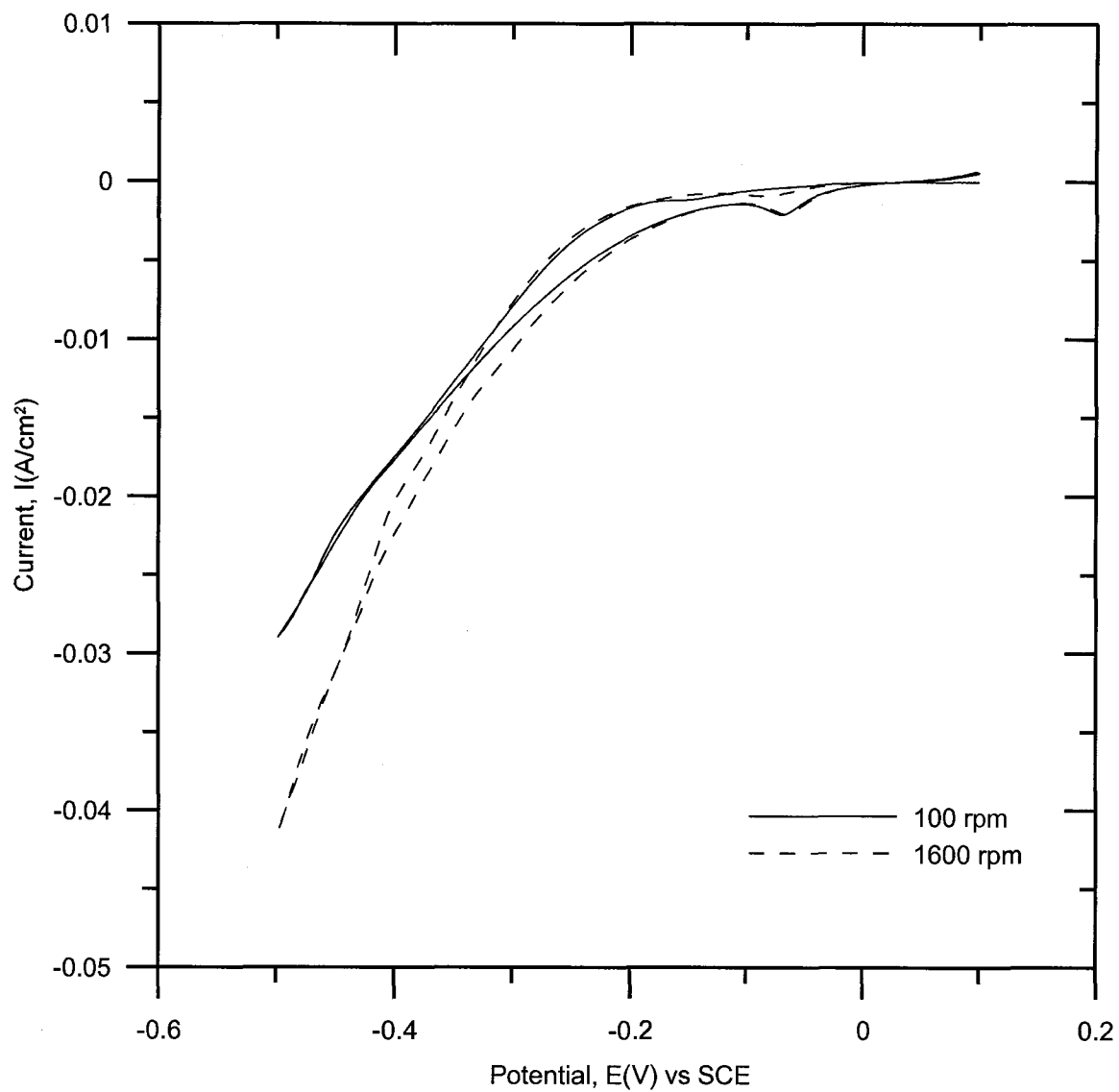


Figure 4.39 Current density vs. potential for 2.5ml/L of Leveler in Bath I

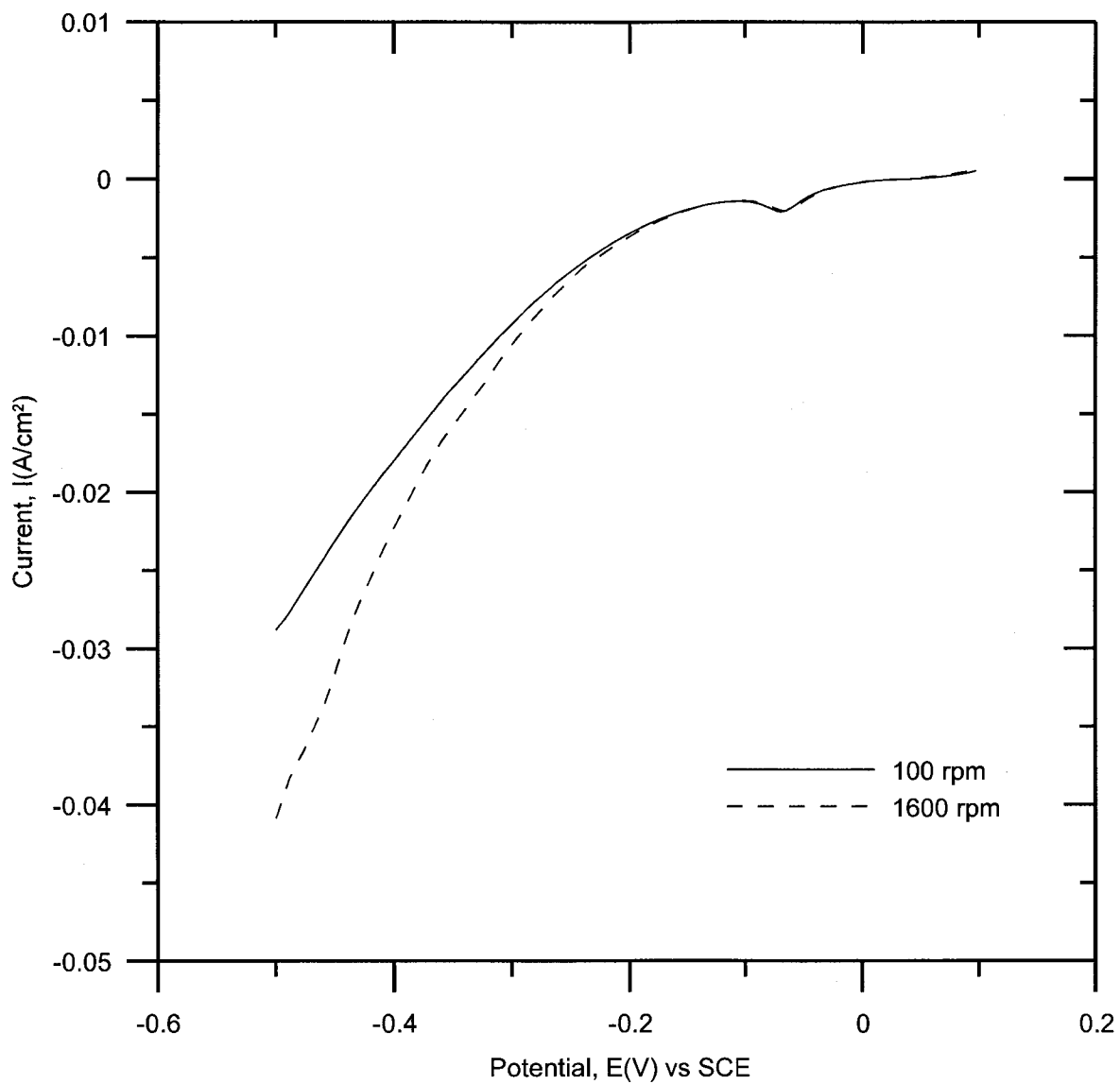


Figure 4.40 Current density vs. potential for 2.5ml/L of Leveler in Bath I – Return scan



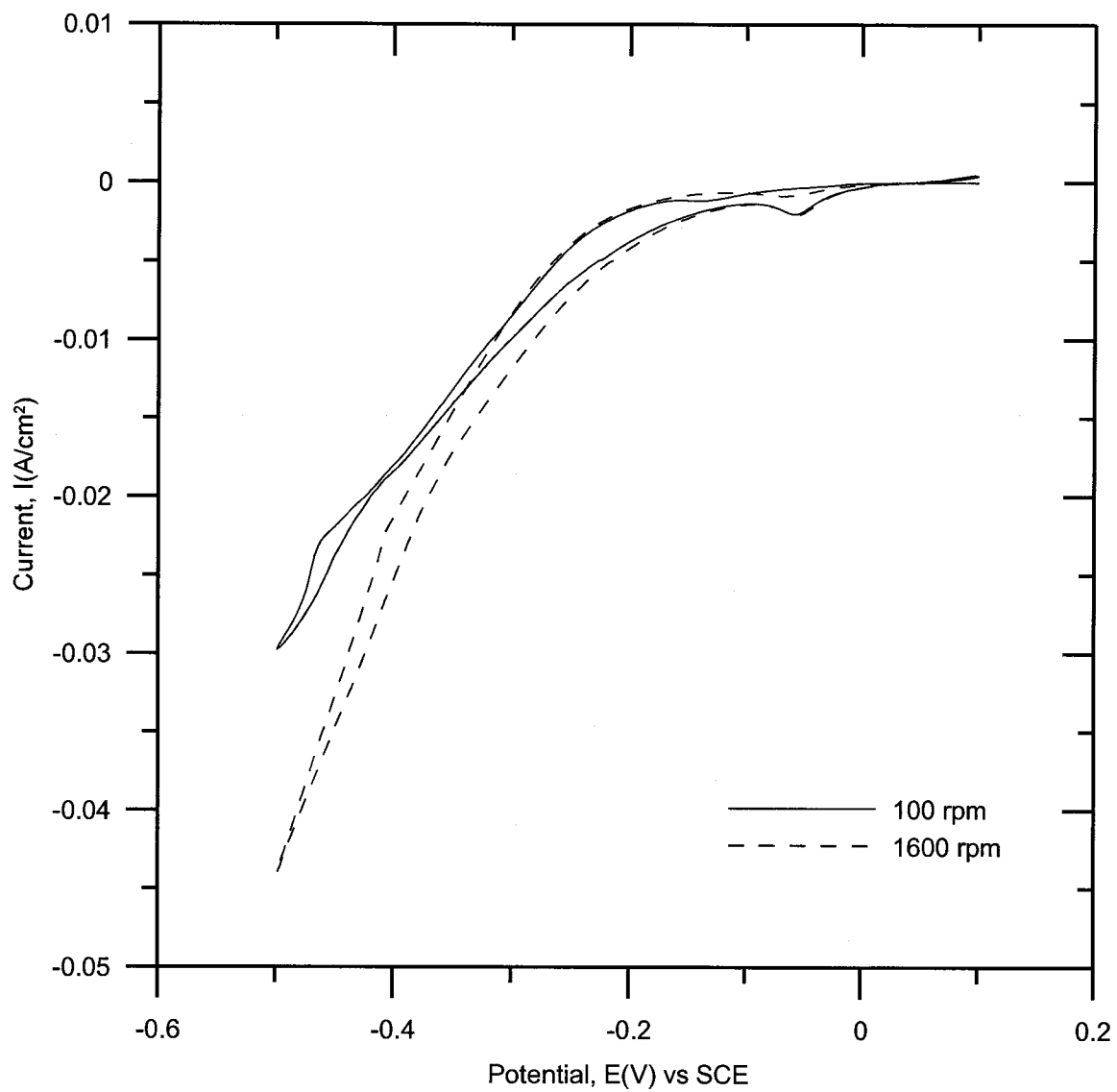


Figure 4.41 Current density vs. potential for 4.5ml/L of Leveler in Bath I

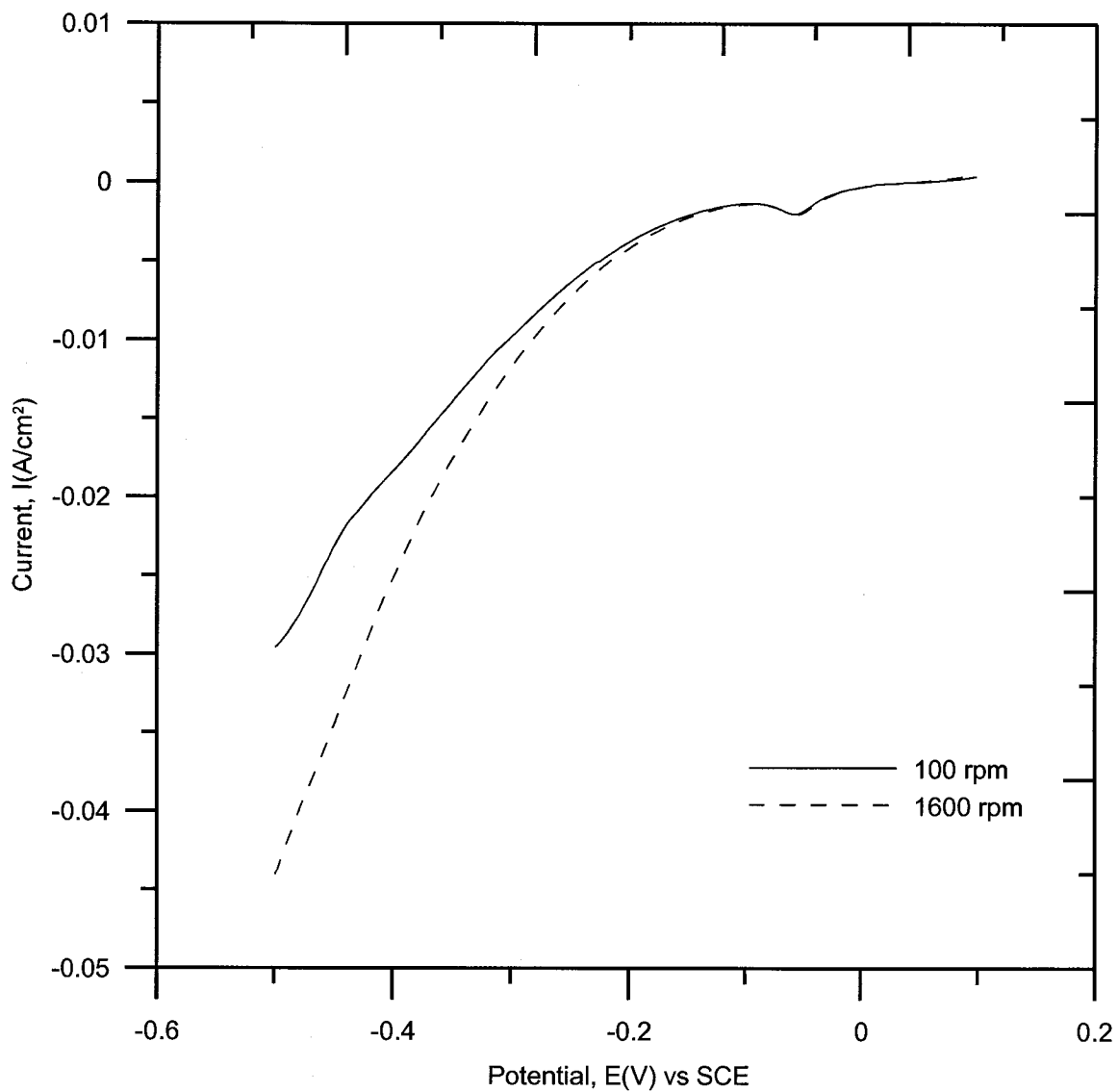


Figure 4.42 Current density vs. potential for 4.5ml/L of Leveler in Bath I – Return scan

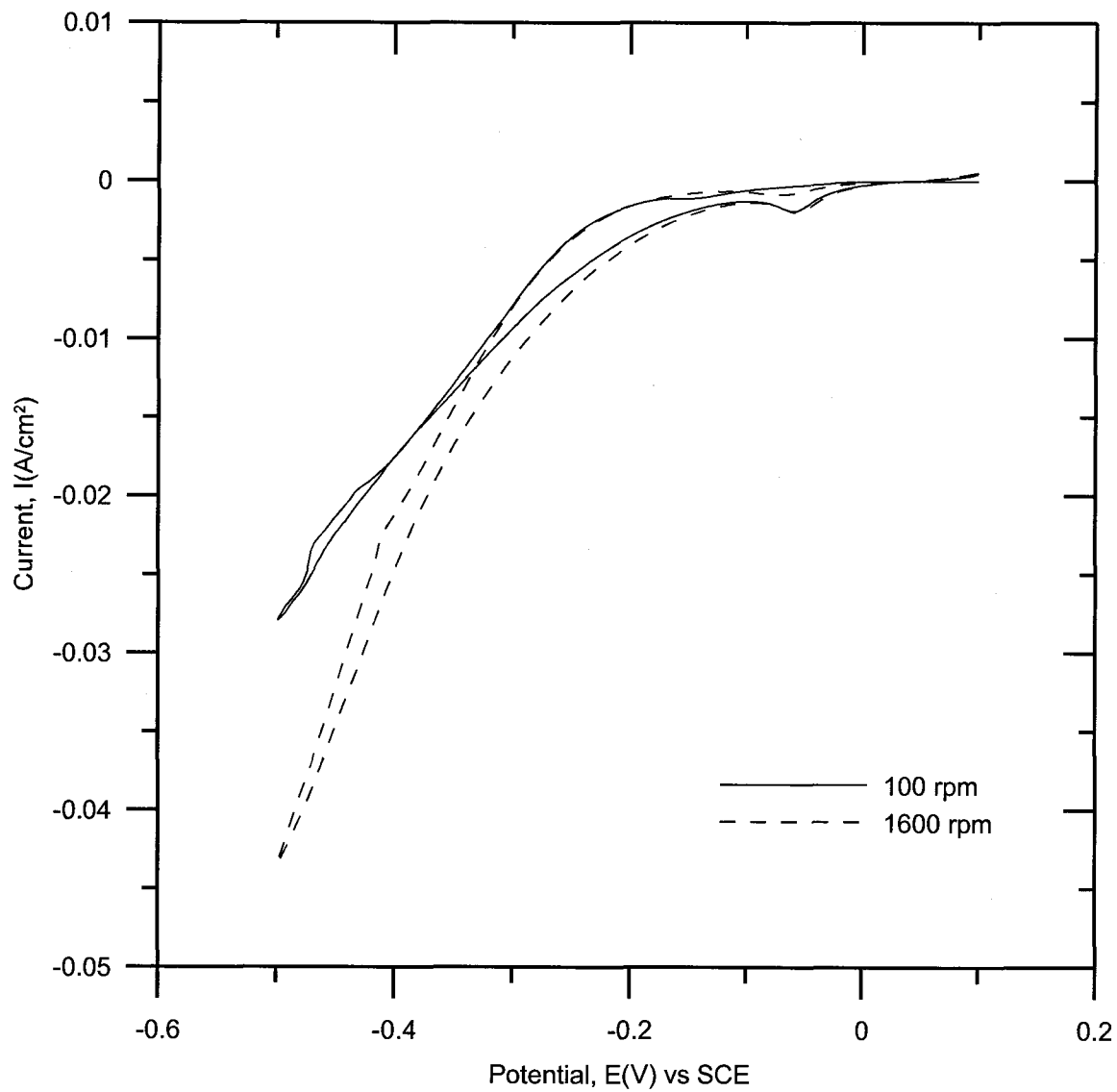


Figure 4.43 Current density vs. potential for 6.5ml/L of Leveler in Bath I

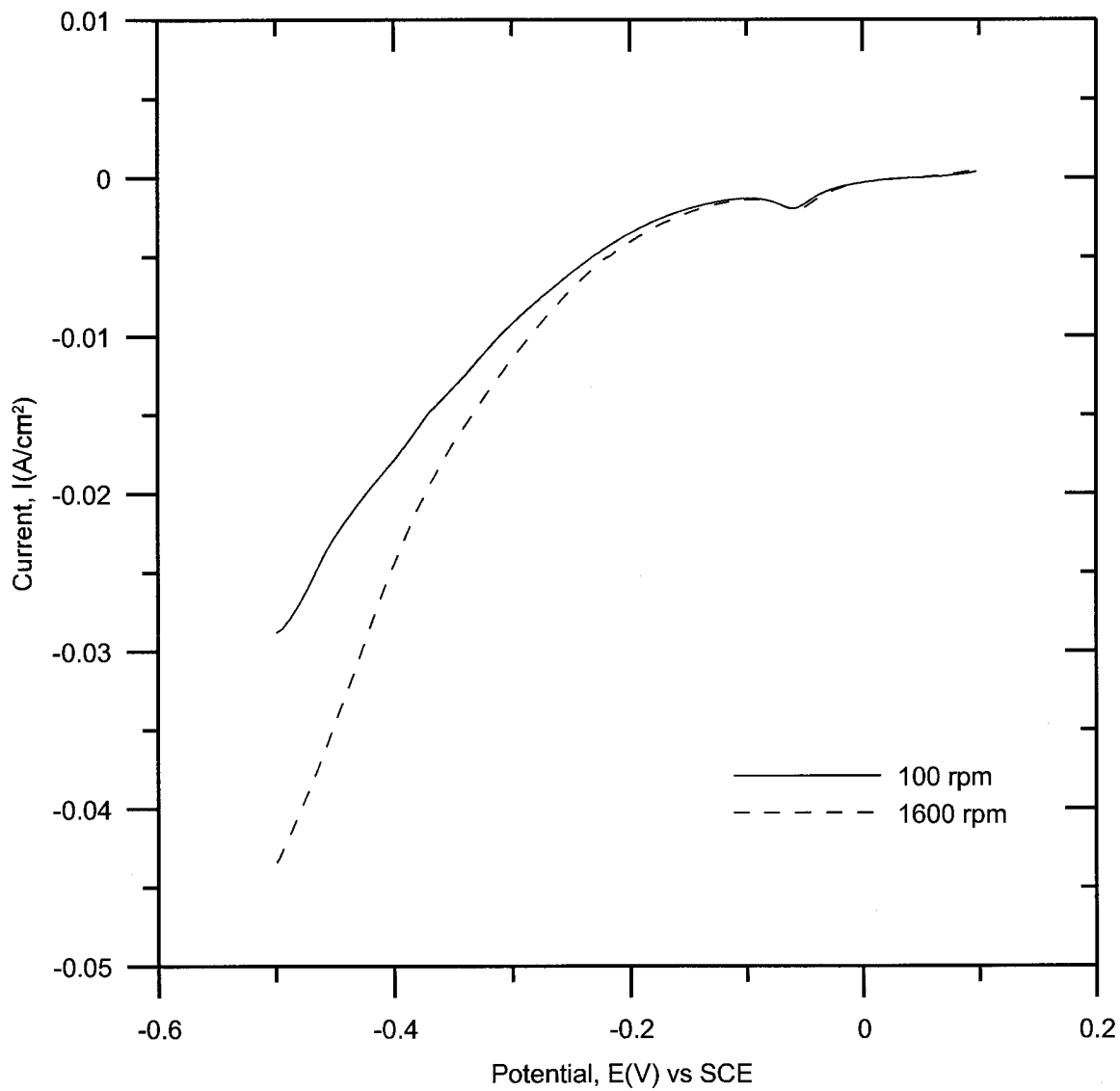


Figure 4.44 Current density vs. potential for 6.5ml/L of Leveler in Bath I – Return scan

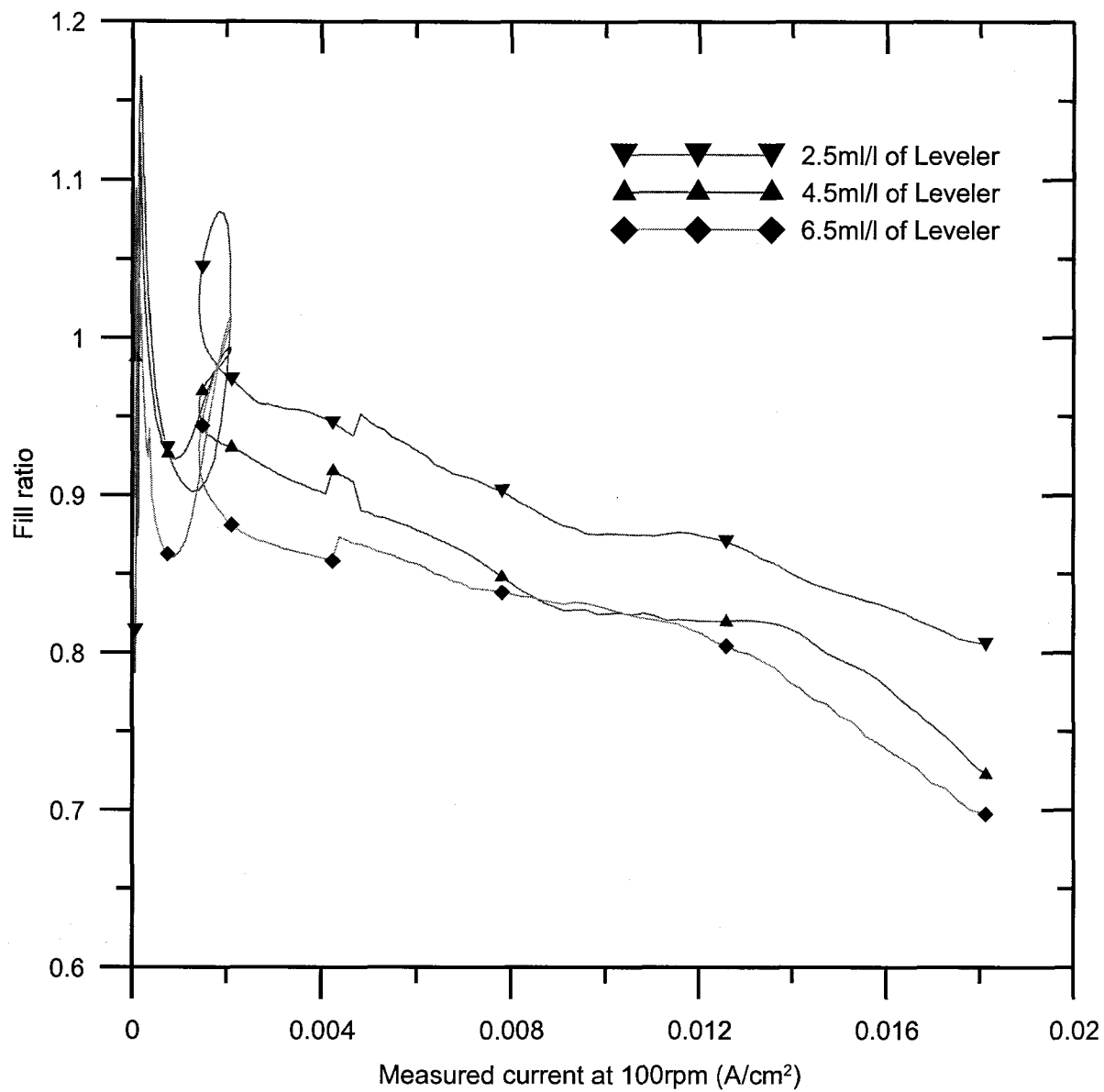


Figure 4.45 Fill ratio vs. current measured at 100rpm of RDE

#### 4.4.2 Analysis of Bath II

Bath II was subjected to cyclic voltammetry analysis by the method described above. Bath II has 3 additives whose optimum concentration in the bath had to be determined. The bath was optimized for concentrations of suppressor, accelerant, and leveler. The accelerant concentration in the electrolyte was varied holding the suppressor and levelers at a constant concentration. Suppressor and leveler concentrations were optimized in the same way. Fill ratio analysis was used.

From Figure 4.46, an accelerant concentration of 10ml/L has a higher fill ratio value compared to that of 15ml/L and 20ml/L. Although 10ml/L of accelerant had a higher number value of fill ratio, 15ml/L was chosen to be the best accelerant concentration as it has a higher current density measured at 100rpm.

In the standard solution with 15ml/l of accelerant and 2.5ml/l of the leveler, the suppressor concentration was varied. The concentrations of the suppressor that were studied are 5ml/l, 7ml/l and 9ml/l. The CV scans at 100rpm and 1600rpm of the RDE was used to evaluate the fill ratios for each of the suppressor concentrations and a plot of the fill ratio vs. the measured current density was constructed. The plot is shown in Figure 4.47. From the plot, each of the suppressor concentrations has its optimum at almost the same current density, i.e. at  $0.0125\text{A}/\text{cm}^2$ . However, the fill ratio is as large as 2 for chemistry with 5ml/l of the suppressor. So, a suppressor concentration of 5ml/l was picked to be the optimum.

The leveler concentration in standard solution (Bath II) was varied. Leveler concentrations of 2.5ml/L, 3.5ml/L and 4.5ml/L were analyzed. CV scans were performed and the reverse sweep data at 100rpm and 1600rpm of the RDE was used to

evaluate the filling efficiency of each of the leveler concentrations analyzed. The plot of the fill ratio vs. the current measured at 100rpm of the RDE is shown in the Figure 4.48. From this plot, a leveler concentration of 2.5ml/L has the highest fill ratio. But the current density is not less when compared with 3.5ml/L and 4.5ml/L of the leveler. There isn't a lot of difference in the fill ratios for different concentrations. Hence, 4.5ml/L of the leveler with a larger current density measured was chosen to be the optimum as higher plating rates are sought.

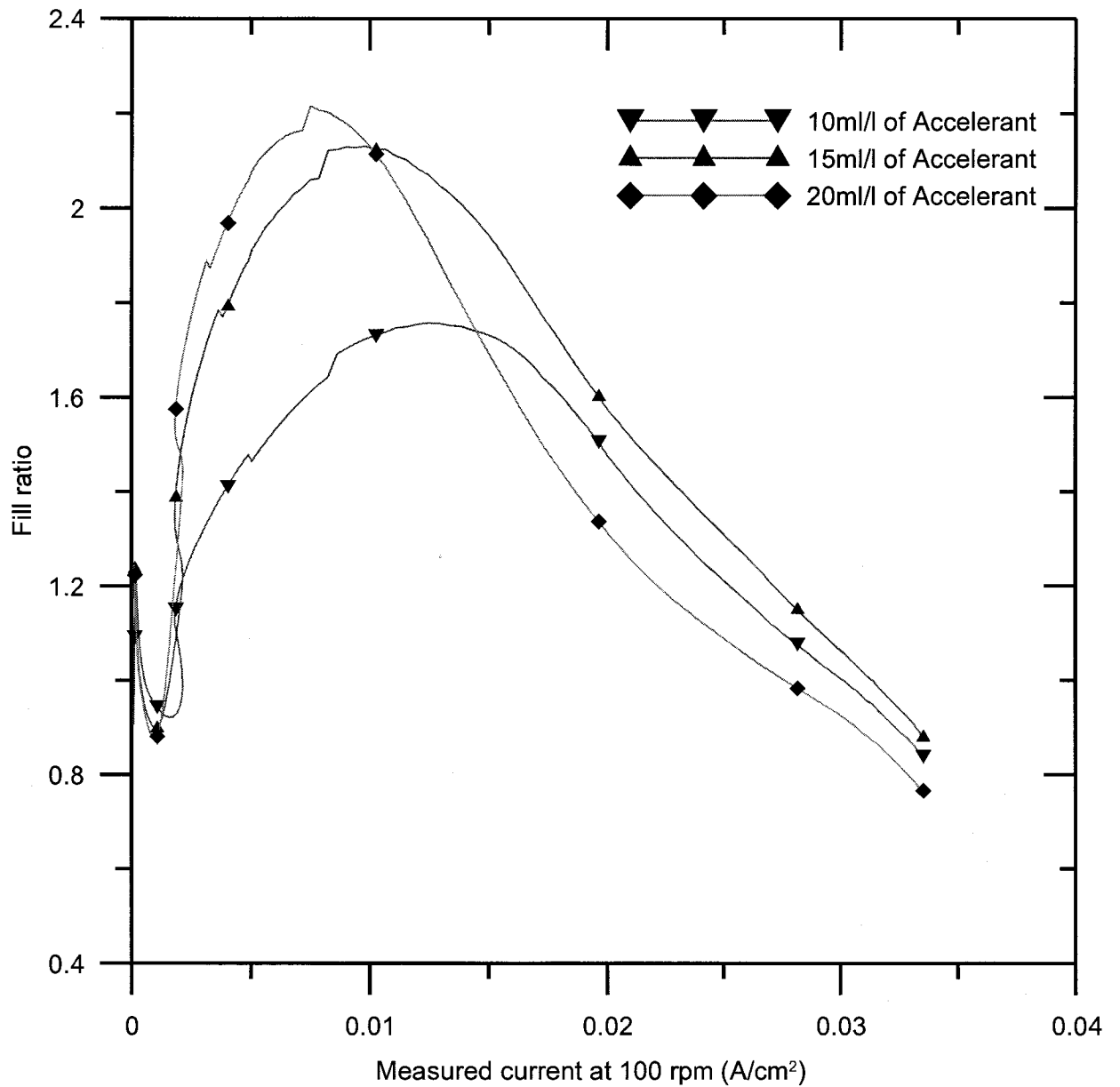


Figure 4.46 Fill ratio vs. current measured at 100rpm of RDE – Accelerant in Bath II



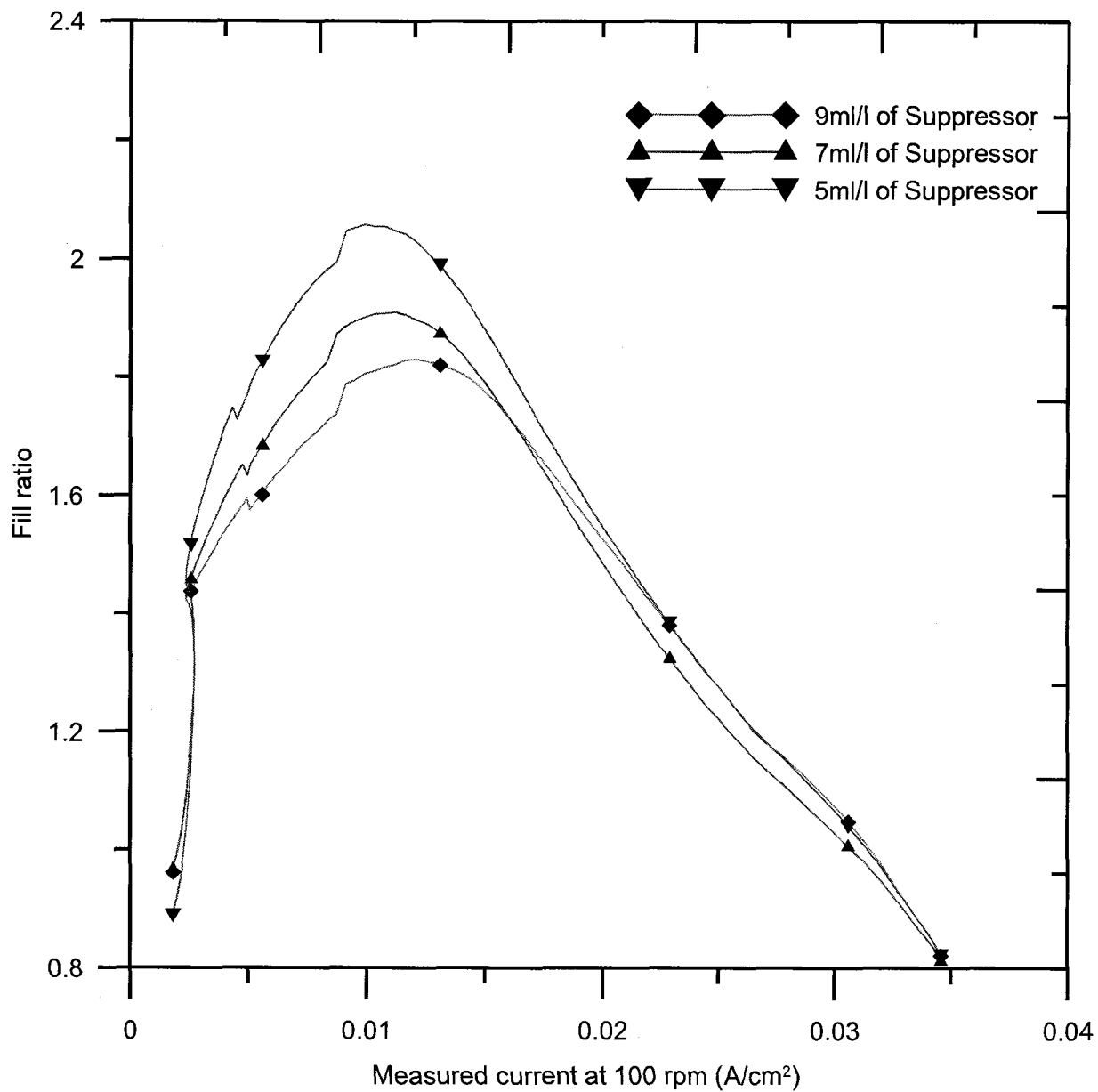


Figure 4.47 Fill ratio vs. current measured at 100rpm of RDE – Suppressor in Bath II

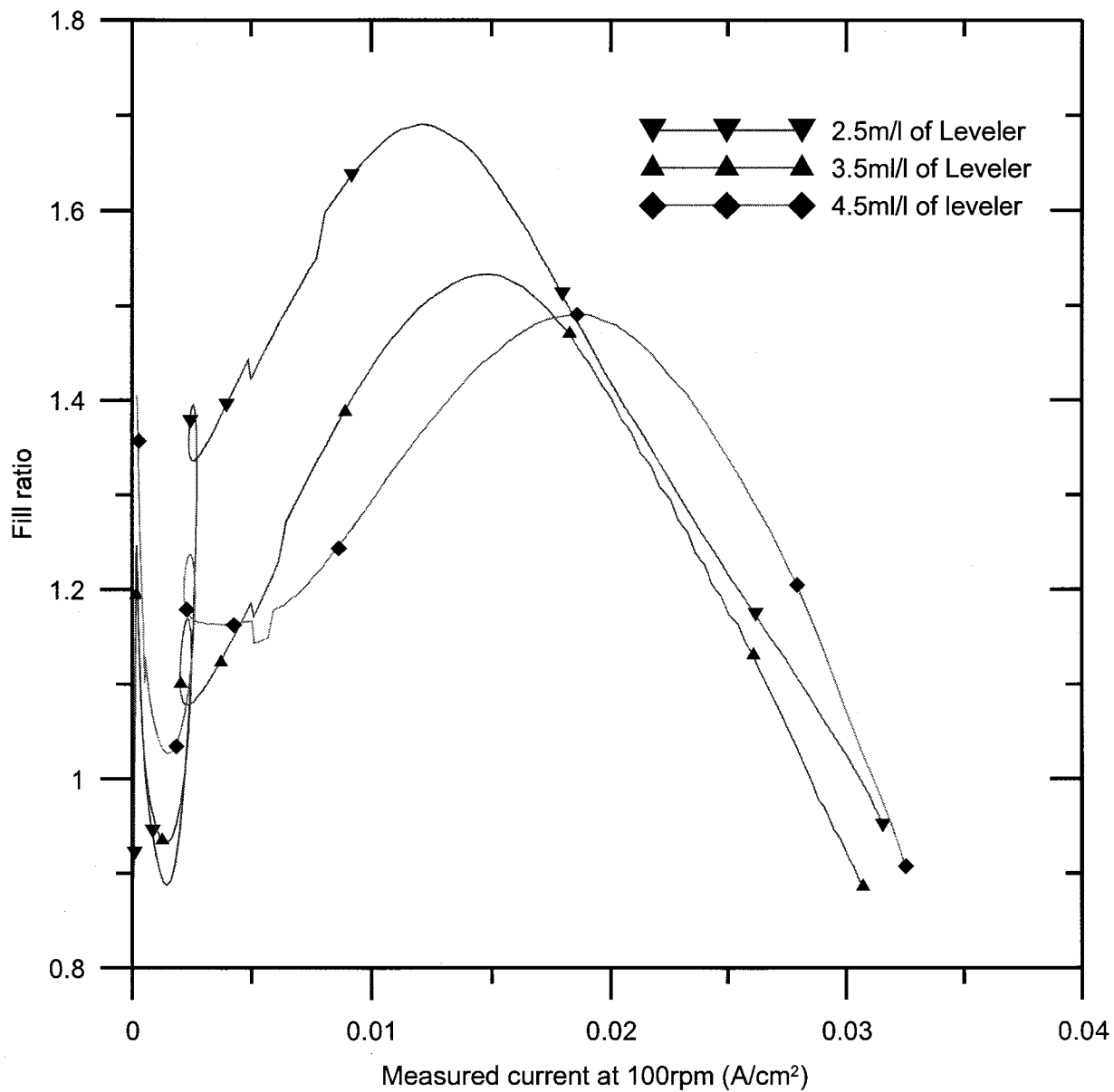


Figure 4.48 Fill ratio vs. current measured at 100rpm of RDE – Leveler in Bath II

#### 4.4.3 Analysis of Bath III – Current/Potential controlled studies

The third bath - Bath III, was analyzed using a combination of galvanic and potential pulse reversal methods. Bath III also has three additives, an accelerant, a suppressor and a leveler. The compositions of these additives are propriety. The copper base electrolyte contains 0.625M of  $\text{CuSO}_4 \cdot 5\text{H}_2\text{O}$ , 0.2M of conc.  $\text{H}_2\text{SO}_4$  and 50ppm of  $\text{Cl}^-$ . The Pt RDE was the working electrode with SCE as the reference. The concentrations of each the additives were varied holding the other two as constant.

For each additive concentration, the first step was a 10min cycle of controlled current chronopotentiometry. A current of 6.56mA was applied with the electrode speed at 160rpm. This step builds up the seed layer. This is then followed by a current wave train of 6.56/-13.12/0mA for 200/10/200ms. At the end of the 60 cycles, the ON/REV/OFF potentials are read out from the last cycle. The electrode is then stripped of any deposited copper by rinsing in a solution containing conc.  $\text{HNO}_3$  and ultrapure water. The electrode is rinsed thoroughly with ultrapure water before being used again.

With the measured potentials, a controlled potential chronoamperometric analysis is run at the same frequency. The current and the charge are measured at different RDE speeds. The ratio of the currents measured is used to compute the fill ratio. The same procedure is followed for varying concentrations of the accelerator, leveler and suppressor. A plot of fill ratio vs. the additive concentration is constructed to determine the optimum concentration. Table 4.5 gives an idea of the whole experimental procedure.

Table 4.5: Experimental procedure for Bath III analysis –Suppressor 1ml/L

Dummying	Galvanostatic	Potentiostatic	rpm	I(mA)	Q(mC)	Transport ratio	
Chronopotentiometry	6.56 / -13.12 / 0 mA	-305/387/88mV	2560	3	35.62	I <sub>40</sub> / I <sub>2560</sub>	1
6.56 mA	200/10/200ms	200/10/200ms	640	3.6	46.18	I <sub>160</sub> / I <sub>2560</sub>	1.55
10 min @ 160 rpm	160 rpm	60 cycles	160	4.65	50.43		
	60 cycles		40	3	35.42		

The concentration of the suppressor was varied holding the accelerant and the leveler concentrations at 15ml/L and 2.5ml/L respectively. The methods were applied at different RDE speeds. From the measured currents, fill ratios of  $I_{40}/I_{2560}$  and  $I_{160}/I_{2560}$  were computed. A plot of fill ratio vs. the suppressor concentration was constructed. This is shown in the Figure 4.49. From the figure, the fill ratio  $I_{160}/I_{2560}$  has a higher value and the optimum concentration of the suppressor lie in between 4ml/L & 6ml/L of the suppressor.

A similar experimental procedure was followed to determine the best accelerant and leveler concentrations in Bath III. The accelerant concentration was varied in-between 5ml/L and 25ml/L in Bath III having 5ml/L of suppressor and 2.5ml/L of leveler. The dummying step was followed by chronopotentiometry and chronoamperometry. Fill ratios of  $I_{40}/I_{2560}$  and  $I_{160}/I_{2560}$  were computed from the currents measured at different RDE speeds. A plot of fill ratio vs. accelerant concentration was constructed. The plot is shown in Figure 4.50. An optimum can be observed at 15ml/L of the accelerant, after which there is fall in both the fill ratios  $I_{40}/I_{2560}$  and  $I_{160}/I_{2560}$ . Hence 15ml/L of accelerant is chosen to be the best concentration of the accelerant to be used in the Bath III. 200ml of Bath III was taken with 15ml/L of accelerant and 5ml/L of suppressor. The procedure was repeated at varying concentration of leveler added to the

200ml of Bath III. The currents measured at different speeds of the RDE were used to determine fill ratios  $I_{40}/I_{2560}$  and  $I_{160}/I_{2560}$ . From fill ratio measurements for leveler concentration variation in Bath III, 3.5ml/L of the leveler has the highest fill ratio. For all other concentrations of the leveler, the fill ratio is very close to unity. That would mean that there is not much of a difference in the surface and bottom current density. So from the three concentrations, 3.5ml/L of the leveler gives the best highest fill ratio. This is shown in Figure 4.51.

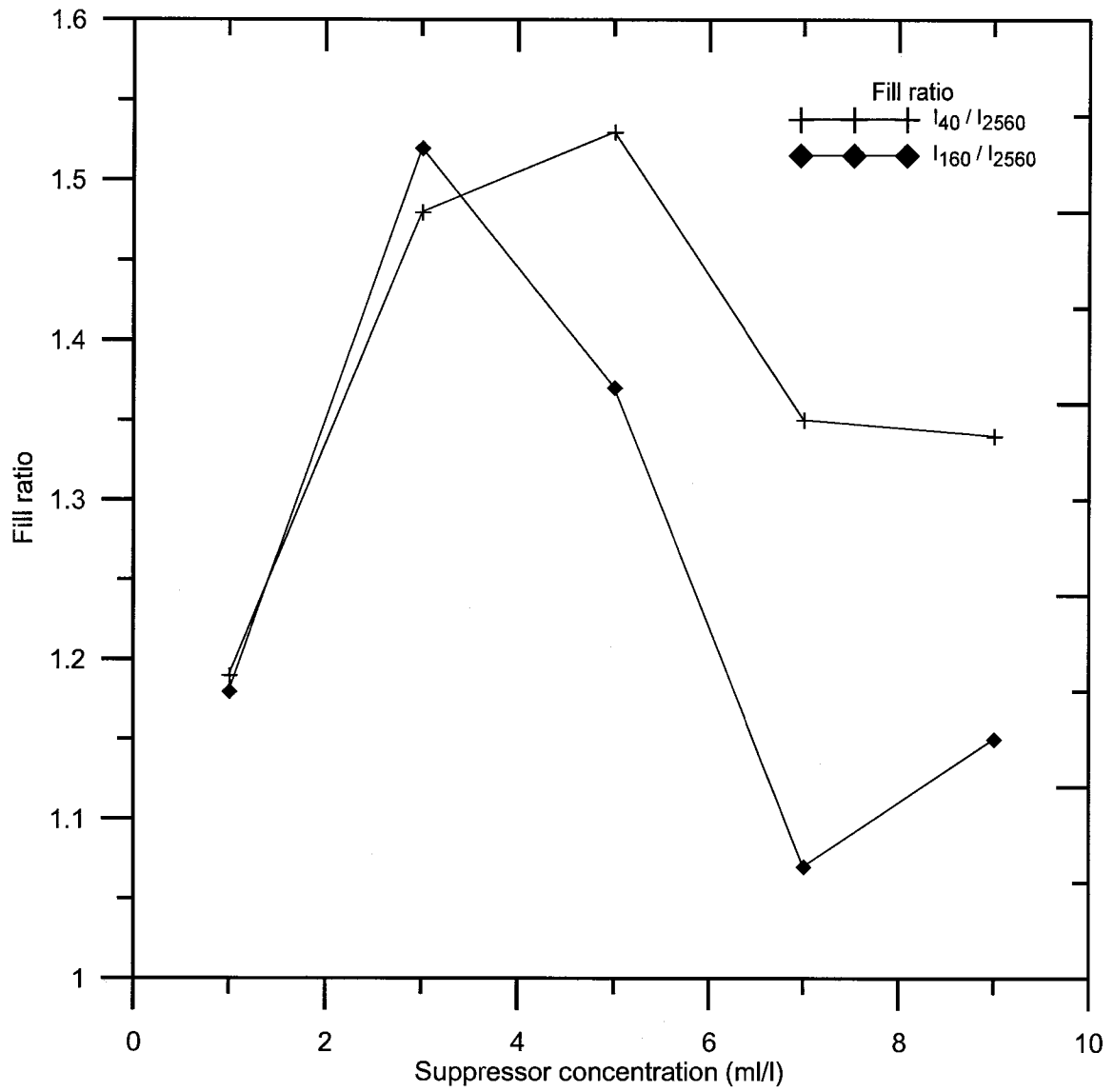


Figure 4.49 Fill ratio vs. suppressor concentration - Bath III

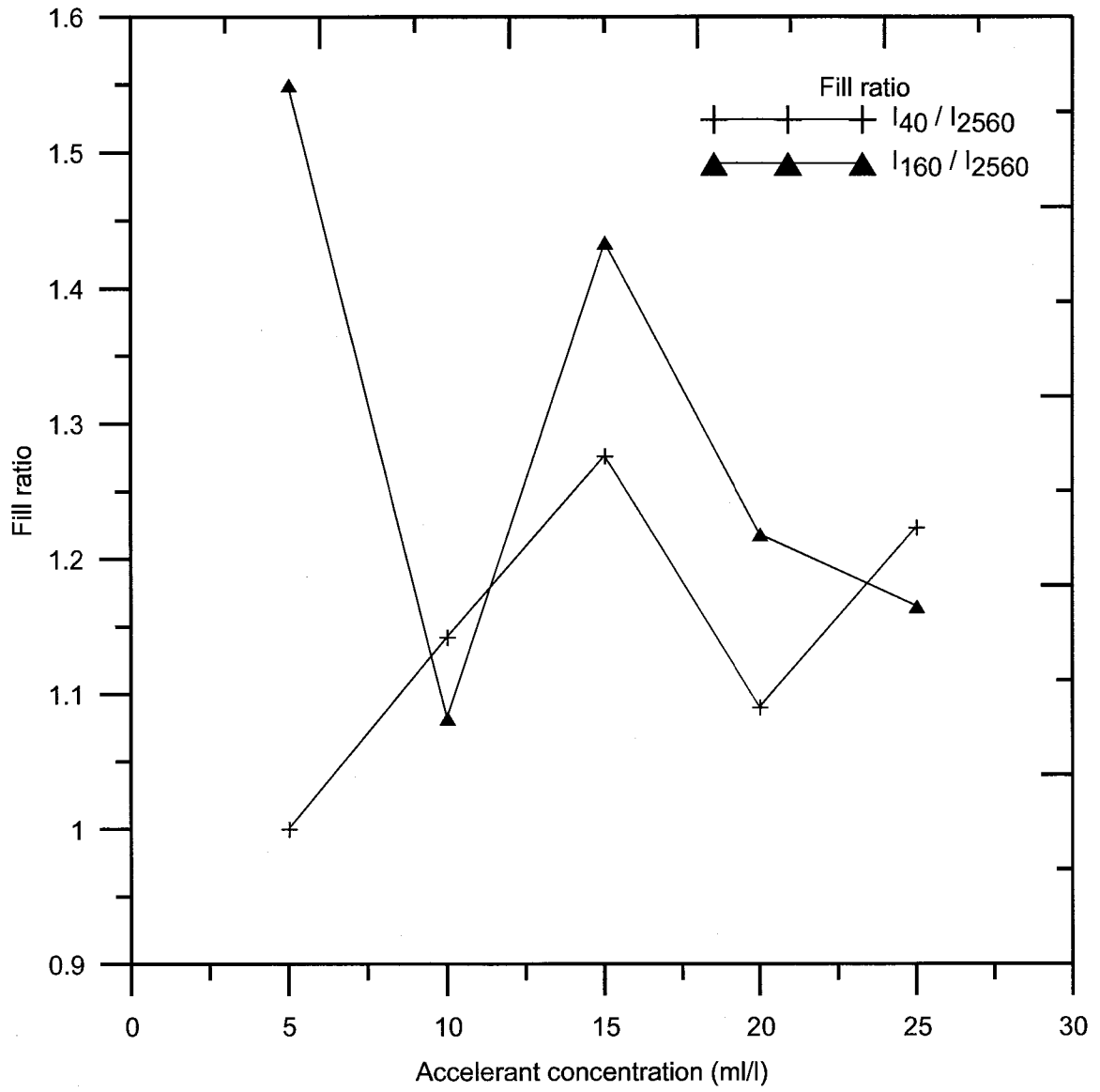


Figure 4.50 Fill ratio vs. accelerant concentration - Bath III

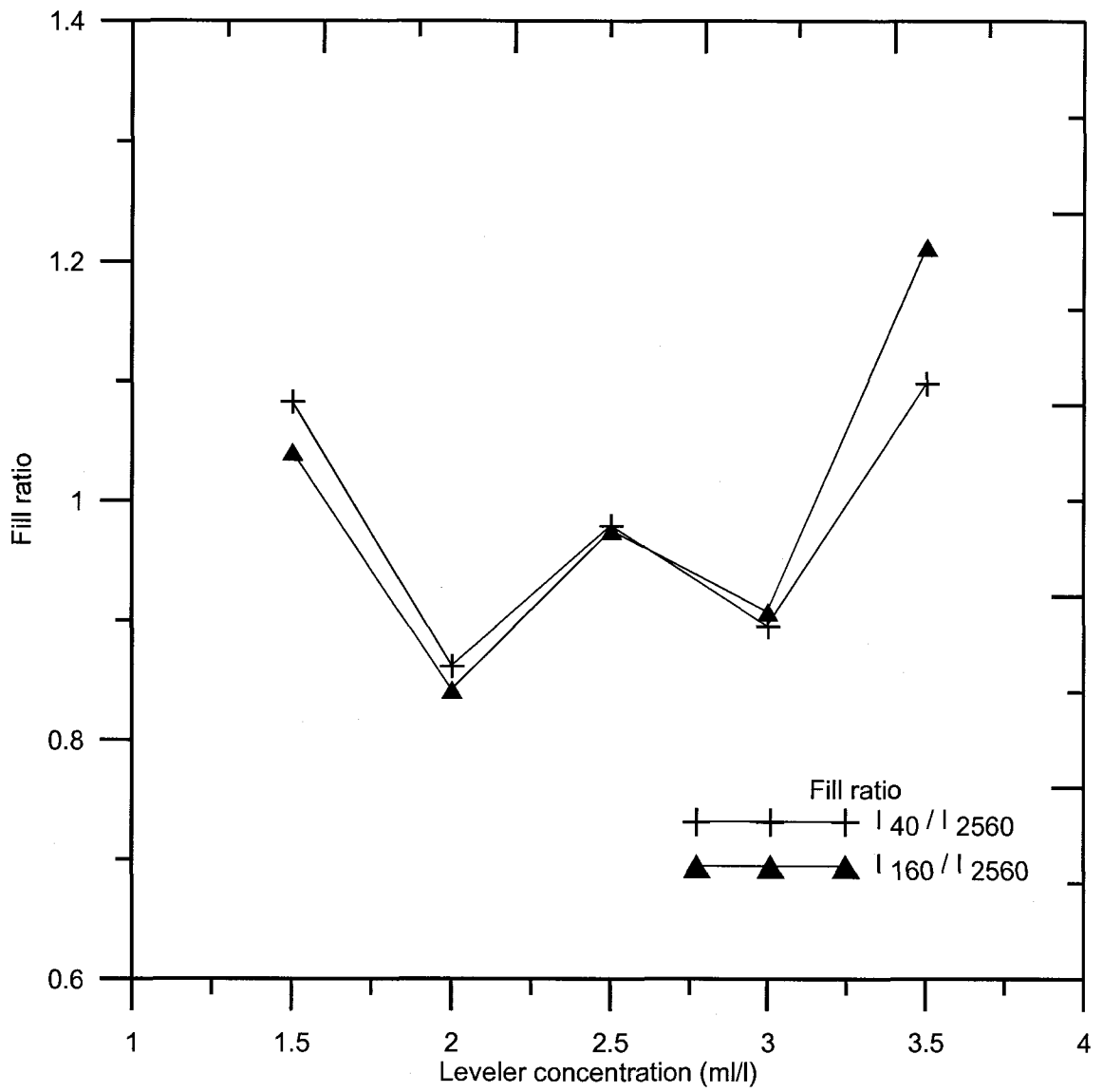


Figure 4.51 Fill ratio vs. leveler concentration - Bath III



#### 4.4.4 Comparison of the via filling electrolytes

From the optimum concentrations of the additives in each of the Baths I, II and III, an evaluation of the best chemistry among the three was performed. The base electrolyte in all the baths is an acidic copper sulfate solute with chloride content. The optimum concentrations of the additives are tabulated below

Table 4.6: Optimum concentration of additives

Additive system	Accelerant (ml/L)	Suppressor (ml/L)	Leveler (ml/L)
I	15	5	2.5
II	15	5	4.5
III	15	5	3.5

Linear sweep voltammetry was carried out to compare the 3 electrolytes. 200ml of each electrolyte batch with the optimized additives was used. A Pt RDE was used as the working electrode, SCE as the reference electrode. The potential was swept from +200mV to -600mV at a scan rate of 5mV/s. The CV scans were done at 100rpm and 1600rpm of the RDE. From the return scan data, the plot of fill ratio vs. the current measured at 100rpm was constructed in a single plot. This is shown in the Figure 4.52.

Bath I is ruled out as it has the lowest fill ratio. The Baths II and III have fill ratios as high as 2.2 and 2. The difference in fill ratios is not big. The current density measured at 100rpm is much larger for Bath III compared to Bath II. The current densities measured at 100rpm (low speed) corresponds to the deposition at the bottom of the via. Each mA/cm<sup>2</sup> corresponds to a filling rate of about 25nm/minute. The current density measured at the bottom of the via would be the desirable operating current density for via filling.

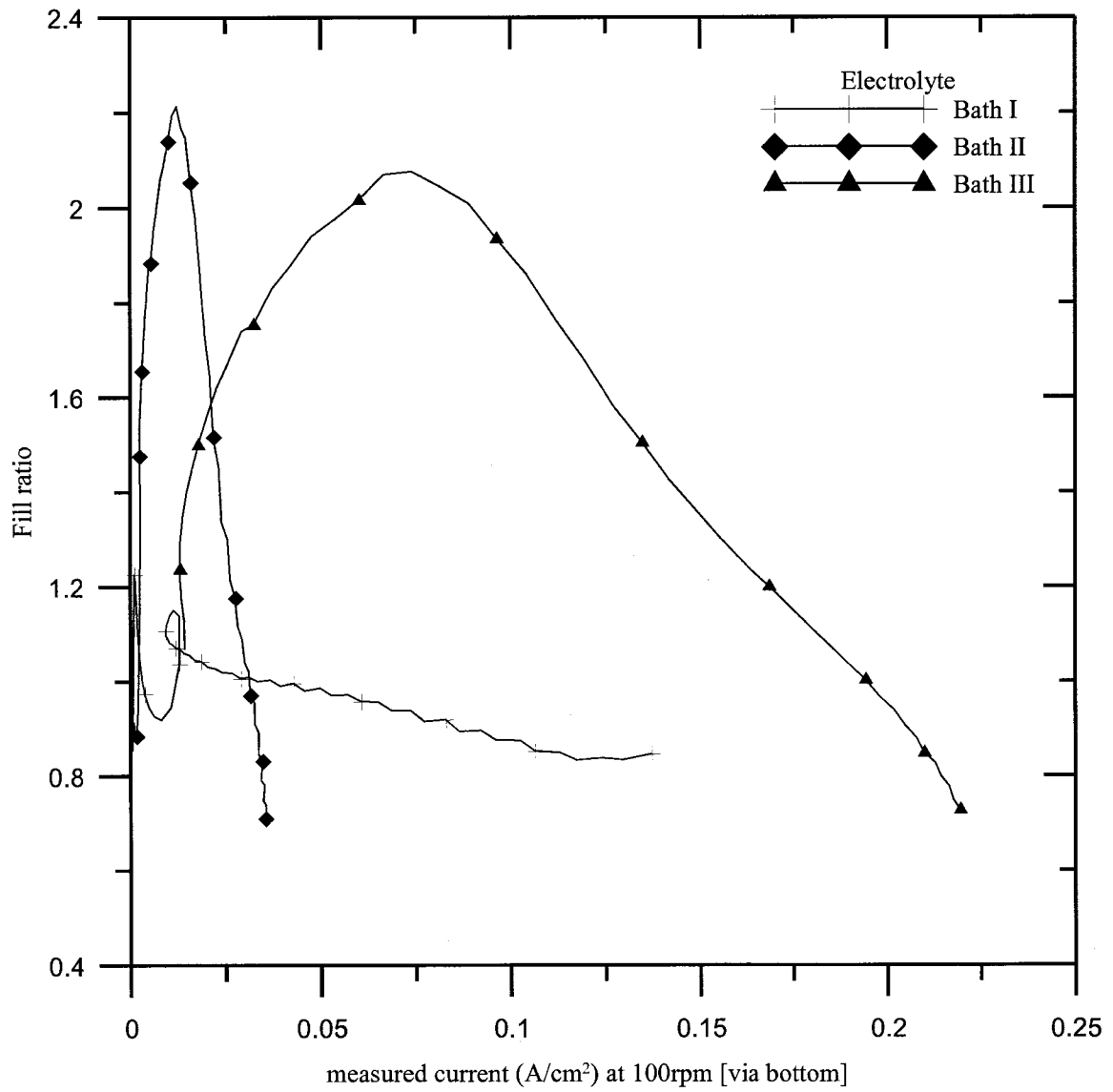


Figure 4.52 Effectiveness of different additive chemistries

## CHAPTER 5

### CONCLUSION AND RECOMMENDATIONS

#### 5.1 Conclusions

The additives used in a via filling chemistry were studied to understand their roles in effectively filling the vias. The additives investigated include 3-mercapto 1-propane sulfonic acid, *bis*-(3-sodiumsulfopropyl)-disulfide, polyethylene glycol, Cl<sup>-</sup> and Br<sup>-</sup> and proprietary systems from Rohm & Haas Electronic Materials Inc.

- (1). Pulse-reverse electrodeposition will result in better bottom-up filling with higher reverse potential.
- (2). SPS acts as a better accelerant than MPSA. Aged MPSA may give filling results as good as SPS
- (3). PEG acts as a plating rate suppressor. This is supported by lower current densities observed with increasing concentration of PEG.
- (4). The suppression effect of PEG is dependent on the molecular weight. A molecular weight in the range 6000-8000g.mol<sup>-1</sup> gives better filling.

- (5). Comparison of filling ability in the presence of  $\text{Cl}^-$  and  $\text{Br}^-$ , presence of chloride ions gives a better fill ratio. This is supported by the difference in potentials observed at different speeds of the RDE.
- (6). The RDE setup serves as a fine screening tool for the analysis of different baths. A good understanding of the model helps in better screening of baths.

## **5.2 Recommendations**

The following recommendations are suggested to further the study of electrochemical deposition of copper:

1. Perform mathematical modeling studies and correlate with experimental data.
2. Use ring disk electrode to study the  $\text{Cu(I)}$  complex formation.
3. Establish one electroanalytical technique as the best screening tool for comparing different via filling chemistries.

## NOMENCLATURE

A	Area of the disk electrode, m <sup>2</sup>
C	Concentration, mol.m <sup>-3</sup>
CE	Counter electrode
D	Diffusion coefficient, m <sup>2</sup> s <sup>-1</sup>
E <sub>a</sub>	Activation energy, V
F	Faradays constant, A.s.mol <sup>-1</sup>
i <sub>L</sub>	Limiting current density, A/cm <sup>2</sup>
J	Flux, mol.cm <sup>-2</sup> s <sup>-1</sup>
n	Number of electrons transferred
O	Oxidized species
Q	Charge, C
ppm	Parts per million
R	Reduced species
R	Gas constant, 8.314J.mol <sup>-1</sup> .K <sup>-1</sup>
RE	Reference electrode
RDE	Rotating disk electrode
SCE	Saturated calomel electrode
T	Absolute temperature, K
t	Time, s

V	Velocity, cm.s <sup>-1</sup>
WE	Working electrode
x	Directional coordinates

## **Greek Letters**

$\Phi$	Potential, V
$\delta$	Diffusion layer thickness, cm
$\omega$	Electrode rotation rate, rad.s <sup>-1</sup>
$\rho$	Resistivity, $\mu\Omega$ .cm

## LITERATURE CITED

- [1] W. -P. Dow, M. -Y. Yen, W. -B. Lin, and S. -W. Ho, "Influence of molecular weight of polyethylene glycol on microvia filling by copper electroplating", *J. Electrochem. Soc.*, 152, 11 (2005)
- [2] Y. Jin, K. Kondo, Y. Suzuki, T. Matsumoto and D. Barkey, "Surface Adsorption of PEG and Cl<sup>-</sup> Additives for Copper Damascene Electrodeposition", *Electrochem. Solid State Lett.*, 8, C6 (2005)
- [3] K. Kondo, T. Yonezawa, D. Mikami, T. Okubo, Y. Taguchi, K. Takahashi and D. Barkey, "High-Aspect-Ratio Copper-Via-Filling for Three-Dimensional Chip Stacking – (2) Reduced Electrodeposition Process- Time", *J. Electrochem. Soc.*, 152, H173 (2005)
- [4] C. Madore, M. Matlosz, and D. Landolt, "Blocking inhibitors in cathodic leveling", *J. Electrochem. Soc.*, 143, 3927 (1996)
- [5] J. Dukovic and C. W. Tobias, "Simulation of leveling in electrodeposition", *J. Electrochem. Soc.*, 137, 3748 (1990)
- [6] S. S. Kruglikov, N. T. Kudriavtsev, G. F. Vorobiova, and A. Ya. Antonov, "On the mechanism of levelling by addition agents in electrodeposition of metals", *Electrochim. Acta*, 10, 253 (1965)
- [7] C. E. Täubert, D. M. Kolb, U. Memmert, H. Meyer, "Adsorption of the Additives MPA, MPSA, and SPS onto Cu(111) from Sulfuric Acid Solutions", *J. Electrochem. Soc.*, 154, 6(2007)
- [8] P. M. Vereecken, R. A. Binstead, H. Deligianni, and P.C. Andricacos, "The chemistry of additives in damascene copper plating", *IBM J. Res. Dev.*, 49, 3 (2005)
- [9] A.C. West, S. Mayer, and J. Reid, "A Superfilling Model that Predicts Bump Formation", *Electrochem. Solid-State Lett.*, 4, C50 (2001)
- [10] T. P. Moffat, J. E. Bonevich, W. H. Huber, A. Stanishevsky, D. R. Kelly, G. R. Stafford, and D. Josell, "Superconformal Electrodeposition of Copper in 500–90 nm Features", *J. Electrochem. Soc.*, 147, 4524 (2000)
- [11] J. Reid and S. Mayer, *Proceedings of the AESF SUR/FIN Annual International Technical Conference*, p.68 (2000)

- [12] D. M. Soares, S. Wasle, "Copper ion reduction catalyzed by chloride ions", *J. Electroanal. Chem.*, 532, (2002)
- [13] W. Shao, G. Pattanaik, G. Zangari, "Influence of chloride anions on the mechanism of copper electrodeposition from acidic sulfate electrolytes", *J. Electrochem. Soc.*, 154, 4 (2007)
- [14] M. Yokoi, S. Konishi, and T. Hayashi, *Denki Kagaku oyobi Kogyo Butsuri Kagaku*, 52, 218 (1984)
- [15] B. -H. Wu, C. -C. Wan, and Y. -Y. Wang, "Void-free anisotropic deposition for IC interconnect with polyethylene glycol as the single additive based on uneven adsorption distribution", *J. Appl. Electrochem.*, 33, 823 (2003)
- [16] J. P. Healy, D. Pletcher, and M. Goodenough, "The chemistry of the additives in an acid copper electroplating bath: Part I. Polyethylene glycol and chloride ion", *J. Electroanal. Chem.*, 338, 155 (1992)
- [17] L. Bonou, M. Eyraud, R. Denoyel, and Y. Massiani, "Influence of additives on Cu electrodeposition mechanisms in acid solution: direct current study supported by non-electrochemical measurements", *Electrochim. Acta*, 47, 4139 (2002)
- [18] Z. V. Feng, X. Li, and A. A. Gewirth, "Inhibition Due to the Interaction of Polyethylene Glycol, Chloride, and Copper in Plating Baths: A Surface-Enhanced Raman Study", *J. Phys. Chem. B*, 107, 9415 (2003)
- [19] K. Doblhofer, S. Wasle, D. M. Soares, K. G. Weil, and G. Ertl, "An EQCM Study of the Electrochemical Copper(II)/Copper(I)/Copper System in the Presence of PEG and Chloride Ions", *J. Electrochem. Soc.*, 150, C657 (2003)
- [20] M. L. Walker, L. J. Richter, and T. P. Moffat, "Competitive Adsorption of PEG, Cl<sup>-</sup>, and SPS/MPS on Cu: An In Situ Ellipsometric Study", *J. Electrochem. Soc.*, 152, C403 (2005)
- [21] M. E. Huerta Garrido and M. D. Pritzker, "Voltammetric Study of the Inhibition Effect of Polyethylene Glycol and Chloride Ions on Copper Deposition", *J. Electrochem. Soc.*, 155, 4 (2008)
- [22] James J. Kelly and A. C. West, "Copper Deposition in the Presence of Polyethylene Glycol", *J. Electrochem. Soc.*, 145, 10 (1998)
- [23] James J. Kelly and A. C. West, "Copper Deposition in the Presence of Polyethylene Glycol – I. Quartz microbalance study", *J. Electrochem. Soc.*, 145, 3477 (1998)
- [24] D. Josell, D. Wheeler, H. Huber, and T.P. Moffat, "Superconformal Electrodeposition in Submicron Features", *Phys. Rev. Lett.*, 87, 016102 (2001)



- [25] T. P. Moffat, D. Wheeler, H. Huber, and D. Josell, "Superconformal Electrodeposition of Copper", *Electrochem. Solid-State Lett.*, 4, C26 (2001)
- [26] J. Reid, S. Mayer, E. Broadbent, E. Klawnhn, and K. Ashtiani, "Factors Influencing Damascene Feature Fill Using Copper PVD and Electroplating", *Solid State Technol.*, 80, (2000)
- [27] T. P. Moffat, B. Baker, D. Wheeler, and D. Josell, "Accelerator Aging Effects During Copper Electrodeposition", *Electrochem. Solid-State Lett.*, 6, C59 (2003)
- [28] Chi-Cheng Hung, Wen-Hsi Lee, Shih-Chieh Chang, Kei-Wei Chen, and Ying-Lang Wang, "Suppression Effect of Low-Concentration Bis-(3-sodiumsulfoethyl disulfide) on Copper Electroplating", *J. Electrochem. Soc.*, 155, 2 (2008)
- [29] J. J. Kim, S. K. Kim, Y. S. Kim, "Catalytic behavior of 3-mercapto-1-propane sulfonic acid on Cu electrodeposition and its effect on Cu film properties for CMOS device metallization", *J. Electroanal. Chem.*, 542, 61 (2003)
- [30] E. Farandon, F.C. Walsh, and S. A. Campbell, "Effect of thiourea, benzotriazole and 4,5-dithiaoctane-1,8-disulphonic acid on the kinetics of copper deposition from dilute acid sulphate solutions", *J. Appl. Electrochem.*, 25, 572 (1995)
- [31] Soo-Kil Kim and Jae Jeong Kim, "Superfilling Evolution in Cu Electrodeposition - Dependence on the Aging Time of the Accelerator", *J. Electrochem. Soc.*, 7, 9 (2004)
- [32] J. O. Dukovic, "Feature-scale simulation of resist-patterned electrodeposition", *IBM J. Res. Dev.*, 37, 125 (1993)
- [33] A. C. West, "Theory of Filling of High-Aspect Ratio Trenches and Vias in Presence of Additives" *J. Electrochem. Soc.*, 147, 227 (2000)
- [34] T. P. Moffat, J. Bonevich, W. Huber, A. Stanishevsky, D. Kelly, G. Stafford, and D. Josell, *J. Electrochem. Soc.*, 147, 4524 (2000)
- [35] Y. Cao, P. Taephaisitphongse, R. Chalupa, and A. C. West, "Three-Additive Model of Superfilling of Copper", *J. Electrochem. Soc.*, 148, C466 (2001)
- [36] P.C. Andricacos, C. Uzoh, J. O. Dukovic, J. Horkans, H. Deligianni, "Damascene copper electroplating for chip interconnections", *IBM J. Res. Dev.*, 42, 5 (1998)
- [37] P. C. Andricacos, "Copper on-chip interconnections: A breakthrough in electrodeposition to make better chips", *The Electrochemical Society Interface*, 8 (1999)
- [38] D. Varandarajan, C. Y. Lee, A. Krishnamoorthy, D. J. Duquette, and W. N. Gill, "A tertiary current distribution model for the pulse plating of copper into high aspect ratios sub-0.25 $\mu\text{m}$  trenches", *J. Electrochem. Soc.*, 147, 9 (2000)

- [39] A. Radisic, A. C. West, and P. C. Searson, "Influence of additives on nucleation and growth of copper on n-Si(111) from acidic sulfate solutions", *J. Electrochem. Soc.*, 149, 2 (2002)
- [40] R. Akolkar, U. Landau, "A time-dependent transport-kinetics model for additive interactions in copper interconnect metallization", *J. Electrochem. Soc.*, 151, 11 (2004)
- [41] Kurt R. Hebert, Saikat Adhikari, and Jerrod E. Houser, "Chemical Mechanism of Suppression of Copper Electrodeposition by Poly(ethylene glycol)", *J. Electrochem. Soc.*, 152, 5 (2005)
- [42] Ken M. Takahashi and Mihal E. Gross, "Transport Phenomena that control Electroplated Copper Filling of Submicron Vias and Trenches", *J. Electrochem. Soc.*, 146, 12 (1999)
- [43] Bioh Kim, Charles Sharbono, Tom Ritzdorf, and Dan Schmauch, "Factors Affecting Copper Filling Process Within High Aspect Ratio Deep Vias for 3D Chip Stacking", 56<sup>th</sup> ECTC Proceedings (2006)
- [44] Sailesh M. Merchant, Seung H. Kang, Mahesh Sangneria Bart V. Schravendijk and Tom Mountsier, "Copper interconnects for semiconductor devices", *JOM Journal of the Minerals, Metals and Materials Society*, 53, 6(2001)